Alena Voit BSc

Expression of human G protein-coupled receptors in *Pichia pastoris*

MASTER'S THESIS

to achieve the university degree of

Diplom-Ingenieurin

Master's degree programme: Biotechnology

submitted to

Graz University of Technology

Supervisor

Assoc.Prof. Dipl.-Ing. Dr.techn. Harald Pichler

Institute of Molecular Biotechnology

Graz, June 2017

AFFIDAVIT

I declare that I have authored this thesis independently, that I have not used other than the declared sources/resources, and that I have explicitly indicated all material which has been quoted either literally or by content from the sources used. The text document uploaded to TUGRAZonline is identical to the present master's thesis.

16 June 2017
Date

Alena Voit
Signature

Danksagung

An erster Stelle möchte ich mich bei meiner ganzen Familie, Freunden, Bekannten und auch meinem Freund bedanken, die mich während meines Studiums durch jegliche Hilfe stets unterstützt haben und immer an mich geglaubt haben. Ein großer Dank gilt Harald Pichler, der mir die Möglichkeit geboten hat, das Projektlabor und die Diplomarbeit über ein interessantes Thema in seiner Arbeitsgruppe zu absolvieren und auch für seine Zeit für Besprechungen und Ratschläge trotz seines ohnehin recht gefüllten Terminplans. Melanie Hirz danke ich für die tolle Betreuung im Labor und die allgemeine Einführung in die Laborarbeiten sowie das spezielle Arbeiten mit *Pichia pastoris*. Ohne sie wären die Experimente wohl nicht annähernd so reibungslos abgelaufen. Weiters danke ich Anita Emmerstorfer-Augustin, die das Projekt mit den GPCRs ins Leben gerufen hat, die Kollaboration mit Christoph Reinhart hergestellt hat und die initialen Vektoren mit den GPCRs konstruiert hat. Natürlich auch Christoph Reinhart vom Max-Planck-Institut für Biophysik in Frankfurt, der uns die cDNAs der GPCRs und die Referenzstämme zur Verfügung gestellt hat und auch bereit war, diverse Stämme auf deren Funktionalität der GPCRs zu analysieren. Weiters gilt ein Dank Karl-Heinz Grillitsch vom Institut für Biochemie an der TU Graz für die Bereitstellung von diversen Antikörpern. Zu guter Letzt auch ein Dank den ganzen Labor- sowie Bürokollegen im ersten Stock sowie der Harald Pichler Gruppe aus dem zweiten Stock, die mir immer, auch bei jeder Kleinigkeit, weitergeholfen haben.

Table of content

Abstract

G protein-coupled receptors (GPCRs) are integral membrane proteins with seven characteristically α-helical transmembrane domains that are found over 800 times in the human genome. As they are involved in many important signal transduction processes, they are associated with various diseases and represent a major target for pharmaceuticals and the development thereof.

Three human GPCRs, the β_2-adrenergic receptor (β_2AR), the human bradykinin 1 receptor (hB1R) and the complement component C3a receptor (C3aR) were cloned in vector constructs with variable promoters and tags. Their expression was analyzed in *Pichia pastoris* strains with different genetic background in order to enhance heterologous receptor production. One strain was engineered to produce cholesterol instead of the native ergosterol in the cellular membranes. This strain yielded the most interesting results as the cholesterol apparently stabilized the expressed β_2AR and was also important for functionality of the receptor. For the hB1R only inactive receptor could be expressed and the C3aR showed no expression at all on the protein level.

Zusammenfassung

G-Protein-gekoppelte Rezeptoren (GPCRs) gehören zu den integralen Membranproteinen, bestehen aus sieben charakteristischen α-helikalen Transmembrandomänen und kommen über 800 Mal in Genom des Menschen vor. Sie werden in Zusammenhang mit diversen Krankheiten gebracht, da sie in viele wichtige Signaltransduktionsprozesse involviert sind und haben daher große Bedeutung für Pharmazeutika und deren Entwicklung.

Drei GPCRs des Menschen, der β_2-Adrenorezeptor (β_2AR), der humane Bradykinin 1 Rezeptor (hB1R) und der Komplementrezeptor für die C3a-Komponente (C3aR) wurden in Vektorkonstrukte mit variablen Promotoren und Tags kloniert. Die Expression wurde in *Pichia pastoris* Stämmen mit unterschiedlichem genetischen Hintergrund untersucht, um die heterologe Produktion der Rezeptoren zu verbessern. Ein Stamm wurde genetisch so verändert, dass er Cholesterin statt dem nativen Ergosterol in den zellulären Membranen produziert. Dieser zeigte die interessantesten Ergebnisse, da das Cholesterin den exprimierten β_2AR offensichtlich stabilisierte und auch positiven Einfluss auf dessen Funktionalität hatte. Vom hB1R konnte nur inaktiver Rezeptor exprimiert werden und der C3aR zeigte keinerlei Expression auf Proteinebene.

List of abbreviations

Table 1: List of abbreviations

aa	amino acids	**Hyg**	hygromycin
Amp	ampicillin	**kDa**	Kilo Dalton
AOX1	Alcohol oxidase 1	**KP_i**	Potassium phosphate buffer
β_2AR	β_2-adrenergic receptor	**MD(H)**	Minimal dextrose medium (+His)
BMGY/ BMMY	Buffered Glycerol-/Methanol-complex Medium	**MeOH**	methanol
		MM(H)	Minimal methanol medium (+His)
cPCR	Colony PCR	**Mut+/MutS**	Methanol utilization plus/slow
bp	Base pair	**OD_{600}**	Optical density at 600 nm
C3aR	Complement component C3a receptor	**ONC**	Overnight culture
		PCR	Polymerase chain reaction
cDNA	Complementary DNA	**P_{AOX1}**	Promoter of *P. pastoris* alcohol oxidase 1
CWW	Cell wet weight		
ddH_2O	Double destilled water	**P_{GAP}**	Promoter of *P. pastoris* glycerinaldehyde-3-phosphate dehydrogenase
DHCR7	Dehydrocholesterol reductase 7		
DHCR24	Dehydrocholesterol reductase 24		
DMSO	Dimethylsulfoxide	**Pma1**	Plasma membrane ATPase 1
dNTP	Deoxynucleotide triphosphate	**PMSF**	Phenylmethylsulfonyl fluoride
DTT	Dithiothreitol	**rpm**	revolutions per minute
DWP	Deep-well plate	**RT**	Room temperature
EtBr	Ethidiumbromide	**SDS-PAGE**	Sodium dodecyl sulfate polyacrylamide gel electrophoresis
EDTA	Ethylenediamine tetraacetic acid		
eGFP	Enhanced green fluorescent protein		
ER	Endoplasmic reticulum	**TCA**	Trichloroacetic acid
ERG5	Sterol C-22 desaturase	**Tm**	Melting temperature
ERG6	Sterol C-24 methyl transferase	**Tris**	2-Amino-2-hydroxymethyl-propane-1,3-diol
EtOH	ethanol		
gDNA	Genomic DNA	**WB**	Western Blot
GEF	GTP exchange factor	**WT**	Wild type
GPCR	G protein-coupled receptor	**YNB**	Yeast nitrogen base
hB1R	Human bradykinin 1 receptor	**YPD**	Yeast extract peptone dextrose media
His	Histidine		
HRP	Horseradish peroxidase		

1 Introduction

1.1 G protein-coupled receptors

G protein-coupled receptors (GPCRs) are integral membrane proteins that are only found in eukaryotes, from lower ones like yeast up to human. In the human genome, for instance, they are annotated about 800 times and represent the largest family of membrane proteins[1–3].

GPCRs are located in the plasma membrane and are built up of seven characteristically α-helical transmembrane domains that are joined by three extracellular and intracellular loops each. The N-terminus is located in the extracellular region which binds the ligands. The C-terminus is intracellular and the cytoplasmic region interacts with different signaling factors like the heterotrimeric G-proteins[4,5].

The so-called GRAFS system was used to cluster human GPCRs based on phylogenetic analysis[1] and lists the five families Glutamate (G), Rhodopsin (R), Adhesion (A), Frizzled/Taste2 (F) and Secretin (S). The rhodopsin family represents the largest one with the most diverse members[6].

About half of the 800 human GPCRs have sensory functions for olfaction, taste and vision whereas the other half is responsible for diverse signal transduction processes[4,7]. GPCRs are activated by the binding of extracellular ligands covering a wide spectrum that varies from small photons and ions up to molecules like lipids, nucleotides, hormones and other proteins[6]. After activation, GPCRs trigger an intracellular signal cascade, mostly by interaction with a heterotrimeric G-protein (Figure 1) but also a G protein-independent signaling pathway has been described which includes arrestins and G protein-coupled receptor kinases (GRKs)[5,8].

GPCRs are involved in various signal transduction processes which associates them with quite a number of diseases in case of malfunction. The diseases range from metabolic disorders like obesity and type 2 diabetes, cardiovascular diseases, osteoporosis, immunological disorders, neurodegenerative diseases, AIDS and cancer[9]. That is why GPCRs represent a major target for the pharmaceutical industry[4,7,10]. Currently, about 50% of all drugs on the market target GPCRs located at the cell surface[11,12]. In order to develop new drugs, much effort is put on the structural characterization of GPCRs[11]. By now, crystal structures of only 10% of all GPCRs involved in signaling processes could be solved[5].

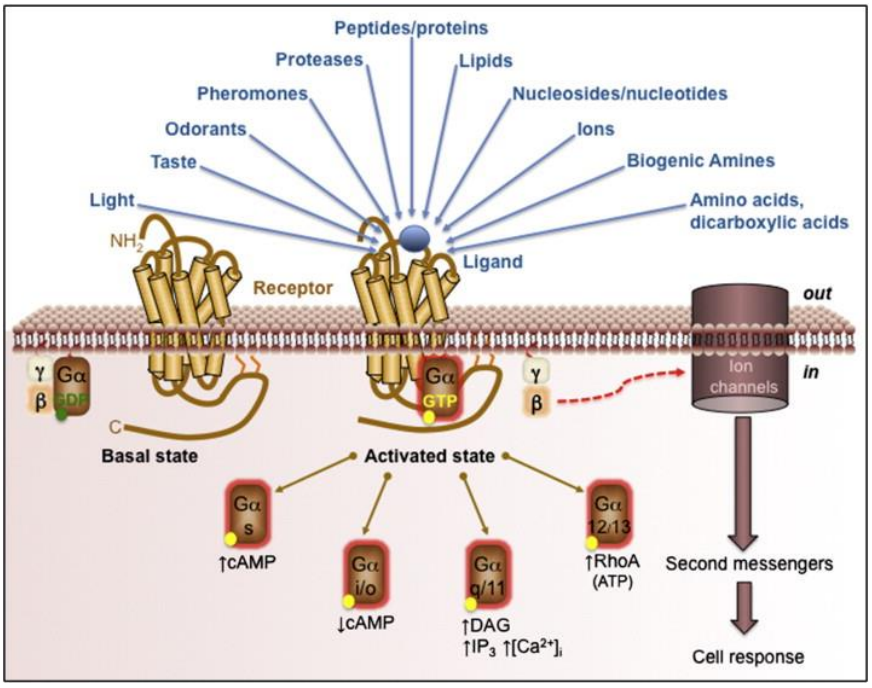

Figure 1: GPCRs are activated by binding of diverse ligands which leads to conformational changes of the receptor. Guanine nucleotide exchange factors (GEFs) exchange GDP for GTP on the α-subunit of the heterotrimeric G-protein which leads to the separation of the Gα and Gβγ subunit. Different Gα subunits influence Ras homologs (RhoA), cyclic AMP (cAMP), diacylglycerol (DAG), inositol-1,4,5-triphosphate (IP_3) and Ca^{2+} levels. The Gβγ subunit can for instance activate ion channels. Image was taken from Heng, B. C. et al. (2013).

Unfortunately, the natural abundance of membrane proteins including GPCRs is quite low which makes crystallization studies difficult as they require high and pure amounts of protein. Other critical factors are stability, functionality and homogeneity especially concerning post-translational modifications[13,14].

Therefore, GPCRs are heterologously expressed in host systems like mammalian cells[15] or insect cells[10,14] but due to the complex and labor-intensive handling of these cells also lower eukaryotes are successfully used. Yeasts like *Saccharomyces cerevisiae* and *Pichia pastoris* are often used hosts as they are easy to manipulate, low in production costs and are capable of eukaryotic post-translational protein processing[13,14,16]. There are two approaches to enhance the heterologous expression of GPCRs. On the one hand, there is the attempt to mutagenize the receptor gene. This was described in a study where they did a directed evolution of GPCRs in *S. cerevisiae* by combining random mutagenesis with a proper screening method for functional receptors[14]. On the other hand, the central point lies in the engineering of the expression host. The Callewaert group developed a modular integrated secretory system in *P. pastoris* in order to enhance GPCR expression[16]. The second strategy is the one this study focusses on.

In this study, the expression of three different GPCRs was analyzed in *P. pastoris*. They all belong to the large rhodopsin family.

1.1.1 β_2-adrenergic receptor

Generally, there are α- and β-adrenergic receptors. β-adrenergic receptors have three subclasses, β_1, β_2, and β_3. They are present in cardiac, airway smooth muscle and adipose tissue, respectively[17]. Mutations of β-adrenergic receptor genes are associated with asthma, hypertension and heart failure[18].

The β_2-adrenergic receptor (β_2AR) in particular is expressed in bronchial and vascular smooth muscle cells and in cardiac myocytes. Therefore, a malfunction is connected to diseases like asthma, vasodilation and inotropy[18]. On the genetic level, different polymorphic forms, point mutations or downregulation of the β_2AR gene can result in nocturnal asthma[19], obesity and type 2 diabetes[18]. The β_2AR also plays a role in heart failure[20,21] and lately, an association between polymorphisms in the β_2AR gene and tuberculosis has been described[22].

Two natural ligands of β_2AR are adrenaline and noradrenaline with a 30-fold higher affinity for adrenaline. Several agonists are used to stimulate the β_2AR whereas antagonists, the so-called β-blockers, reduce signaling of β-adrenergic receptors. Agonists as well as antagonists are used for the treatment of symptoms and diseases[4,18,23].

Once activated, the β_2AR stimulates a wide range of intracellular signal cascades that have been analyzed well and are summarized in Figure 2. There are stimulating (Gs) and inhibiting (Gi) G protein-signaling pathways as well as a G protein-independent pathway that is mediated by arrestin and induces the mitogen-activated protein (MAP) kinase pathway.

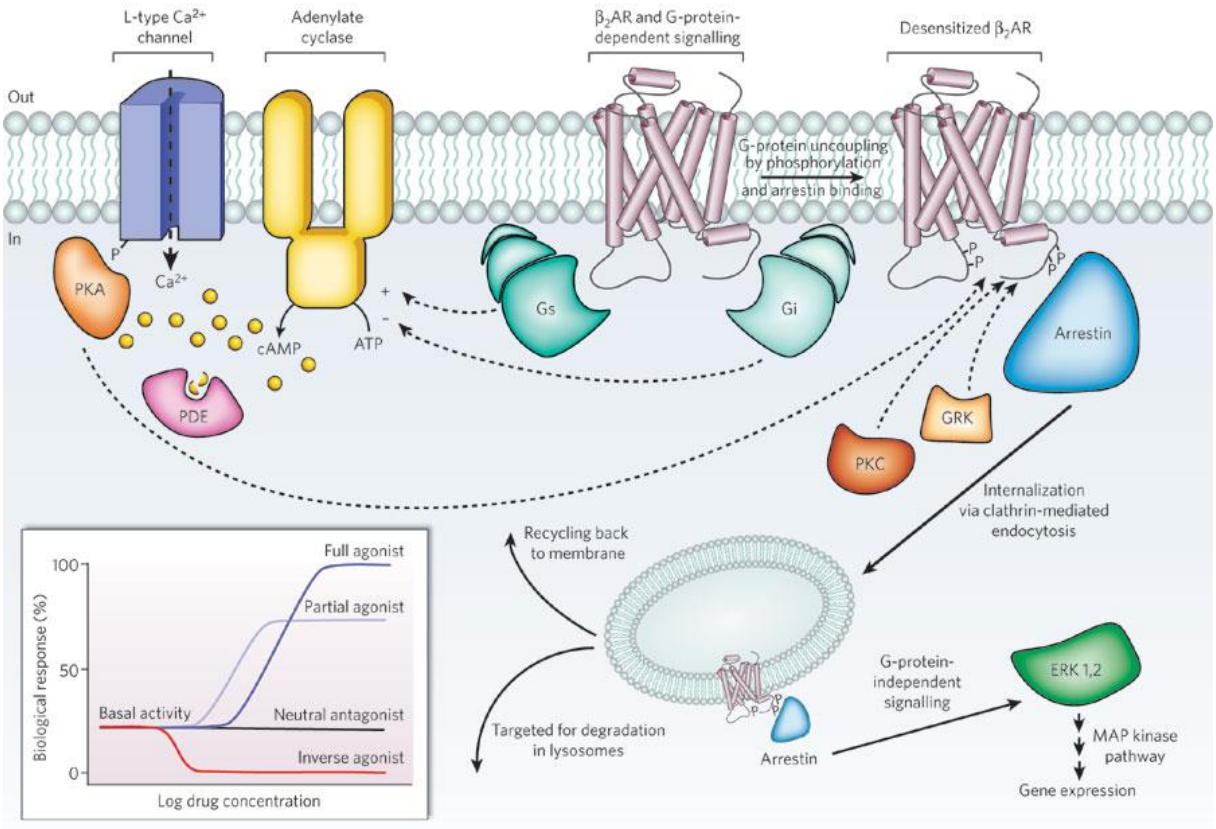

Figure 2: Signaling pathways regulated by the β_2AR. It can activate Gαs and Gαi which regulate adenylate cyclase up or down. Adenylate cyclase produces cAMP which activates protein kinase A (PKA). PKA regulates phosphorylation of L-type Ca^{2+} channels and of the β_2AR itself after activation. Phosphodiesterase proteins (PDEs) downregulate cAMP levels. The β_2AR is also phosphorylated by protein kinase C (PKC) and a GRK and is then coupled to arrestin, which activates extracellular signal-regulated kinases (ERK), prevents the activation of G proteins and internalizes the receptor through clathrin-coated pits. GPCRs have basal activity without any agonist. Inverse agonists inhibit basal activity; neutral antagonists have no effect and agonists and partial agonists stimulate biological responses. Image was taken from Rosenbaum, D. M. et al. (2009).

The β_2AR was the first GPCR that was cloned and sequenced[24,25] and the second GPCR of which a crystal structure has been determined. This was accomplished by the insertion of a T4 lysozyme in the third intracellular loop of the receptor[10]. By the way, the first GPCR structure was obtained from the eukaryotic GPCR bovine rhodopsin as it is the only GPCR that is highly abundant in native tissue[10,26–28]. Today, the β_2AR serves as a model GPCR for heterologous expression[29] as there is much information already known about this receptor. Moreover, it has already been successfully expressed in *P. pastoris* strains[30] and it is known to be easily and well expressed in this host system.

It has also been shown that the β_2AR has a conserved cholesterol binding site[31] (Figure 3A), that cholesterol in the cell membrane improves stability of the receptor[32,33] and cholesterol seems to be important for crystallization attempts (Figure 3B)[10,33].

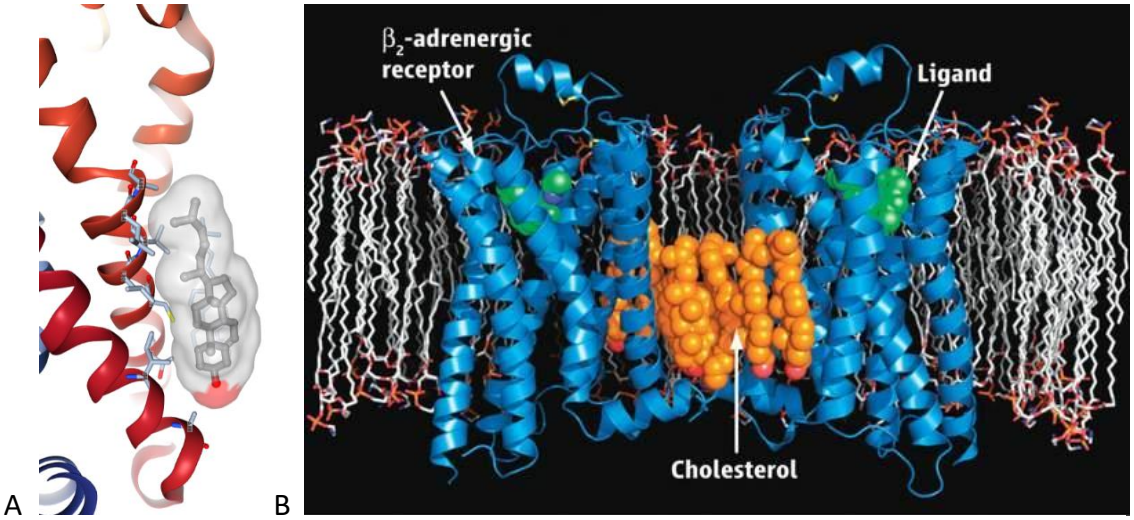

Figure 3: (A) Cholesterol binding site in the β_2AR (PDB 3D4S). (B) Figure: Structure of the human β_2AR (blue) in the surrounding of a lipid membrane. The receptor is bound to a diffusible ligand (green) and cholesterol and palmitic acid (orange) are present between the two receptor molecules. Image B was taken from the Author's Summary of Cherezov, V. et al. (2007).

The β_2AR structure could be solved in complex with a Gs protein[34] too (Figure 4).

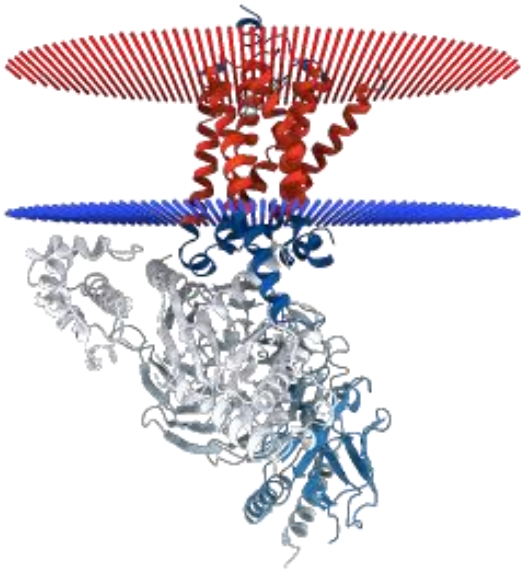

Figure 4: Crystal structure of the β_2AR-Gs protein complex (PDB 3SN6).

1.1.2 Complement component C3a receptor

The complement component C3a receptor (C3aR) is involved in the complement system, an essential part of the innate immune response. Its ligand, the complement component C3a, is formed by proteolytic cleavage of the complement component C3. C3a, C4a and C5a are small peptides of about 10 kDa that are also called anaphylatoxins as they can trigger anaphylactic shock[35]. They cause pro-inflammatory effects like smooth muscle contraction, vasodilation, increased vascular permeability and release of Histamine and reactive oxygen species[9,35]. Therefore, C3aR is responsible for allergic diseases like bronchial asthma[36]. It is expressed in different human mast cell lines and the binding of C3a mediates Ca^{2+} mobilization, substantial degranulation and chemokine generation via Gi-protein activation[37] but also leads to the production of IL-6 and TNF-α by B-lymphocytes and monocytes [38].

C3aR has already been cloned and characterized[39] but the crystal structure still remains to be solved.

1.1.3 Human bradykinin 1 receptor

There are two bradykinin receptor subtypes called the human bradykinin 1 receptor (hB1R) and human bradykinin 2 receptor (hB2R). Their ligand bradykinin is a vasoactive nonapeptide, whose structure[40] is shown in Figure 5. The peptide has a short plasma half-life of about 15 s and binds the endothelial bradykinin receptors in pathophysiological states as well as inflammatory processes. The classical symptoms of inflammation like redness, heat, swelling and pain result from vasodilation and increased vascular permeability[41,42].

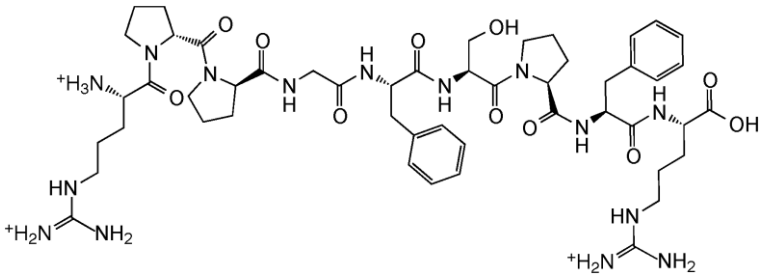

Figure 5: Structure of bradykinin. The nonapeptide has the sequence Arg-Pro-Pro-Gly-Phe-Ser-Pro-Phe-Arg. Image was taken from Voronina, L. et al. (2015).

There are two differences between the hB1R and hB2R. On the one hand it is the natural ligand: hB1R recognizes the degradation product des-Arg^{9}-bradykinin and hB2R binds bradykinin itself[42]. On the other hand, the expression of hB1R is inducible and it has a slow agonist desensitization, whereas hB2R is constitutively expressed and has a rapid agonist desensitization[41]. hB2R is normally stable in the cell membrane, but when bradykinin is bound the receptor gets internalized by endocytosis and recycled[41,43]. By contrast, hB1R is only expressed and stabilized at the cell surface when the ligand des-Arg^{9}-bradykinin is bound and this happens during injury and inflammation[44]. Without ligand binding the receptor is internalized by endocytosis and degraded[41]. hB2R[45] as well as hB1R[46] have been cloned but crystal structures are still missing.

1.2 *P. pastoris* as expression host

By now, the methylotrophic yeast *P. pastoris* is a well understood host for the production of different proteins, especially enzymes as well as biopharmaceuticals[13,47]. A well annotated genome sequence of the CBS7435 strain is available,[48] which facilitates genetic manipulations. Moreover, several selection markers, inducible and constitutive promoter systems, signal sequences for secretory expression and different host strains for special applications are established. Especially the very strong, methanol inducible *AOX1* promoter is used in most vector constructs in order to obtain high level expression of heterologous proteins[13]. *P. pastoris* is also a proper host for the expression of membrane proteins from higher eukaryotes including human. Its eukaryotic background provides a good starting point concerning protein processing[47] and also a more similar membrane surrounding compared to bacterial hosts. The crystal structure of two GPCRs could be solved by using the protease deficient *P. pastoris* SMD1163 as expression host [49–51].

1.2.1 Cholesterol as stabilizing factor

A critical factor for the expression of GPCRs are stabilizing lipids in the cellular membranes. Cholesterol plays a major role in the regulation of the structure and function of eukaryotic membranes and is also important for membrane proteins including GPCR function and related pharmacology[33]. For GPCRs and also other membrane proteins, a cholesterol consensus interaction motif has been found[31].

It is known that mammals and fungi differ in their sterol composition. They initially share parts of the sterol metabolic pathway but at a certain point their pathways differ (Figure 6). Fungi synthesize mainly ergosterol by adding a methyl group at C-24 via the sterol C-24 methyl transferase (Erg6p) and by introducing a double bond at C-22 via the sterol C-22 desaturase (Erg5p). Mammals, on the other hand, produce cholesterol by saturating sterols at the positions C-7 and C-24 via the dehydrocholesterol reductases 7 (*DHCR7*) and 24 (*DHCR24*). Although these two sterols seem to be quite similar and have only small differences in the chemical structures, they have a distinct impact concerning the lipid environment of membrane proteins[52,53].

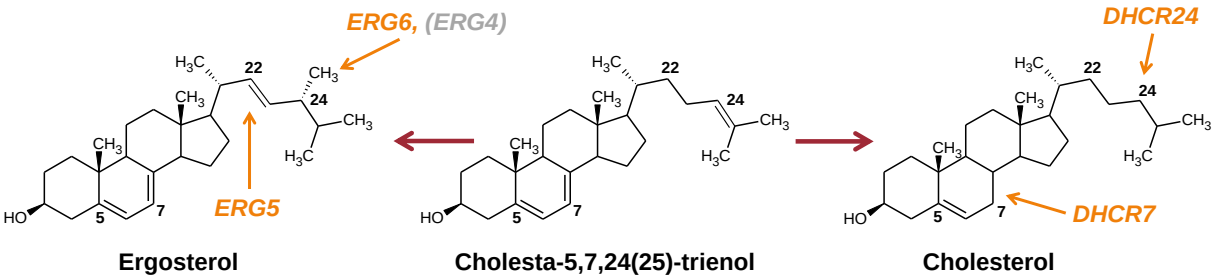

Figure 6: Structures of ergosterol and cholesterol. The sterol C-22 desaturase (*ERG5*) and the sterol C-24 methyl transferase (*ERG6*) are responsible for ergosterol synthesis whereas the dehydrocholesterol reductases 7 and 24 (*DHCR7*, *DHCR24*) mediate cholesterol production. Cholesta-5,7,24(25)-trienol is a possible intermediate. Image was taken from Hirz, M. et al. (2013).

In order to combine the advantages of the expression host *P. pastoris* and cholesterol as the major sterol, the *P. pastoris* CBS7435 Δ*ku70* strain was engineered to produce cholesterol instead of the native ergosterol in the cellular membranes by replacing the genes *ERG5* and *ERG6* by the *DHCR7* and *DHCR24* genes. During methanol induction conditions, up to 90% of total sterols in this cholesterol strain are actually cholesterol. This study focusses mainly on this strain as it has already shown to be a proper host for the expression of a human membrane protein[52].

1.3 Workflow of this thesis

The different *P. pastoris* strains were transformed with variable N- and C-terminally tagged GPCR constructs under the inducible *AOX1* as well as the constitutive GAP promoter.

To analyze the heterologous expression of the receptors in the total cell lysates as well as in the microsomal fractions, different methods were applied. The 10xHis and StrepII-tags were visualized with immunodetection methods like WB or DotBlot, whereas the eGFP was screened with a fluorescence assay. Cell fractionation and fluorescence microscopy was used to localize the receptor and, finally, also a functional analysis of different receptors was applied.

The aim of this work was to confirm the existing data of the stabilizing effect of cholesterol in the cellular membranes, especially for the β_2AR. Additionally, heterologous GPCR production in *P. pastoris* should be optimized for further analysis, in particular for the C3aR and hB1R. For these two receptors, no crystal structures are currently available. Thus, it was the aim to increase basic knowledge in this field.

2 Materials and methods

2.1 Materials

All used materials, including instruments, reagents, enzymes, antibodies, media, buffers, strains, primers and vectors are listed in this section.

2.1.1 Instruments and devices

Table 2: Instruments for different tasks and the corresponding manufacturer.

Task	Instrument/Device	Manufacturer
Absorption and fluorescence measurement	FLUOstar Omega	BMG Labtech, Germany
	SynergyMx	BioTek Instruments, Inc., USA
	Micro plate, 96-well, PS, F-bottom, clear/ µCLEAR®, black	Greiner bio-one GmbH, Germany
Agarose gel electrophoresis	PowerPacTM Basic + Sub-Cell GT	BIO-RAD, USA
	GelDoc-It (Benchtop 2 UV transilluminator)	UVP, Canada
Cell cultivation	Certomat BS-1	Sartorius AG, Germany
	HT Orbitron	Infors AG, Switzerland
	RS 306	Infors AG, Switzerland
Cell fractionation	MSK Homogenizer	B. Braun Biotech International GmbH, Germany
	Optima LE-80K Ultracentrifuge (70 Ti, SW41 Ti)	Beckman Coulter GmbH, USA
	Optima TLX Ultracentrifuge 120.000 rpm	Beckman Coulter GmbH, USA
	Avanti J-20XP (JA-10, JA-25.50)	Beckman Coulter GmbH, USA
	Hand homogenizer, strong (30 ml)	Sartorius AG, Germany
	Dounce tissue grinder set (Tissue Grind Tube size, Tissue Grind Pstl LC)	Sigma Aldrich, USA
Desalting	MF™ (0.025 µm VSWP)	Merck Millipore, USA
DNA concentration measurement	NanoDrop 2000C Spectrophotometer	Thermo Fisher Scientific, USA
Electrotransformation	Micro Pulser™	BIO-RAD, USA
	Electroporation Cuvettes (2 mm gap)	Biozym Scientific GmbH
Harvest of cells	Tabletop centrifuge 5810, 5810R	Eppendorf, Germany
Imaging of Western Blots	Syngene G:Box	Syngene, UK
Incubation 28°C	BINDER Incubators	Binder GmbH, Germany

Laminar Flow	Gelaire Flow Laboratories BSB 4A	UNIEQUIP, Germany
Magnetic stirrer	MR 3001	Heidolph Instruments, Germany
Microcentrifuge	Centrifuge 5415, 5415R	Eppendorf, Germany
Mixing	Vortex – Genie 2	Scientific Industries Inc., USA
OD_{600} measurement	Bio Photometer	Eppendorf, Germany
	Cuvettes (10 x 10 x 45 mm)	Greiner bio-one GmbH, Germany
Optical microscopy	DM LB2 (HCX PL Fluotar 100x, 1.30 OIL PH 3; filter cubes A, D, I3, N2.1)	Leica microsystems GmbH, Germany
	Ebq100 (100 W mercury)	Leistungselektronik Jena GmbH, Germany
PCR	GeneAmp® PCR System 2700 or 2720	Applied Biosystems, USA
pH measurement	Inolab pH720	WTW, Germany
Pipetting	Pipetman P20, P200, P1000	Gilson, Inc., USA
qPCR	7500 Real Time PCR System	Applied Biosystems, USA
	MicroAmp Optical 96-well Reaction Plate	Applied Biosystems, USA
	Optical Adhesive Covers	Applied Biosystems, USA
	Filter tips (10, 100, 200, 1000)	Greiner bio-one GmbH, Germany
SDS-PAGE and Western Blot	Power Ease 500 Power Supply	Thermo Fisher Scientific, USA
	Mighty Small II Mini Vertical Unit	Amersham Bioscience, Sweden
	TE22 Mini Tank Transfer Unit	Amersham Bioscience, Sweden
	Roti®-NC	Roth GmbH, Germany
	GFL 3013	GFL, Germany
Thermomixer	Thermomixer comfort	Eppendorf, Germany
Weighing	M-prove CP 6201	Sartorius AG, Germany
	Practum®	Sartorius AG, Germany

2.1.2 Reagents

Table 3: Reagents and their supplier.

Reagent	Supplier
Acrylamide 30%	Sigma Aldrich, USA
Agar-Agar Kobe I	Roth GmbH, Germany
Agarose LE	Biozyme, Germany
Albumin Fraction V (BSA)	Roth GmbH, Germany
Ammonium persulfate (APS)	Roth GmbH, Germany
Aqua bidest.	Fresenius Kabi GmbH, Austria
Bacto™ Peptone	Becton, Dickinson and Company, USA
Bacto™ Yeast extract	Becton, Dickinson and Company, USA

Bicine	Roth GmbH, Germany
Biotin	Roth GmbH, Germany
Protein Assay Dye Reagent Concentrate	BIO-RAD, USA
cOmplete™ ULTRA tablets, mini, EASY pack	Roche, Switzerland
D-Glucose	Roth GmbH, Germany
Difco™ Yeast Nitrogen Base w/o Amino Acids	Becton, Dickinson and Company, USA
Dimethylsulfoxyde (DMSO)	Roth GmbH, Germany
Dithiothreitol (DTT)	Roth GmbH, Germany
Di-Potassium hydrogen phosphate	Roth GmbH, Germany
dNTPs	Thermo Fisher Scientific, USA
D-Sorbitol	Roth GmbH, Germany
D-Sucrose	Roth GmbH, Germany
Ethanol	CHEM-LAB NV, Belgium
Ethidiumbromide (EtBr)	Roth GmbH, Germany
Ethylenediamine tetraacetic acid (EDTA)	Roth GmbH, Germany
Gene Jet™ Plasmid Miniprep Kit	Thermo Fisher Scientific, USA
Gene Ruler™ DNA Ladder Mix	Thermo Fisher Scientific, USA
Glass-beads (ø 0.25-0.5 mm)	Roth GmbH, Germany
Glycerol	Roth GmbH, Germany
Glycine	Roth GmbH, Germany
L-Histidine	Roth GmbH, Germany
Hydrochloric acid	Roth GmbH, Germany
Hygromycin B	ForMedium™, United Kingdom
Lambda DNA/HindIII Marker	Thermo Fisher Scientific, USA
LB (Luria Bertani)	Roth GmbH, Germany
Lithiumacetate	Roth GmbH, Germany
Loading Dye 6x	Thermo Fisher Scientific, USA
Magnesium chloride	Roth GmbH, Germany
Methanol (MeOH)	CHEM-LAB NV, Belgium
Milk powder	Roth GmbH, Germany
NAD	Roth GmbH, Germany
PageRuler™ Prestained Protein Ladder	Thermo Fisher Scientific, USA
PEG-8000	Sigma Aldrich, USA
Phenol/Chloroform/Isoamylalkohol 25:24:1	Roth GmbH, Germany
Phenylmethylsulfonyl fluoride (PMSF)	Roche, Switzerland
2x Power SYBR Green Master Mix	Applied Biosystems, USA
Poly-L-Lysine	Sigma Aldrich, USA
PonceauS	Sigma Aldrich, USA
Potassium Chloride	Roth GmbH, Germany
Potassium dihydrogen phosphate	Roth GmbH, Germany
SDS	Roth GmbH, Germany
Sodium acetate	Roth GmbH, Germany
Sodium azide	Sigma Aldrich, USA
Sodium chloride	Roth GmbH, Germany
Sodium hydroxide	Roth GmbH, Germany

SuperSignal West Pico Chemiluminescent Substrate	Thermo Fisher Scientific, USA
TEMED	Roth GmbH, Germany
Trichloroacetic acid	Roth GmbH, Germany
Tris	Roth GmbH, Germany
Triton X-100	Roth GmbH, Germany
Tween 20	Roth GmbH, Germany
Immersion oil	Sigma Aldrich, USA
Wizard® SV Gel and PCR Clean Up System	Promega Corporation, USA
β-Mercaptoethanol	SERVA Electrophoresis GmbH, Germany

2.1.3 Enzymes

Table 4: Enzymes and their supplier.

Enzyme	Supplier
DreamTaq™ polymerase	Thermo Fisher Scientific, USA
FastDigest™ restriction enzymes	Thermo Fisher Scientific, USA
Phusion High-Fidelity DNA Polymerase (2 U/µl)	Thermo Fisher Scientific, USA
Restriction enzymes	Thermo Fisher Scientific, USA
T4 DNA Ligase 3 U/µl	Promega Corporation, USA
Taq DNA ligase 40 U/µl	New England Biolabs, USA
T5 exonuclease 10 U/µl	New England Biolabs, USA
RNAse	Thermo Fisher Scientific, USA
Zymolyase 20T	Seikagaku Biobusiness, Japan

2.1.4 Antibodies

Antibodies are listed in Table 5. The mouse primary monoclonal antibodies (mAB) anti-His and anti-StrepII recognized the 10xHis and StrepII-tag on the N- or C-terminus of the expression constructs, respectively. The rabbit primary antibodies against plasma membrane H^+-ATPase (Pma1p), plasma membrane GPI-anchored β-(1,3)-glucanosyl transferase (Gas1p)[54], a 40 kDa protein of the ER (ER 40 kDa) and the 30 kDa porin of the outer mitochondrial membrane (Por1p) were raised against the proteins of *S. cerevisiae*. HDEL is the ER retention signal and was raised against a synthetic HDEL peptide that represents the C-terminus of yeast BiP[55,56], an ER chaperone. The antibodies directed against *S. cerevisiae* proteins cross-react with their counterparts in *P. pastoris*. The rabbit anti-Aox1p antibody was obtained by immunization with the alcohol oxidase 1 protein of *P. pastoris.*

Table 5: Primary and secondary antibodies, their dilutions, buffers and suppliers.

Primary antibodies	Supplier
Mouse anti-His mAB, (H1029) 1:2500 in 2% BSA-TBST	Sigma Aldrich, USA
Mouse anti-StrepII mAB 1:1000 in 0.2% BSA-PBS-T, (2–1507-001)	IBA GmbH, Germany
Rabbit anti-*S. cerevisiae* Pma1p 1:10000 in 5% TBST-milk	Provided by K. Grillitsch, Institute of Biochemistry, TU Graz
Rabbit anti-*S. cerevisiae* ER 40 kDa 1:5000 in 5% TBST-milk	Provided by K. Grillitsch, Institute of Biochemistry, TU Graz
Rabbit anti-*S. cerevisiae* α–porin 1:1000 in 5% TBST-milk	Provided by K. Grillitsch, Institute of Biochemistry, TU Graz
Rabbit anti-*S. cerevisiae* Gas1p 1:10000 in 2.5% BSA-TBST	Provided by K. Grillitsch, Institute of Biochemistry, TU Graz
Mouse anti-HDEL mAB; (2E7) 1:1000 in 2.5% BSA-TBST	Provided by K. Grillitsch, Institute of Biochemistry, TU Graz; bought at Santa Cruz Biotechnology, Inc.
Rabbit anti-*P. pastoris* Aox1p 1:500 in 5% milk powder	Provided by K. Grillitsch, Institute of Biochemistry, TU Graz
Secondary antibodies	**Supplier**
Goat anti-mouse IgG antibody – HRP (A4416) 1:5000 in 5% TBST-milk	Sigma Aldrich, USA
Goat anti-rabbit IgG antibody – HRP (A9169) 1:5000 in 5% TBST-milk	Sigma Aldrich, USA

2.1.5 Media and Buffers

Table 6: Media, buffers and their composition.

Media/Buffer	Composition
LB, LB-Hyg^{100}	2% LB (+ 1.5% agar, + 100 µg/ml hygromycin)
YPD, YPD-Hyg^{300}	1% yeast extract, 2% peptone, 2% D-glucose (+ 2% agar, + 300 µg/ml hygromycin)
10x YNB	13.4 % yeast nitrogen base with ammonium sulfate without amino acids
10x D-glucose	200 g/l D-glucose
10x Glycerol	100 ml glycerol, 900 ml water
10x Methanol	5 ml methanol, 95 ml water
1 M potassium phosphate buffer, pH 6.0	132 ml of 1 M K_2HPO_4 (174.18 g/L), 868 ml of 1 M KH_2PO_4 (136.09 g/l)
BEDS (10 ml)	1 ml of 0.1 M bicine NaOH (10 x), 300 µl ethylene glycol, 500 µl DMSO, 2 ml 5 M sorbitol, 6.2 ml H_2O
0.1 M Bicine	1.63 g N,N-Bis-(2-hydroxyethyl)-glycine in 100 ml H_2O, with NaOH to pH 8.3
1 M DTT	1.54 g DTT dissolved in 10 ml H_2O
5 M sorbitol	91.1 g sorbitol in 100 ml H_2O

500 x Biotin		0.2 g/l Biotin
MD agar plates		15 g/l agar, 100 ml 10x YNB, 2 ml 500x Biotin, 100 ml 10x D-glucose, 800 ml H_2O
MDH agar plates		15 g/l agar, 100 ml 10x YNB, 2 ml 500x Biotin, 100 ml 10x D-glucose, 10 ml 100 x Histidine, 800 ml H_2O
MMH agar plates		15 g/l agar, 100 ml 10x YNB, 2 ml 500x Biotin, 100 ml 10x Methanol, 10 ml 100x Histidine, 800 ml H_2O
100x Histidine		0.4% L-Histidine
BMGY medium		10 g/l yeast extract, 20 g/l peptone, 100 ml 1 M potassium phosphate buffer pH 6.0, 100 ml 10x YNB, 2 ml 500x Biotin, 100 ml 10x Glycerol, 700 ml H_2O
BMMY medium/agar		10 g/l yeast extract, 20 g/l peptone, 100 ml 1 M potassium phosphate buffer pH 6.0, 100 ml 10x YNB, 2 ml 500x Biotin, 700 ml H_2O, methanol for desired concentration (+ 15 g/l agar)
BMMSY		10 g/l yeast extract, 20 g/l peptone, 100 ml 1 M potassium phosphate buffer pH 6.0, 100 ml 10x YNB, 2 ml 500x Biotin, 700 ml H_2O, 100 ml 1 M sorbitol, methanol for desired concentration
Breaking Buffer, pH 7.4		6 g/l sodium phosphate (monobasic), 372 mg/l EDTA, 50 ml glycerol, 900 ml H_2O, 1 mM PMSF (add freshly)
10x SDS running buffer		28 g/l Tris, 144 g/l Glycine, 10 g/l SDS
20x transfer buffer		29 g/l Tris, 144 g/l Glycine
1x transfer buffer		50 ml 20x transfer buffer, 100 ml methanol, 850 ml H_2O
10x TBS buffer, pH 7.5		30.3 g/l Tris, 87.6 g/l NaCl, adjust pH with HCl
1x TBST buffer		100 ml TBS buffer, pH 7.5, 300 µl Tween-20, fill to 1 l with water
TBST - milk		5 g whey powder per 100 ml 1x TBST
PonceauS staining solution		0.1% PonceauS in acetic acid (5%)
Tris-HCl buffer, pH 6.8		60.5 g/l Tris, adjust pH with HCl
Tris-HCl buffer, pH 8.8		181.7 g/l Tris, adjust pH with HCl
SDS-PAGE sample buffer		780 µl dissociation buffer, 200 µl Tris-HCl buffer, pH 8.8, 20 µl β-mercaptoethanol
SDS-PAGE resolving gel	12.5%	11.3 ml acrylamide (30%), 10.5 ml Tris-HCl buffer (1.5 M, pH 8.8), 6 ml dH_2O, 281.3 µl SDS (10%), 140.6 µl APS (10%), 28.1 µl TEMED
	10%	13.3 ml acrylamide (30%), 10 ml Tris-HCl buffer (1.5 M, pH 8.8), 15.8 ml dH_2O, 400 µl SDS (10%), 400 µl APS (10%), 40 µl TEMED
SDS-PAGE stacking gel (3%)		2.45 ml acrylamide (30%), 4.9 ml Tris-HCl buffer (0.5 M, pH 6.8), 13.9 ml dH_2O, 187.5 µl SDS (10%), 93.8 µl APS (10%), 18.8 µl TEMED

Dissociation buffer		20 mM KH_2PO_4, 6 mM EDTA, 6% SDS, 10% glycine, 0.05% bromophenolblue
TE-buffer		10 mM Tris/HCl, pH 7.5; 1 mM EDTA, 100 mM NaCl, 5% (v/v) glycerol, 1 mM PMSF
Tris/HCl buffer 10 mM, pH 7.4		120 mM NaCl, 10% (v/v) glycerol
SP-A		0.1 M Tris/SO_4, pH 9.4
SP-B		1.2 M sorbitol, 20 mM KH_2PO_4, pH 7.4 with KOH, 1 mM PMSF
Sucrose gradient		20-60% sucrose in TE, 15 mM sodium azide
5x isothermal reaction buffer (ISO)		25% PEG-8000, 500 mM Tris/Cl pH 7.5, 50 mM $MgCl_2$, 50 mM DTT, 1 mM dATP, 1 mM dCTP, 1 mM dGTP, 1 mM dTTP, 5 mM NAD
Gibson assembly master mix		320 µl of 5x ISO reaction buffer, 0.64 µl T5 exonuclease (10 U/µl), 20 µl Phusion® High-Fidelity DNA Polymerase (2 U/µl), 160 µl Taq DNA ligase (40 U/µl), 699.36 µl sterile ddH_2O
Yeast lysis buffer		4 ml Triton X-100, 20 ml of 10% SDS, 4 ml of 5 M NaCl, 400 µl of 0.5 M EDTA, 2 ml of 1 M Tris, pH 8, ddH_2O to 200 ml
DotBlot	Solution I	100 mM Tris 7.0, 1 mM EDTA, 1 mM PMSF
	Solution II	2 M Lithiumacetate
	Solution III	0.2 M NaOH
	Solution IV	4% SDS, 1.25% β-Mercaptoethanol, 5% Glycerin, 20 mM Tris, pH 7.0, 1 mM EDTA

2.1.6 Strains

The GPCRs were cloned and transformed into different *P. pastoris* strains listed in Table 7. The used strains were *P. pastoris* CBS7435 WT Δ*his4* and CBS7435 WT Δ*his4* Δ*ku70*[57], which is deficient for the non-homologous end joining mechanism, making homologous recombination more likely. One strain was the commercially available protease deficient strain *P. pastoris* SMD1168 Δ*his4* Δ*pep4* that is deficient in a major vacuolar aspartyl protease also called protease A[13,47]. The fourth *P. pastoris* strain was the strain that produces cholesterol instead of the native ergosterol (see section 1.2.1).

Additionally, different protease-deficient cholesterol strains were used that were deficient in protease A (Δ*pep4)*, protease B (Δ*prb1)* or both (Δ*pep4* Δ*prb1).*

Later, reference strains, kindly provided by Christoph Reinhart, were compared to the newly created strains. These protease-deficient *P. pastoris* SMD1163 strains have a double knockout of protease A and B and express the β_2AR either to 20 pmol per mg of total membrane proteins (-StrepII-tagged) or to 50 pmol per mg (-biotinylated).

Table 7: Strains, description of their genetic background and source.

Strain	Description	Source
E. coli		
Top10 F'	F'{lacIq Tn10 (TetR)} mcrA Δ(mrr-hsdRMS-mcrBC) Φ80 lacZΔM 15 ΔlacX74 recA1 araD139 Δ(ara-leu)7697 galU galK rpsL endA1 nupG	Life Technologies, Carlsbad, CA
P. pastoris		
WT	CBS7435 Δ*his*	Näätsaari, L. et al.[57]
Δ*ku70*	CBS7435 Δ*his* Δ*ku70*	Näätsaari, L. et al.[57]
SMD1168	*P. pastoris* SMD1168 Δ*his* Δ*pep4*	Life Technologies, Carlsbad, CA
Cholesterol strain	CBS7435 Δ*his* Δ*ku70* Δ*erg5*::pPpGAP-Zeocin™-[*DHCR*7] Δ*erg6*::pGAP-G418[*DHCR*24]	Melanie Hirz, Gerald Richter
Cholesterol strain Δ*prb1*	CBS7435 Δ*his* Δ*ku70* Δ*erg5*::pPpGAP-Zeocin™-[*DHCR*7] Δ*erg6*::pGAP-G418[*DHCR*24] Δ*prb1*	Melanie Hirz
Cholesterol strain Δ*pep4*	CBS7435 Δ*his* Δ*ku70* Δ*erg5*::pPpGAP-Zeocin™-[*DHCR*7] Δ*erg6*::pGAP-G418[*DHCR*24] Δ*pep4*	This study
Cholesterol strain Δ*prb1* Δ*pep4*	CBS7435 Δ*his* Δ*ku70* Δ*erg5*::pPpGAP-Zeocin™-[*DHCR*7] Δ*erg6*::pGAP-G418[*DHCR*24] Δ*prb1* Δ*pep4*	This study
SMD1163 20 pmol/mg	SMD1163 Δ*pep4* Δ*prb1* pPIC9KFlagHis10TevΔGβ_2ARStrepII	Christoph Reinhart
SMD1163 50 pmol/mg	SMD1163 Δ*pep4* Δ*prb1* pPIC9KFlagHis10ΔGβ_2AR-Bio	Christoph Reinhart

2.1.7 Primers

Table 8: Primers for different tasks, their sequences and Tm.

Task	Name	sequence	Tm
Sequencing, cPCR	Fw(seq_pPpHygalpha)	GAAAGAATTCCGAAACG	47°C
	Rv(Seq_pPpHygstrep)	CATCTCTCAGGCAAATG	48°C
Gibson Cloning eGFP-tagged vectors	Fw_GPCR	GCAGGTACCACTGAGCGTCAGAC	70°C
	Rv_TEV-b2AR	**ACCTTGAAAGTACAGGTTTTC**CAGCAG TGAGTCATTTGTACTACAATTCCT	67°C
	Rv_TEV-C3aR	**ACCTTGAAAGTACAGGTTTTC**GCGGCC GCCCACAGTTGTA	72°C
	Rv_TEV-hB1R	**ACCTTGAAAGTACAGGTTTTC**GCGGCC GCCGTTACGC	72°C
	Fw_eGFP-Hyg	TGGATGAATTGTACAAGTAATCAAGAG GATGTCAGAATGC	60°C
	Rv_Hyg	AAGAAGATCCTTTGATCTTTTCTACG	60°C
	Fw_TEV-eGFP	**GAAAACCTGTACTTTCAAGGT**GCTAGC AAAGGAGAAGAACTTTTC	62°C
	Rv_Hyg-eGFP	AAATGGCATTCTGACATCCTCTTGATTA CTT GTA CAA TTC ATC CAT GC	59°C
qPCR	RT_Hyg_fw	GCTTTCAGCTTCGATGTAGGA	62°C
	RT_Hyg_rev	CGATGCAAAGTGCCGATAAAC	62°C
	ARG4-own-F-rtqpcr	GGCAGATGCTTATTCTACTGGA	62°C
	ARG4-own-R-rtqpcr	GGCCCCAAAACATCTACCAGA	64°C
control cPCRs *PEP4* knockout	Fw_5'UTR pep4	ATGATATTTGACGGTACTACGATGT	53°C
	Rv_3'UTR pep4	CTAAATAGACTTGGCTAAACCTACT	52°C
	Fw_upstr_5'UTRpep4	TCCAACAATTCGGTTAGGTGTC	55°C
	Rv downstr_3'UTRpep4	TGTGGGTTAATTGCAGAGCT	54°C
	Fw_seq_pUCori	TCGGAACAGGAGAGCGC	58°C
	Rv_seq_pAOX1	GGGTGTTGAGGAGAAGAGGA	57°C
Gibson cloning pGAP vectors	Fw Hyg-pGAP	CAGTTATTATTCATTTAAATTTTTTGTAG AAATGTCTTGGTGTCCTCGTC	71°C
	Rv alpha-pGAP	ATCTCATCGTTTCGGAATTCTGTGTTTTG ATAGTTGTTCAATTGATTGAA	67°C
	Fw pGAP-GPCR	TGAACAACTATCAAAACACAGAATTCCG AAACGATGAGATTCC	66°C
	Rv GPCR	GCTCGTACGAGAAGAAACAA	60°C
	Fw Hyg	CCTATATAGTATAGGATTTTTTTTGTCAT T	59°C
	Rv pGAP-Hyg	CCAAGACATTTCTACAAAAAATTTAAAT GAATAATAACTGTGTATTTTTC	58°C

underlined: binding regions on vector (region for Tm calculation), **bold**: TEV sequence

2.1.8 Vectors

Table 9: Vectors, their description and source.

Name	Description	Source
pPpHygαHisGPCRStrepII	Hyg-marker, P_{AOX1}, N-term 10xHis-tag, C-term StrepII-tag	Anita Emmerstorfer-Augustin
10pPpRSFCMFαCeGFP	eGFP	Mudassar Ahmad
pPpHygαHisGPCRTeveGFP	Hyg-marker, P_{AOX1}, N-term 10xHis-tag, C-term eGFP	This study
pHGKTef1Swa_ScKex2_FLAG	P_{GAP}	Melanie Hirz
pPpHygpGAPαHisGPCRStrepII	Hyg-marker, P_{GAP}, N-term 10xHis-tag, C-term StrepII-tag	This study
pPpHygpGAPαHisGPCRTeveGFP	Hyg-marker, P_{GAP}, N-term 10xHis-tag, C-term eGFP	This study
pPpKC3	*HIS4*-marker	Mudassar Ahmad
pPpKC1_pep4	5'/3' UTR of *PEP4*	Mudassar Ahmad
pPpKC3_pep4	*HIS4*-marker, 5'/3' UTR of *PEP4*	This study

The cDNAs of the GPCRs were kindly provided by Christoph Reinhart (Max-Planck Institute for Biophysics, Frankfurt). The vector pPpHyg and the GPCR cDNA fragments were assembled by Gibson cloning and sequenced afterwards. In the first vector constructs (Figure 7A, β_2AR shown as example), the GPCRs were encoded with an N-terminal His 6-10x-tag and a C-terminal StrepII-tag, that consists of the eight amino acid residues Trp-Ser-His-Pro-Gln-Phe-Glu-Lys[58]. This was to detect the receptor at both ends via specific antibodies. The vectors were linearized with *SwaI* (=*SmiI*) prior to transformation to enable integration into the genome. In the second vector construct (Figure 7B, β_2AR shown as example) the C-terminal StrepII-tag was replaced by a TEV protease cleavage site and an eGFP in order to detect the expressed receptor via a fluorescence signal.

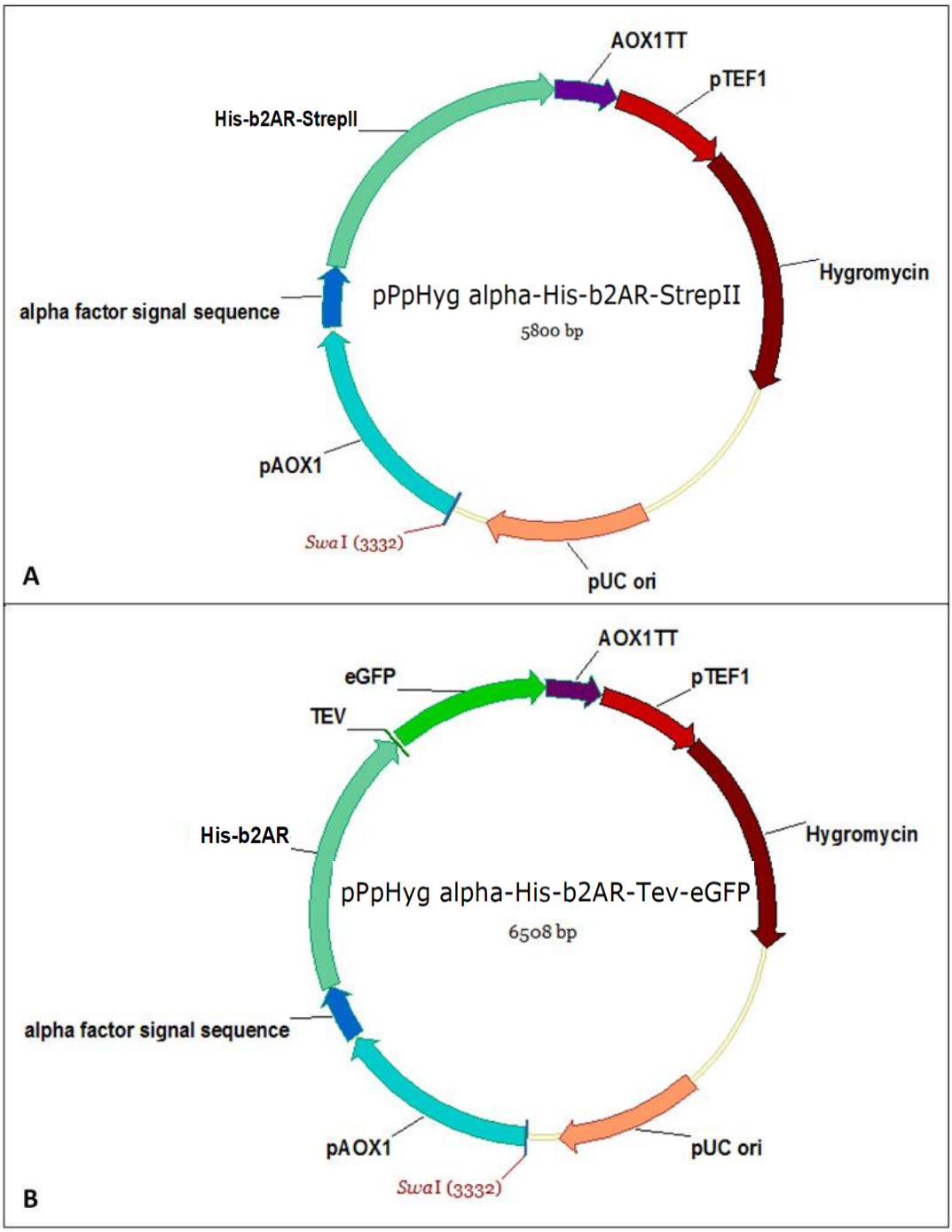

Figure 7: pPpHygαHisβ_2ARStrepII and pPpHygαHisβ_2ARTeveGFP vectors. They encode β_2AR with an N-terminal His 6-10x-tag and a C-terminal StrepII-tag (7A) or a C-terminal eGFP and a TEV protease cleavage site (7B). The following genetic elements were employed: the inducible P_{AOX1} for expression, the α-mating factor signal sequence of *S. cerevisiae* for plasma membrane targeting, the *AOX1* terminator for transcription termination, the hygromycin resistance gene under the constitutive *TEF1* promoter for selection in *P. pastoris* and *E. coli,* the pUC origin for replication in *E. coli* and a *SwaI* (=*SmiI*) linearization site.

The third vector construct contained the constitutive GAP promoter instead of the inducible *AOX1* promoter. These vectors were once assembled with the C-terminal StrepII-tag (Figure 8A) and once with the C-terminal eGFP (Figure 8B).

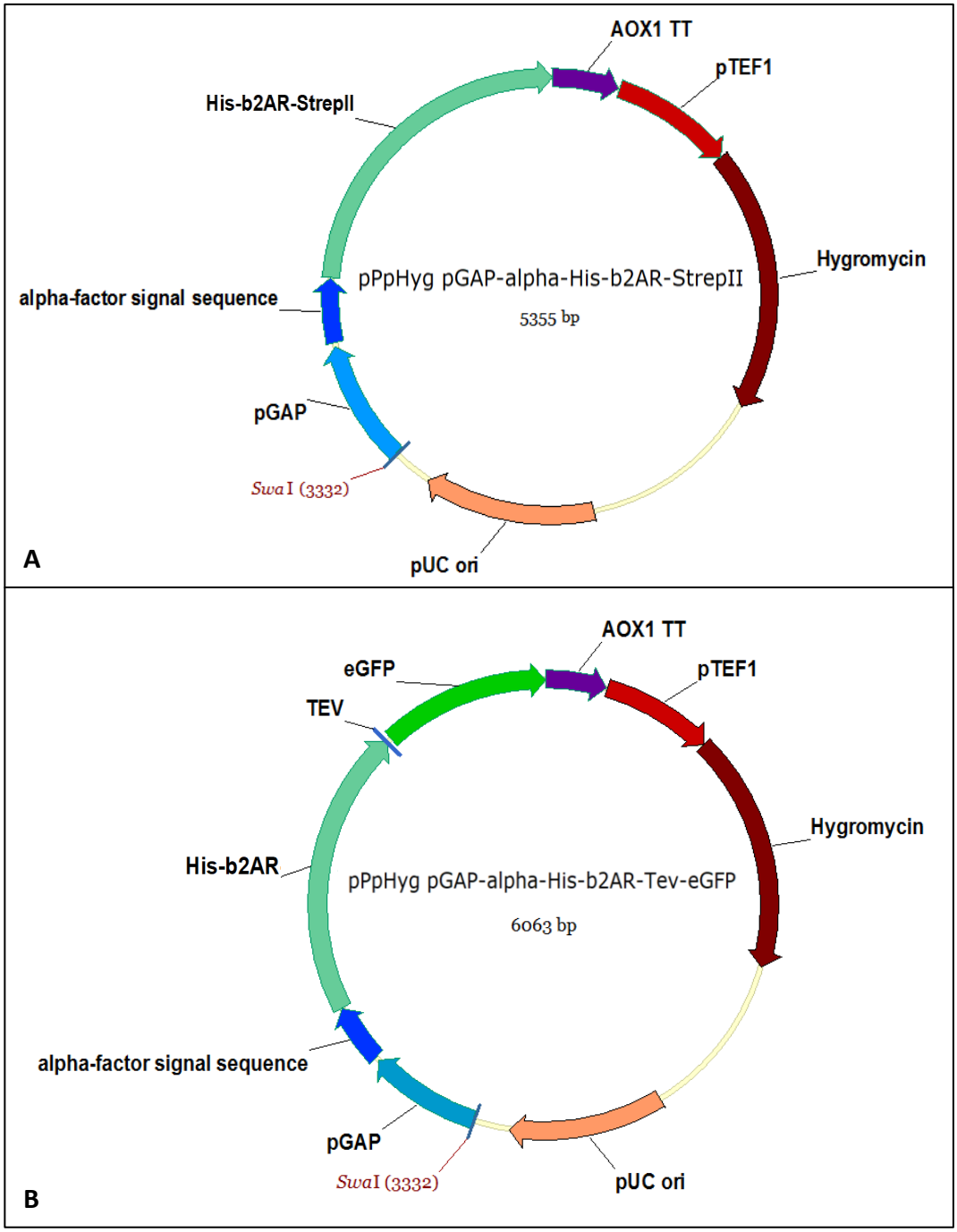

Figure 8: (A) pPpHygpGAPαHisβ_2ARStrepII vector; (B) pPpHygpGAPαHisβ_2ARTeveGFP vector. The inducible *AOX1* promoter was replaced by the constitutive GAP promoter. Otherwise, the genetic elements were as described in Figure 7.

The vector pPpKC3_pep4 was constructed for the knockout of the *PEP4* gene of *P. pastoris* (Figure 9). It contains the 5' and 3' untranslated regions (UTRs) of the *PEP4* gene flanked by FRT sites which are recognized by the FLP recombinase under the inducible *AOX1* promoter and the *AOX1* terminator for the recycling of the marker gene. The start (ATG) and stop-codon of the *PEP4* gene were marked too. The *HIS4* gene was used as selection marker under the control of a constitutive *ARG4* promoter and the *ARG4* terminator. An ampicillin resistance gene and a pUC origin of replication are responsible for the selection and replication in *E. coli*. The *SfiI* restriction sites were used for the cloning and the *SmaI* restriction site for linearization of the vector.

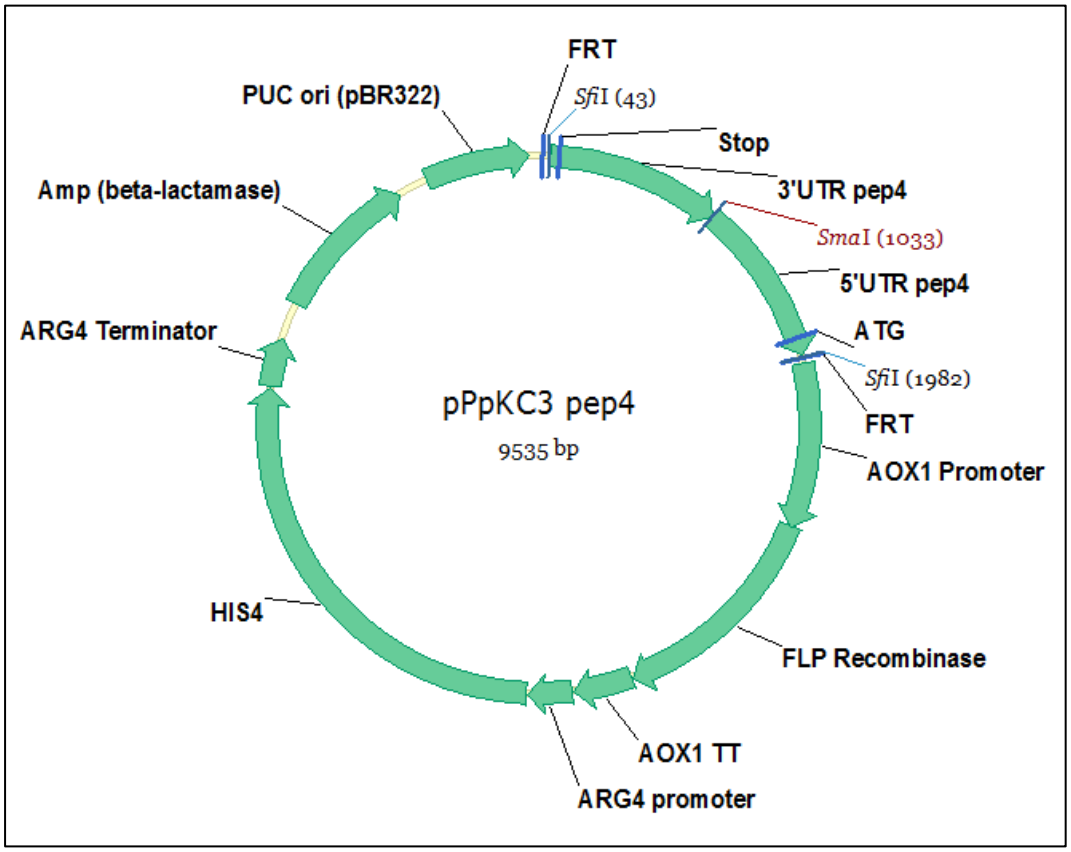

Figure 9: pPpKC3_pep4 vector. It contains the 5' and 3' UTRs of the *PEP4* gene, two FRT sites recognized by the FLP recombinase under the inducible *AOX1* promoter for marker recycling, the *HIS4* gene as selection marker under the constitutive *ARG4* promoter, an ampicillin resistance gene for selection and a pUC origin for replication in *E. coli*, *SfiI* restriction sites for cloning and the *SmaI* resctriction site for linearization.

2.2 Methods

2.2.1 General methods

2.2.1.1 DNA visualization and quantification

Agarose gel electrophoresis was performed by mixing 1% agarose, 1x TAE buffer and some µl of 1% EtBr. Control gels were run for 45 min at 120 V, for preparative gels 120 min at 90 V in 1x TAE buffer. As standards, five µl of the GeneRuler™ DNA Ladder Mix and, for gDNA samples, the Lambda DNA/HindIII Marker (Figure 10) were loaded. For DNA quantification, 1 µl was applied to a NanoDrop 2000C spectrophotometer.

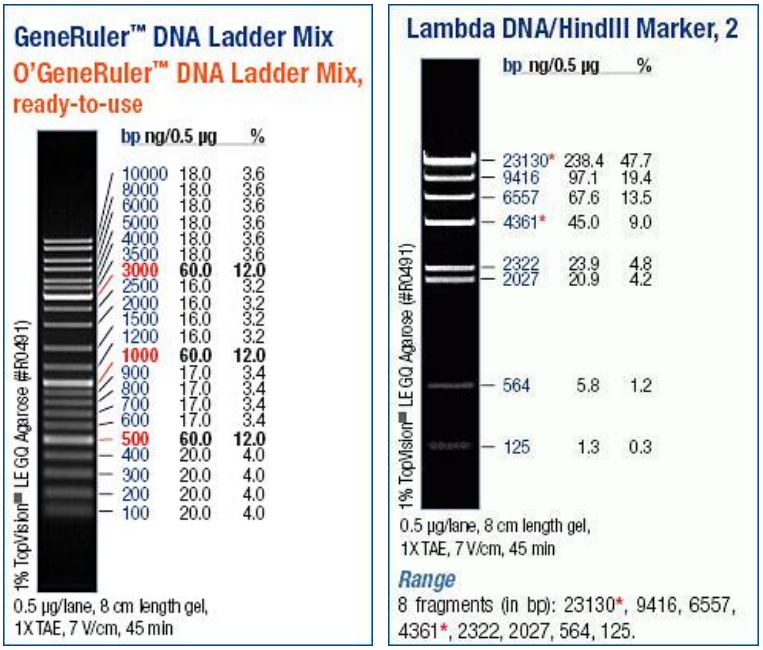

Figure 10: GeneRuler™ DNA Ladder Mix and Lambda DNA/HindIII Marker were used as standards for agarose gel electrophoresis.

2.2.1.2 DNA purification

DNA was purified from agarose gels, PCR or restriction reactions via the Wizard® SV Gel and PCR Clean Up System. The DNA was eluted in 30 µl of ddH_20.

2.2.1.3 Plasmid DNA isolation from *E. coli*

The isolation of plasmid-DNA from freshly streaked *E. coli* was done with the Gene Jet™ Plasmid Miniprep Kit. In order to pellet cell debris and chromosomal DNA, the lysate was centrifuged for 10 min. DNA was eluted in 50 µl ddH_20.

2.2.1.4 DNA restriction

After Gibson assembly, several plasmids were isolated and analyzed for right fragment sizes via restriction analysis.

3-5 µl plasmid (depending on concentration)
1 µl *SacI* FD
1 µl *PstI* FD
2 µl 10x FD green buffer
x µl ddH_20 (to 20 µl)
---
20 µl total

The mixture was incubated at 37°C for about 30 min, and then loaded onto a control agarose gel to visualize the fragments.

2.2.1.5 Vector linearization

For transformation into electrocompetent *P. pastoris* cells, the expression vector was linearized with *SwaI* (=*SmiI*) to facilitate integration into the genome.

10-16 µl plasmid (depending on concentration)
2 µl *SmiI* FD
2 µl FD 10x buffer
x µl H_20 (to 20 µl)
---
20 µl total

The mixture was incubated at 37°C for about 30-60 min depending on the plasmid concentration, inactivated for 15 min at 65°C and then purified using the Wizard® SV Gel and PCR Clean Up System. One µl of the linearized vector was loaded onto an agarose gel to check the integrity of the DNA and complete linearization by comparing the band of the cut vector to an uncut control vector. The DNA concentration was measured by the NanoDrop 2000C spectrophotometer.

2.2.1.6 Sequencing

Ten µl vector DNA with a concentration of about 100 ng/µl were mixed with 4 µl of 5 µM sequencing primer and were sent for sequencing to LGC Genomics GmbH, Berlin, Germany. Sequence files were evaluated with SnapGene Viewer 3.3.1 and the LALIGN tool of the website FASTA Sequence Comparison at the University of Virginia.

2.2.1.7 Transformation of electrocompetent *E. coli* cells

Eighty µl of electrocompetent *E. coli* cells were mixed with 50-100 ng DNA. After 2 min of incubation on ice, cells were transferred to electroporation cuvettes and pulsed in the Ec.2 mode for 5-6 ms at 2.5 kV. After the pulse, 1 ml of LB media was added to the cells. The regeneration was done for 30 min at 37°C and 500 rpm. Then, cells were plated onto LB agar containing the proper antibiotic and were incubated at 37°C overnight.

2.2.1.8 Transformation of electrocompetent *P. pastoris* cells

Generally, the condensed protocol from Lin-Cereghino et al. (2005)[59] was used. To ensure the right OD_{600} for the transformation, the 5 ml ONC was used to inoculate a 50 ml YPD main culture to an OD_{600} of 0.01 for overnight cultivation. Eighty µl of competent *P. pastoris* cells were mixed with 1.5 µg of linearized DNA. Cells were regenerated for 2 h at 28°C before 100 µl and the rest of the cell suspension were plated on YPD hygromycin. They were incubated at 28°C for at least two days or until colonies appeared.

2.2.1.9 Preparation of SDS-PAGE gels

The resolving gel (Table 6) was poured, covered with n-butanol and polymerized for at least 1 h. Then, n-butanol was washed away with ddH_2O and the residual water was removed by filter papers. The stacking gel (Table 6) was poured on top, the combs were placed into it and polymerized for at least 30 min. The gels were stored at 4°C or used immediately.

2.2.1.10 Preparation of glycerol stocks

The strains were grown in 5 ml YPD for 24-48 h. 500 µl of 50% glycerol were mixed with 1 ml of the cell suspension and frozen at -80°C.

2.2.2 Colony PCR

P. pastoris transformants were streaked out freshly on YPD with 300 µg/ml hygromycin or MD agar, respectively, and grown at 28°C for 2-3 days. Some cell material was resuspended in 20 µl ddH_2O. The cells were frozen for 10-15 min at -20°C and then incubated for 10 min at 95°C. The pellets were centrifuged for 2 min at max. speed and 1.5 µl of the supernatant were used for cPCR. The reaction was set up as follows:

1.5 µl colony supernatant
1.25 µl forward primer
1.25 µl reverse primer
5 µl 5x GoTaq Buffer Green
0.5 µl dNTPs (10 mM)
0.25 µl DreamTaq Polymerase
15.25 µl ddH_2O
25 µl total

95°C	4 min	
95°C	30 s	35 cycles
50-70°C	30 s	
72°C	1 min/kb	
72°C	7 min	
4°C	∞	

Figure 11: PCR program for cPCR.

For the negative controls or no template controls, the *P. pastoris* CBS7435 WT strain was used as well as another set-up which contained ddH_2O instead of the template.

2.2.3 Determination of possible multiple integration events

DWPs with 300 µl YPD were inoculated with different clones and were cultivated for 48 h at 28°C and 320 rpm. The cells were pinned onto YPD agar with increasing hygromycin concentrations of 300 µg/ml, 500 µg/ml, 1000 µg/ml, 2000 µg/ml and 4000 µg/ml.

In addition, the strains were streaked onto YPD agar plates with 300 µg/ml and 4000 µg/ml hygromycin. For the negative control, the *P. pastoris* CBS7435 WT strain without transformation was streaked onto the YPD agar.

2.2.4 Determination of Mut+/MutS phenotype

For the determination of either Mut+ or MutS phenotypes, the strains were streaked onto MDH and MMH agar plates and grown at 28°C until differences were visible.

2.2.5 Cultivation of *P. pastoris*

2.2.5.1 96-well DWP

For cultivation with transformants expressing under the *AOX1* promoter, wells were filled with 250 µl BMGY, inoculated with single colonies and grown for 48-72 h. The induction was done by adding 250 µl BMMY(1%) initially, and by adding further 50 µl BMMY(10%) every 8 or 16 h. After 48 h of induction the cells were analyzed.

P_{GAP} cultivation was done in 300 µl YPD or BMGY media. After 48-72 h of growth, another 300 µl YPD or BMGY were added, cells were further grown for 24 h and then were used for further steps.

2.2.5.2 300 ml shake flasks

Cultivation was started by inoculating a 5-10 ml ONC in YPD which was grown for 24-48 h. The main culture of 25 ml BMGY in 300 ml Erlenmeyer flasks was then inoculated to an OD_{600} of 0.05 (WT, Δ*ku70*, SMD1168 strains) or 0.2 (cholesterol strain). The cells were grown for 72 h and were induced by adding 25 ml BMMY(2%). Induction was continued daily in the mornings and evenings over 72 h by adding 500 µl of 100% methanol or 2.5 ml BMMY(10%). Samples were taken after 0, 8, 24, 48 and 72 h, centrifuged and cell pellets were stored at -20°C.

2.2.5.3 2 l shake flasks

After growing the cells in a 5 ml ONC in YPD, a 2 l shaking flask with 100 ml BMGY was inoculated to an OD_{600} of 0.1 (WT, Δ*ku70*, SMD1168 strains) or 0.3 (cholesterol strain), respectively. Cells were grown for 72 h and were then induced by adding 100 ml BMMY(2%). Induction was continued over 48 h by adding 10 ml BMMY(10%) daily in the morning and in the evening.

2.2.6 Protein isolation

2.2.6.1 Glass bead-disruption

2.2.6.1.1 Small scale

One ml samples taken from cultivations were centrifuged for 10 min at 13,200 rpm and 4°C. The supernatants were discarded. The pellets, which were always kept on ice, were resuspended in 200 µl of ice-cold Breaking Buffer containing freshly added 1 mM PMSF and were vortexed vigorously. An equal volume of glass-beads (0.25 - 0.5 mm) was added and the cells were disrupted in 8 subsequent 30 s long vortexing and cooling steps. The cell debris was centrifuged at 5000 rpm for 10 min at 4°C, and the clear supernatant was transferred into a fresh microcentrifuge tube. For further isolation of total microsomes the residual glass beads were washed with 200 µl breaking buffer.

2.2.6.1.2 Large scale

Two-hundred ml of cell cultures were centrifuged at 5000 rpm for 5 min at 4°C. The supernatant was discarded and the pellets were washed with ice-cold deionized water. The cells were again centrifuged at 5000 rpm for 5 min at 4°C. Then, the cell wet weight (CWW) was determined. The pellet was resuspended in approximately 5 ml TE-Buffer with 1 mM PMSF. The suspension was transferred into a Merckenschlager vessel that finally contained 1/3 glass beads, 1/3 cell suspension and 1/3 air. The Merckenschlager vessels were pre-cooled with CO_2 and the cells were disrupted for 4 min with CO_2 cooling every 30 s. The cell lysate without glass beads was transferred into a centrifugation vessel with caps for the JA 25.5 rotor and were centrifuged at 5000 x g for 10 min at 4°C to remove unbroken cells, cell debris and residual glass beads. The resulting supernatant represented the homogenate.

2.2.6.2 Disruption via spheroplasting using a Dounce Homogenizer

Cells were harvested by centrifugation at 3000 x g for 5 min, washed with water and resuspended at 0.5 g cell wet weight per ml in SP-A buffer containing 10 mM DTT. Cells were incubated for 10 min at 28°C while shaking. The cell pellet was washed with SP-B buffer and was resuspended in pre-warmed SP-B at 0.15 g CWW per ml. Cells were then converted to spheroplasts using 2 mg zymolyase per g CWW and incubating for at least 60 min at 28°C with shaking. Spheroplasts were harvested by centrifugation at 3000 x g and 4°C for 5 min and

washed twice with SP-B. For homogenization, spheroplasts were resuspended in 15 ml of ice-cold SP-B containing 1 mM PMSF and ¼ of a protease inhibitor tablet and were homogenized with 15 strokes in a tight-fitting pestle Dounce Homogenizer. The homogenous suspension was centrifuged for 5 min at 3000 x g and 4°C. The resulting pellet was resuspended in 10 ml of the same buffer, homogenized and centrifuged again. After centrifugation, both supernatants were pooled to form the homogenate.

2.2.7 Cell fractionation

2.2.7.1 Isolation of total microsomes

2.2.7.1.1 Small scale

The lysate was centrifuged for 1 h at 100,000 x g in a Beckman TLX 120,000 ultracentrifuge at 4°C. The small microsome pellet was resuspended in 50 µl Tris-HCl buffer. Three-hundred fifty µl water and 100 µl of ice-cold 50% TCA were added and the proteins were precipitated over night at 4°C.

2.2.7.1.2 Large scale

The homogenate was transferred into ultracentrifugation vessels and centrifuged at 45,000 rpm for 1 h at 4°C in a 70Ti fixed angle rotor. The resulting supernatant represented the cytosolic fraction, the pellet contained the total microsome fraction and was resuspended in 2 ml Tris-HCl buffer.

2.2.7.2 Sucrose gradient

Cells were cultivated in 2 l flasks, cell lysis was done by spheroplasting and the resulting homogenate was ultracentrifuged in a 70Ti fixed angle rotor for 45 min at 45,000 rpm and 4°C. The supernatant that contained the cytosolic fraction was preserved for further analysis. The microsomal pellet was resuspended in 1-2 ml TE buffer containing 1 mM PMSF and was loaded onto a sucrose gradient. The gradient had been formed by pipetting 1 ml of each sucrose solution one after the other in the proper centrifugation vessel for the SW41Ti swing-out rotor. The gradient started with 60% sucrose at the bottom and consisted of 5% steps up to 20% sucrose. After centrifugation in a SW41Ti swing-out rotor for 16 h at 34,000 rpm and 4°C,

1 ml fractions were taken from the top of the gradient and were used for further analysis of the proteins.

2.2.8 Determination of protein concentration with a Bio-Rad Assay

For the calibration curve, 20 mg of bovine serum albumin (BSA) were dissolved in 10 ml ddH_2O to obtain a concentration of 2 mg/ml. Serial dilutions were done with water to obtain 1 mg/ml, 0.5 mg/ml, 0.25 mg/ml, 0.1 mg/ml and 0.05 mg/ml. Ten µl of the different dilutions were placed into a 96-well microtiter plate as well as 10 µl ddH_2O which was used as blank. The total cell lysate samples were diluted 1:10 with ddH_2O. Ten µl of the dilutions were placed into the microtiter plate. One part of Bio-Rad reagent was mixed with four parts of ddH_2O and 200 µl of the mixture were then added to the samples in the microtiter plate. All measurements were performed in triplicates. The absorption at 595 nm was measured with the plate reader after an incubation time of about 10 min at RT.

2.2.9 TCA precipitation

For protein precipitation, 400 µl ice-cold ddH_2O were placed in a microcentrifuge tube. A defined amount of protein, usually 100 µg, calculated from the Bio-Rad Assay, was added to the water. Then, 100 µl of ice-cold 50% TCA were added, vortexed briefly and incubated for at least 1 h on ice for protein precipitation. The proteins were pelleted for 10 min at 13,200 rpm and 4°C, and the supernatants were discarded. The pellets were washed with 500 µl ice-cold water, centrifuged for 5 min at 13,200 rpm and 4°C, and the supernatants were discarded again. The pellets were resuspended in 50 µl SDS sample buffer and 10-15 µl were loaded onto a SDS gel. The thermal denaturation of the protein samples was omitted in order to decrease aggregation phenomena.

2.2.10 SDS-PAGE

For SDS-PAGE, 5 µl of the PageRuler™ Prestained Protein Ladder (Figure 12), a positive control as well as 10-15 µl of the samples were loaded onto the gel, corresponding to 20-30 µg protein. The chamber of the Mighty small II cassette was filled with 1 x SDS running buffer and the running conditions for electrophoresis were set to 35 mA, 125 V and 35 W for 90 min.

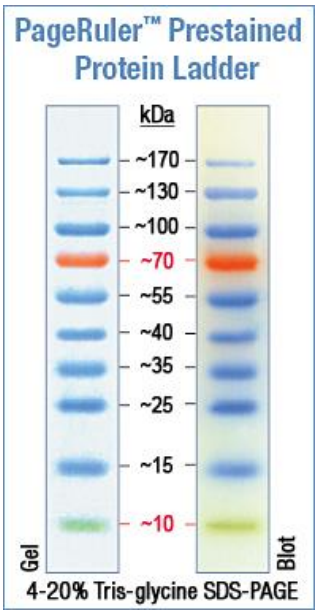

Figure 12: PageRuler™ Prestained Protein Ladder was used as standard for SDS-PAGE

2.2.11 Western Blot & Immunodetection

The SDS-PA gels were blotted onto nitrocellulose membranes with a Hoefer™ TE22 Mini Tank Blotting Unit. The Sandwich was built up as shown in Figure 13 and the inner chamber was filled with 1 x transfer buffer. The blotting conditions were set to 500 V, 500 mA, 50 W and the transfer was performed for 90 min while stirring. After blotting, the membrane was stained with PonceauS to prove transfer efficiency and uniform loading and was destained with 1xTBST before immunodetection.

Figure 13: Setup of Western Blot.

For immunodetection, the membrane was blocked with 5% milk powder in 1 x TBST for 1 h at RT with moderate shaking and was then rinsed with 1 x TBST. The membrane was incubated with the primary antibody solution overnight at 4°C with moderate shaking. The next day the membrane was washed three times with 1 x TBST buffer for 10 min with moderate shaking. The secondary antibody solution was added to the membrane and moderately shaken for 1 h

at RT. The membrane was washed again twice for 10 min. The enhancer solution and the peroxide solution from the "SuperSignal West Pico Chemiluminescent Substrate" detection Kit were mixed in a 1:1 ratio and protected from sunlight. The membrane was incubated with 1.5 ml of the mixed solution and the chemiluminescent signal was then captured with the G:BOX Bioimaging System.

2.2.12 Quantitative PCR

2.2.12.1 gDNA isolation from *P. pastoris*

The isolation of gDNA was adapted from the protocol of Hoffman and Winston [60]. A 10-15 ml ONC was grown in YPD at 28 °C. The next day cells were spun down for 5 min at 500 rpm. The supernatant was discarded, the cell pellet was resuspended in 0.5 ml sterile distilled water and spun down for 1.5 min in the Eppendorf centrifuge at maximum speed (13,200 rpm). The supernatant was taken off and the cell pellet was resuspended in 200 µl of Yeast lysis buffer. Then, 200 µl phenol:chloroform:isoamyl alcohol (25:24:1) and 0.3 g of acid-washed beads were added and vortexed for 8 min. Two-hundred µl TE buffer were added and spun for 5 min in a microfuge at 13,200 rpm. The aqueous phase was transferred to a new tube, 1 ml of ice-cold 100% EtOH was added and mixed by inversion. DNA was precipitated for 30 min at -20°C and then spun out for 5 min at 4°C in a microfuge. The supernatant was taken off, the pellet was air-dried at 60°C, resuspended in 400 µl TE buffer and 5 µl RNAse A (10 mg/ml) and was incubated at 37°C for more than two h. Then, 10 µl of 3 M sodium acetate and 1 ml of ice-cold 100% EtOH were added, mixed by inversion and DNA was precipitated overnight at -20°C. DNA was collected by spinning for 5 min at 4°C in a microfuge, the supernatant was taken off and the pellet was washed with 1 ml of 70% EtOH. The pellet was air-dried at 60°C and resuspended in 50 µl of ddH_20.

2.2.12.2 Determination of DNA concentration and purity

gDNA concentration was determined by the NanoDrop 2000c spectrophotometer. Ratios for 280 nm/260 nm and 260 nm/230 nm should be higher than 1.8. Additionally, 2 µl of the gDNA samples were loaded onto an agarose gel and were checked for integrity of the gDNA. Samples were stored at 4°C.

2.2.12.3 Control PCR of gDNA

Prior to qPCR, a control PCR of the isolated gDNA was done in order to check if expected PCR products were formed. The components for one PCR reaction were:

Maxima Hot Start Green PCR Master Mix (2X)	12.5 µl
10 µM Forward Primer	0.5 µl
10 µM Reverse Primer	0.5 µl
Template DNA	ca. 1 µl (5 ng)
Nuclease-free water	10.5 µl
	25 µl total

Two primer pairs were used to amplify the target and the reference gene (Table 10, Figure 14).

Table 10: Primer for the amplification of the target and reference gene and the PCR product size.

	Primer	PCR product size
Target gene	RT_Hyg_fw RT_Hyg_rev	102 bp
Reference gene	ARG4-own-F-rtqpcr ARG4-own-R-rtqpcr	100 bp

95°C	4 min	
95°C	30 s	30 cycles
57°C	30 s	
72°C	30 s	
72°C	7 min	
4°C	∞	

Figure 14: PCR program for control PCR of gDNA.

2.2.12.4 Quantitative PCR

Quantitative PCR was largely performed according to the protocol described by Abad et al. (2010)[61] . Details were adapted from the Master thesis of Anja Schiefer[62]. The hygromycin marker was used as target gene for the determination of the copy number and the *ARG4* gene was used as housekeeping gene in *P. pastoris* with one copy in the genome. The WT strain #4 expressing β_2AR-StrepII was used as reference strain as it was assumed that it had only one copy of the expression cassette integrated due to a lack of signals in the WB analysis.

All gDNA dilutions were done in a final volume of 200 µl. The calibration curve was done with the reference strain. The starting concentration was 11 ng/µl which was then further diluted in 1:3 steps to reach the lowest concentration of 0.033 ng/µl. The other strains were diluted to 0.66 ng/µl.

The PCR mixture for one reaction is shown in the following. This mixture was done once for the *ARG4* primers and once for the Hyg primers.

2x Power SYBR Green Master Mix	20 µl
Forward primer 5 µM	2 µl
Reverse primer 5 µM	2 µl
ddH_2O	12 µl
Template gDNA	6 µl
	42 µl

From this master mix of 42 µl two times 19 µl aliquots were taken and placed into two wells of the qPCR reaction plate to perform double measurements. The wells on the edge of the plates were not used. The reaction plates were covered with an optical adhesive cover and centrifuged for 1 min at 4000 rpm and 4°C to remove air bubbles.

The qPCR thermocycler profile was set up as shown in Figure 15.

Holding stage	95°C	10 min
Cycling stage (40 cycles)	95°C	15 s
	60°C	1 min
Melt Curve stage	95°C	15 s
	60°C	1 min
	in 1% steps to 95°C	30 s per step
	60°C	15 s

Figure 15: PCR program for qPCR that included 40 cycles of product amplification and a melting curve stage.

2.2.12.5 Calculation of copy number

Equation 1 was chosen to calculate the copy quantity. The genome size of *P. pastoris* CBS7435 of 9.4 Mb[48] was taken for calculation and the resulting copy quantity of a single copy gene in 1 ng of *P. pastoris* gDNA is about 97,066 copies.

Equation 1: Calculation of the copy quantity of the target gene in a certain amount of genomic DNA (gDNA). N = size of gDNA in bp, m = mass, DNA amount in gram, Avogadro's number = 6.02×10^{23} copies/mol, average molecular weight of a dsDNA molecule = 660 g/mol/bp

$$DNA\ (copy\ quantity) = \frac{6.02 \times 10^{23} (copy/mol) \times m\ (g)}{n\ (bp) \times 660\ (g/mol\ /bp)}$$

For the calculation of the copy number, the standard deviations should be lower than 0.5 and the non-template control should be negative. Absolute and relative quantification was performed to calculate the copy number of the target gene. The absolute quantification used the following equation 2 from Lee, C et al. (2006)[63]:

Equation 2: Calculation of the copy number with absolute quantification.

$$Copy\ number_{TARGET\ GENE} = \frac{Copy\ quantity_{TARGET\ GENE}}{Copy\ quantity_{REFERENCE\ GENE}}$$

The relative quantification was implemented on the basis of the $2^{-\Delta\Delta Ct}$ method described by Livak and Schmittgen (2001)[64]. For comparison, a second method for relative quantification from Pfaffl M.W. (2001) was applied[65].

2.2.13 Assembly of pPpHygαHisGPCRStrepII vectors

The construction of the starting vectors pPpHygαHisGPCRStrepII was done by Anita Emmerstorfer-Augustin via Gibson Assembly. Transformants were checked for integration of the expression cassette via cPCR, several clones per strain were cultivated, protein expression was induced and the proteins were analyzed via WB and detected with anti-His or anti-StrepII antibodies.

2.2.14 Cloning of eGFP-tagged GPCRs

The cloning was done by Gibson Cloning Protocol #122[66,67]. As starting points, the vectors pPpHygαHisGPCRStrepII, the eGFP containing 10pPpRSFC-MFalpha-C-eGFP vector as well as the corresponding primers (Table 8) were used. The fragments were amplified using Q5 high-fidelity DNA Polymerase and 2 ng of template DNA as described in the manual. The PCR program and setup are shown in Figure 16 and Table 11.

98°C	30 s	
98°C	10 s	30 cycles
60-72°C	30 s	
72°C	1-2 min	
72°C	7 min	
4°C	∞	

Figure 16: PCR program for amplification of fragments with Q5 polymerase.

Table 11: PCR setup for cloning of eGFP-tagged GPCRs.

	Template	Primers	Fragment size	Extension time	Annealing temperature
GPCR-fragments	pPpHygαHisβ_2AR-StrepII	Fw_GPCR Rv_TEV-b2AR	3312 bp	2 min	70°C
	pPpHygαHisC3aR-StrepII	Fw_GPCR Rv_TEV-C3aR	3594 bp	2 min	72°C
	pPpHygαHishB1R-StrepII	Fw_GPCR Rv_TEV-hB1R	3207 bp	2 min	72°C
Hyg-fragment	pPpHygαHisβ_2AR-StrepII	Fw_eGFP-Hyg Rv_Hyg	2550 bp	1 min 30 s	63°
eGFP-fragment	10pPpRSFC-MFalpha-C-eGFP	Fw_TEV-eGFP Rv_Hyg-eGFP	763 bp	1 min	62°C

The PCR fragments were loaded onto a preparative agarose gel, purified and assembled to the final vectors pPpHygαHisGPCRTeveGFP using 50 ng of the smallest fragment. After transformation into *E. coli*, vectors were isolated, verified by restriction enzyme digestion with *SacI* and *PstI* and sent to sequencing. Correct vectors were linearized with *SmiI* and transformed into *P. pastoris* strains. Transformants were directly used for inoculation of DWPs and screened for fluorescence signals.

2.2.15 Cloning of GPCRs under P_{GAP}

The cloning was again done by Gibson assembly. As starting point, the vectors pPpHygαHisGPCRStrepII and pPpHygαHisGPCRTeveGFP, the P_{GAP} containing pHGKTef1Swa_ScKex2_FLAG vector as well as the corresponding primers (Table 8) were used. The fragments were amplified using Phusion DNA Polymerase, 5x Phusion HF buffer and about 3 ng of template DNA as described in the manual. The PCR program and setup is shown in Figure 17 and Table 12.

98°C	30 s	
98°C	10 s	⎫
60-70°C	30 s	⎬ 30 cycles
72°C	30 s -1 min 45 s	⎭
72°C	7 min	
4°C	∞	

Figure 17: PCR program for amplification of fragments with Phusion DNA Polymerase.

Table 12: PCR setup for cloning of GPCRs under P_{GAP}

	Template	Primers	Fragment size	Extension time	Annealing temperature
GPCR-fragments	pPpHygαHisβ$_2$AR-StrepII	Fw pGAP-GPCR Rv GPCR	1674 bp	1 min 30 s	60°C
	pPpHygαHisC3aR-StrepII		1956 bp	1 min 30 s	
	pPpHygαHishB1R-StrepII		1569 bp	1 min 30 s	
	pPpHygαHisβ$_2$AR-TeveGFP		2382 bp	1 min 30 s	
	pPpHygαHisC3aR-TeveGFP		2664 bp	1 min 30 s	
	pPpHygαHishB1R-TeveGFP		2277 bp	1 min 30 s	
Hyg-fragment	pPpHygαHisβ$_2$AR-StrepII	Fw Hyg Rv pGAP-Hyg	3285 bp	1 min 45 s	61°C
pGAP-fragment	pHGKTef1Swa_ScKex2_FLAG	Fw Hyg-pGAP Rv alpha-pGAP	526 bp	30 s	70°C

The PCR fragments were loaded onto a preparative agarose gel, purified and assembled to the final vectors pPpHygpGAPαHisGPCRStrepII and pPpHygpGAPαHisGPCRTeveGFP using 50 ng of the smallest fragment. After transformation into *E. coli*, vectors were isolated, verified by restriction enzyme digestion with *SacI* and *PstI*, and were sent to sequencing. Correct vectors were linearized with *SmiI* and transformed into *P. pastoris* strains. Transformants were directly used for inoculation of DWPs and screened for fluorescence signal (eGFP-tag) or for signals in the DotBlot (StrepII-tag).

2.2.16 Fluorescence screening in DWPs

Cells were cultivated directly from the transformation plates in 96-DWPs as described in section 2.2.5.1. The *P. pastoris* WT was used as negative control. For P_{AOX1} cultivation, several *P. pastoris* clones expressing β_2AR-GFP were used. For the first P_{GAP} screening, positive controls were not available. After specific cultivation, cells were pinned onto YDP-Hyg^{100} agar for conservation. For fluorescence screening, two times 10 µl of the cell suspension were mixed with 190 µl ddH_2O in special 96-microtiter plates and the OD_{600} as well as the fluorescence signal of the eGFP (excitation max. 488 nm, emission max. 509 nm) were measured with the plate reader.

2.2.17 Fluorescence microscopy

Cells were cultivated in shake flasks (2.2.5.2) for P_{AOX1} induction or simply grown as ONCs in YPD or BMGY under P_{GAP}. For microscopy, cultures were induced with a special methanol/sorbitol co-feeding strategy. Instead of standard BMMY, a combined BMMSY with 2% sorbitol and 0.2% methanol was used for the first induction after the growth phase. Further induction was done by adding BMMY(10%) to a final methanol concentration of 0.1%.

Slides were covered with poly-L-lysine and 2-5 µl of diluted cells were put onto the slide. Light images were taken using the 100x objective and corresponding phase contrast. For imaging the fluorescence, the I.3 filter was used and the exposure time in milliseconds (ms) was chosen depending on the strength of the fluorescence signal.

2.2.18 Functional analysis

Functional analysis of the GPCRs was performed by Christoph Reinhart at the Max-Planck Institute in Frankfurt, Germany. The strains expressing the GPCRs were streaked out freshly onto YPD-Hyg^{300} agar plates and were sent to Germany. The strains were cultivated, protein expression was induced and the membranes were isolated. Functional analysis was done with the radio-labelled ligand [3H](-)CGP-12177, an antagonist of the β_2AR[4].

2.2.19 DotBlot in 96-well format

The protocol was kindly provided by Christoph Reinhart and adapted, depending on the application, as described below.

2.2.19.1 Cell cultivation

A 96-DWP was filled with 200 µl YPD, inoculated with single colonies from the transformation plates and four positive as well as four negative controls were added. The DWP was incubated at 28°C for two days. Then, the DWP was replicated in a new DWP with 200 µl YPD per well and was again incubated at 28°C for two days. After incubation, the cells were pinned onto a sterile nitrocellulose membrane on top of a 0.5 and 2.5% BMMY agar plate for P_{AOX1} induction and on a YPD agar plate for P_{GAP} induction. The plates were incubated at 28°C for 3-4 days or until the colonies had grown well.

2.2.19.2 Cell lysis

Filter papers in 96-well format were soaked with different solutions (I-IV) and the nitrocellulose membrane with the cells on top was applied to the filter paper and incubated for a defined time and at a defined temperature (Figure 18).

Solution I	5 min	RT
Solution II	10 min	RT
Solution III	10 min	RT
Solution I	5 min	RT
Solution IV	30 min	60°C

Figure 18: Incubation conditions for the different solutions in the DotBlot.

The cells were washed off with ddH_2O. The membrane was then directly used for the immunoblot, starting with the blocking step with milk powder (section 2.2.11). Detection was done against the N-terminal His-tag or the C-terminal StrepII-tag.

2.2.20 Construction of protease deficient cholesterol strains

For the knockout of the *PEP4* gene in the *P. pastoris* cholesterol strain and the pre-existing cholesterol strain Δ*prb1*, the sequences of the 5' and 3' UTR of the *PEP4* gene were cloned in the pPpKC3 vector. For this purpose, the pPpKC1_pep4 vector containing the 5' and 3' UTRs as well as the pPpKC3 vector with the *HIS4* marker gene were cut with *SfiI* in the following set-up:

30 µl DNA
2 µl *SfiI*
5 µl 10x Cut Smart Buffer
13 µl ddH_20

50 µl total

The mixture was incubated at 50°C overnight. The pPpKC3 vector was dephosphorylated for 20 min at 37°C and was inactivated for 5 min at 75°C. The preparations were loaded onto a preparative agarose gel, the vector backbone of pPpKC3 and the *PEP4* UTR insert were cut out and purified with the Wizard® SV Gel and PCR Clean Up System. One-hundred ng of the vector backbone were ligated with a 3-fold molar excess of the insert at 16°C overnight. The ligase was inactivated for 10 min at 70°C and the whole ligation was desalted for 30 min. Five µl were then transformed into electrocompetent *E. coli* Top10 cells. Fifteen clones were re-streaked onto LB-Amp and the plasmids were isolated. The constructs were analyzed via control-cuts with *SfiI* to confirm the right insert:

2 µl DNA
1 µl *SfiI*
2 µl 10x Cut Smart Buffer
15 µl ddH_20

20 µl total

The mixture was incubated at 50°C for 45 min. The vector that showed the correct fragments was linearized with the set-up:

10 µl vector
2 µl *SmaI*
2 µl 10x Tango buffer
6 µl ddH_20

20 µl total

The reaction was incubated at 30°C overnight, inactivated at 65°C for 20 min, purified and transformed into *P. pastoris* cholesterol strain and cholesterol strain Δ*prb1*. Selection was done on MD plates for His+ transformants. Twenty-four clones of each strain were re-streaked onto MD plates and the integration of the expression cassette in the *PEP4* locus was verified by cPCR 1 and 2 (Figure 19 and Table 13).

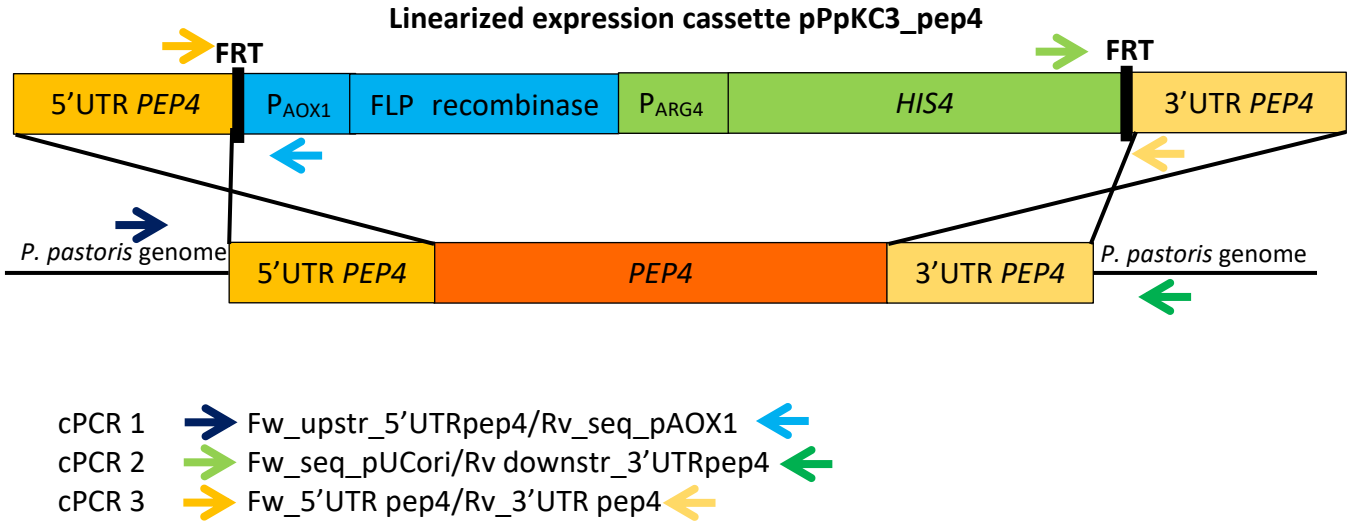

Figure 19: Schematic *PEP4* knockout strategy. The 5' and 3' UTRs of the *PEP4* gene on the edge of the linearized pPpKC3_pep4 vector do a double cross-over with the homologous regions on the *P. pastoris* genome to integrate the expression cassette into the *PEP4* locus.

Table 13: cPCR 1 and 2 for verification of expression cassette integration into the *PEP4* locus

	Primer	PCR product size	Annealing temperature	Extension time
cPCR 1 (5'UTR)	Fw_upstr_5'UTRpep4 Rv_seq_pAOX1	1568 bp	50°C	1 min 45 s
cPCR 2 (3'UTR)	Fw_seq_pUCori Rv downstr_3'UTRpep4	1568 bp		

For marker recycling, several positive clones were cultivated in BMMY(1%) for 24 h, plated onto YPD agar in different dilutions and analyzed via cPCR 3 for the *pep4* knockout and for successful marker recycling. Figure 20 shows the constellation in the *P. pastoris* genome and Table 14 the set-up and specific PCR program steps for cPCR 3.

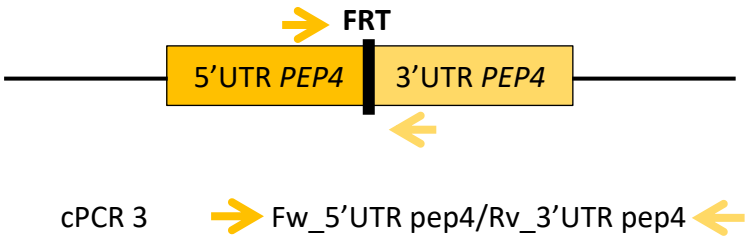

Figure 20: 5'UTR and 3'UTR of the *PEP4* gene in the *P. pastoris* genome after successful knockout and marker recycling.

Table 14: cPCR 3 for verification of *pep4* knockout and marker recycling

Primers	PCR product size	Reason	Annealing temperature	Extension time
Fw_5'UTR pep4 Rv_3'UTR pep4	1233 bp	original *PEP4* gene is still there	50°C	8 min
	180 bp	*PEP4* gene is knocked out		
	7761 bp OR no product	marker is not recycled yet; expression cassette is still there		

To ensure complete marker recycling, single clones were cultivated in DWPs with 250 µl YPD for 48 h and then pinned onto MD and MDH plates to see which clones had fully lost their ability to grow on MD.

3 Results

3.1 StrepII-tagged GPCR expression

3.1.1 Verification of gene integration by cPCR

Eight clones of each GPCR in the *P. pastoris* WT (Figure 21), SMD1168 (Figure 22) and Δ*ku70* strain (Figure 24) backgrounds and five clones of each GPCR in the cholesterol strain (Figure 23) background were tested for expression cassette integration via cPCR. In general, all tested clones had the gene of interest successfully integrated into the genome and showed the correct PCR product size. The expected size for the β_2AR was 1541 bp, for the hB1R 1436 bp and for the C3aR 1823 bp. In the lanes where no band was visible, there was not sufficient cell material available as these clones grew worse than the others. Those strains were either neglected for further analysis (WT β_2AR 3, WT C3aR 2, Figure 21) or tested again via cPCR (Chol hB1R 3-4, Figures 23, 24). Neither the *P. pastoris* WT negative control without any expression cassette nor the no template control showed any unspecific signal (Figure 23).

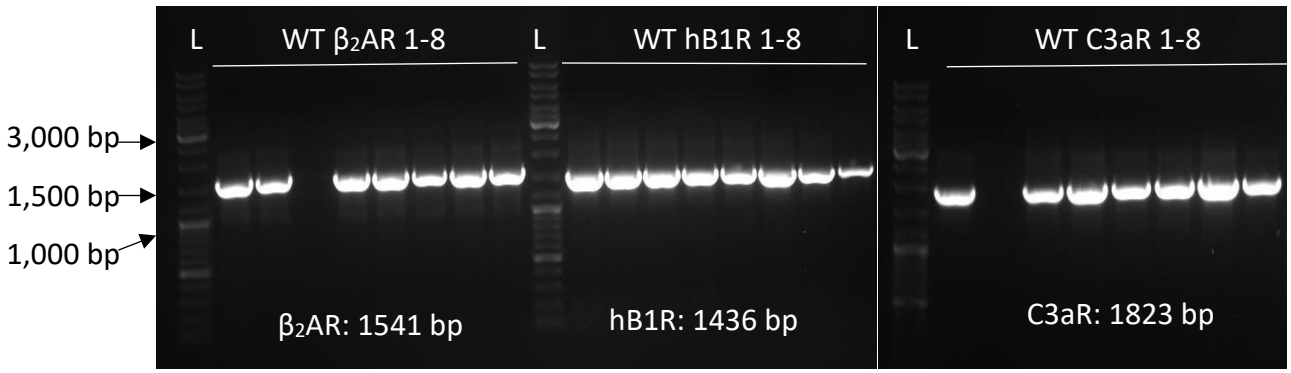

Figure 21: Results of cPCR for verification of gene integration. *P. pastoris* WT β_2AR, hB1R and C3aR transformants 1-8, L: GeneRuler™ DNA Ladder Mix

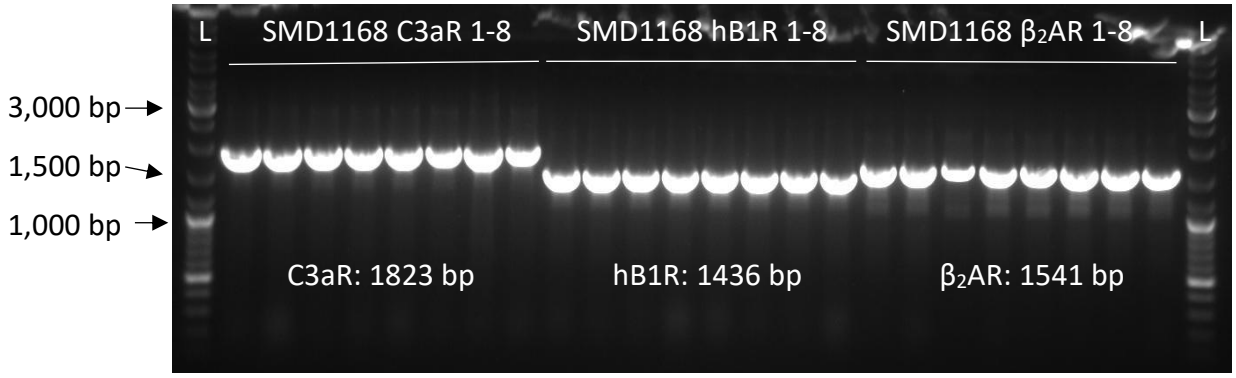

Figure 22: Results of cPCR for verification of gene integration. *P. pastoris* SMD1168 C3aR, hB1R and β_2AR transformants 1-8, L: GeneRuler™ DNA Ladder Mix

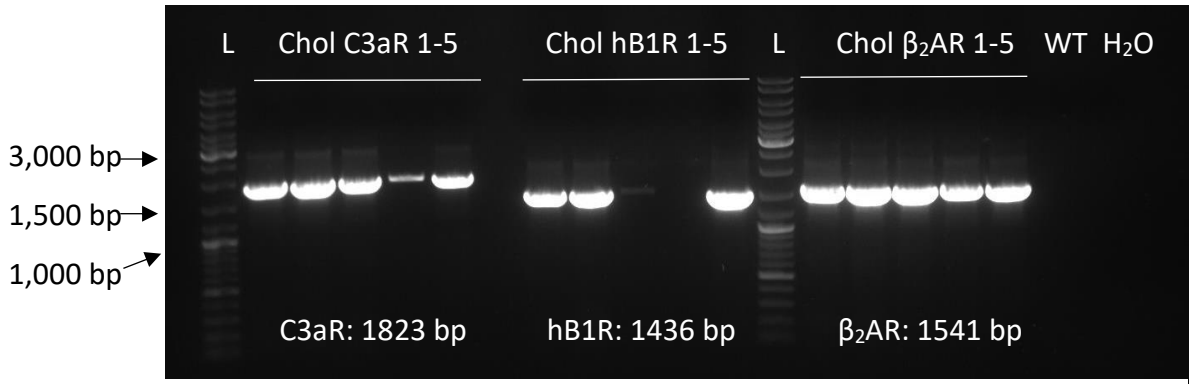

Figure 23: Results of cPCR for verification of gene integration. *P. pastoris* cholesterol strain C3aR, hB1R and β_2AR transformants 1-5, L: GeneRuler™ DNA Ladder Mix, WT, H_2O: negative controls

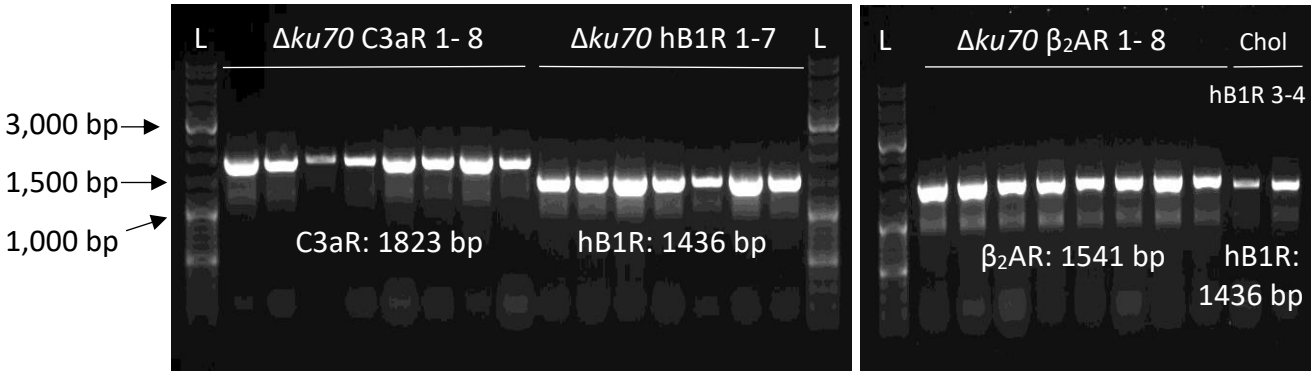

Figure 24: Results of cPCR for verification of gene integration. *P. pastoris* Δ*ku70* strain C3aR transformants 1-8, Δ*ku70* strain hB1R transformants 1-7, Δ*ku70* strain β_2AR transformants 1-8, cholesterol strain hB1R transformants 3-4, L: GeneRuler™ DNA Ladder Mix

3.1.2 Cultivation, protein isolation and Western Blot

3.1.2.1 β_2AR-StrepII

3.1.2.1.1 Total cell lysate

Five clones per strain that had been positively tested in the cPCR for the β_2AR gene were cultivated, expression of β_2AR was induced and the proteins of the total cell lysate were analyzed via WB at indicated time points of induction.

The five cultivated WT strains 1, 2, 4, 5, and 6 showed no signal except some unspecific bands as seen in Figure 25 for the WT strains 5 and 6. The cholesterol strains 2, 3 and 5 showed an increasing signal over time at about 55 kDa and at an undefined high molecular weight, whereas the cholesterol strains 1 and 4 showed no signal at all. Figure 25 shows the cholesterol strains 3, 4 and 5 as example for the anti-StrepII detection.

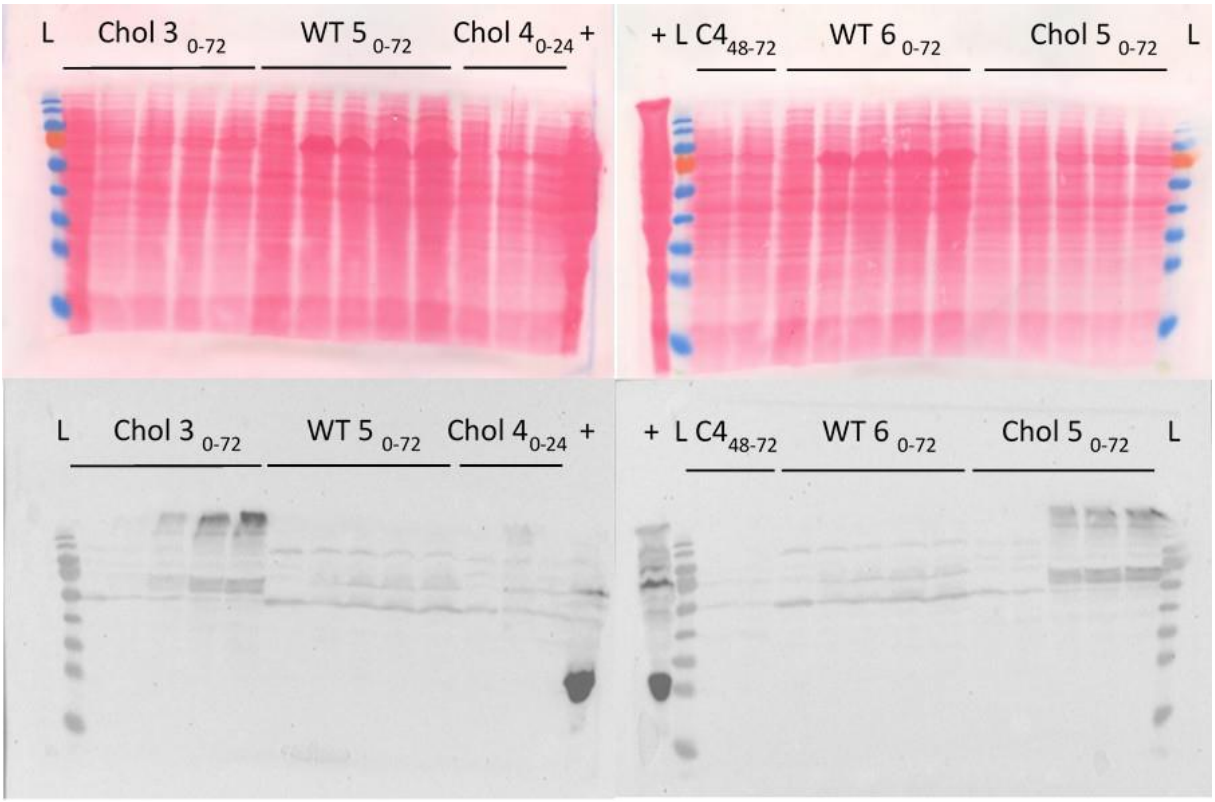

Figure 25: SDS-PAGE (12.5%) and WB of 40 µg protein of the total cell lysate after 0 - 72 h of MeOH induction (t_{0-72}) with *P. pastoris* clones expressing β_2AR-StrepII, top: PonceauS staining of nitrocellulose membranes, bottom: immunodetection with anti-StrepII antibody; L: PageRuler™ Prestained Protein Ladder, +: positive control: protein with StrepII-tag overexpressed in *P. pastoris*

The WB analysis of the cultivated strains *P. pastoris* Δ*ku70* 1-3 and SMD1168 1-2 yielded no signal, neither against the StrepII-tag nor against the His-tag.

The analysis of the Δ*ku70* strains 4-5 and SMD1168 strains 3-5 gave a slightly positive signal (Figure 26). Here, only the anti-StrepII antibody was used as it seemed to give the stronger signals. The SMD1168 strains 3 and 5 as well as the Δ*ku70* strain 4 showed some signal after 8 h of induction (t_8) but the signal decreased over induction time. The size of the expressed receptor could not be defined exactly as there were several bands that had the same intensity. Nevertheless, there were faint bands at about 55 kDa and at a high molecular weight.

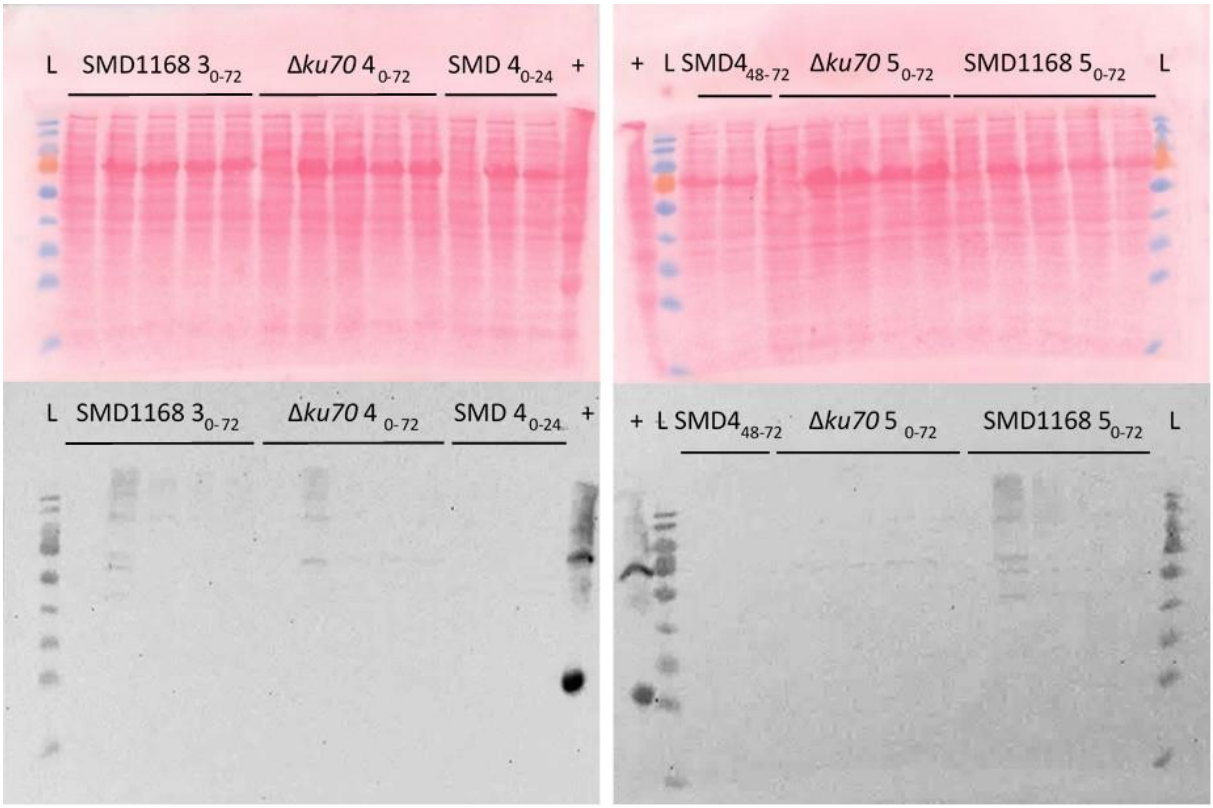

Figure 26: SDS-PAGE (12.5%) and WB of 30 µg protein of the total cell lysate after 0 -72 h of MeOH induction (t_{0-72}) with *P. pastoris* clones expressing β_2AR-StrepII, top: PonceauS staining of nitrocellulose membranes, bottom: immunodetection with anti-StrepII antibody; L: PageRuler™ Prestained Protein Ladder, +: positive control: protein with StrepII-tag overexpressed in *P. pastoris*

3.1.2.1.2 Isolation of total microsomes

One clone per strain that had shown a signal in the WB of the total cell lysate samples was cultivated again, induced and the total microsomes were isolated. The following WB analysis confirmed the previous results. The isolated protein samples of the cytosol, the homogenate and the total microsomes after 48 h of induction were analyzed. In Figure 27, the left membranes show the WB/Immunoblot against the His-tag and the right membranes the WB/Immunoblot against StrepII-epitope-tag.

The WT 4 strain did not show any band as already seen in the WB with the total cell lysate samples. The Δ*ku70* 4 strain showed no signal either, although there had been a faint signal with the total cell lysate at t_8. The SMD1168 strain 5 gave weak signals at an undefined size in the homogenate and in the total microsome fraction but only with the anti-StrepII detection. The cholesterol strain 3 showed signals with both antibodies in the homogenate and in the total microsome fraction. The bands could be seen at a very high molecular weight size of more than 180 kDa and a strong band was also visible at about 55 kDa.

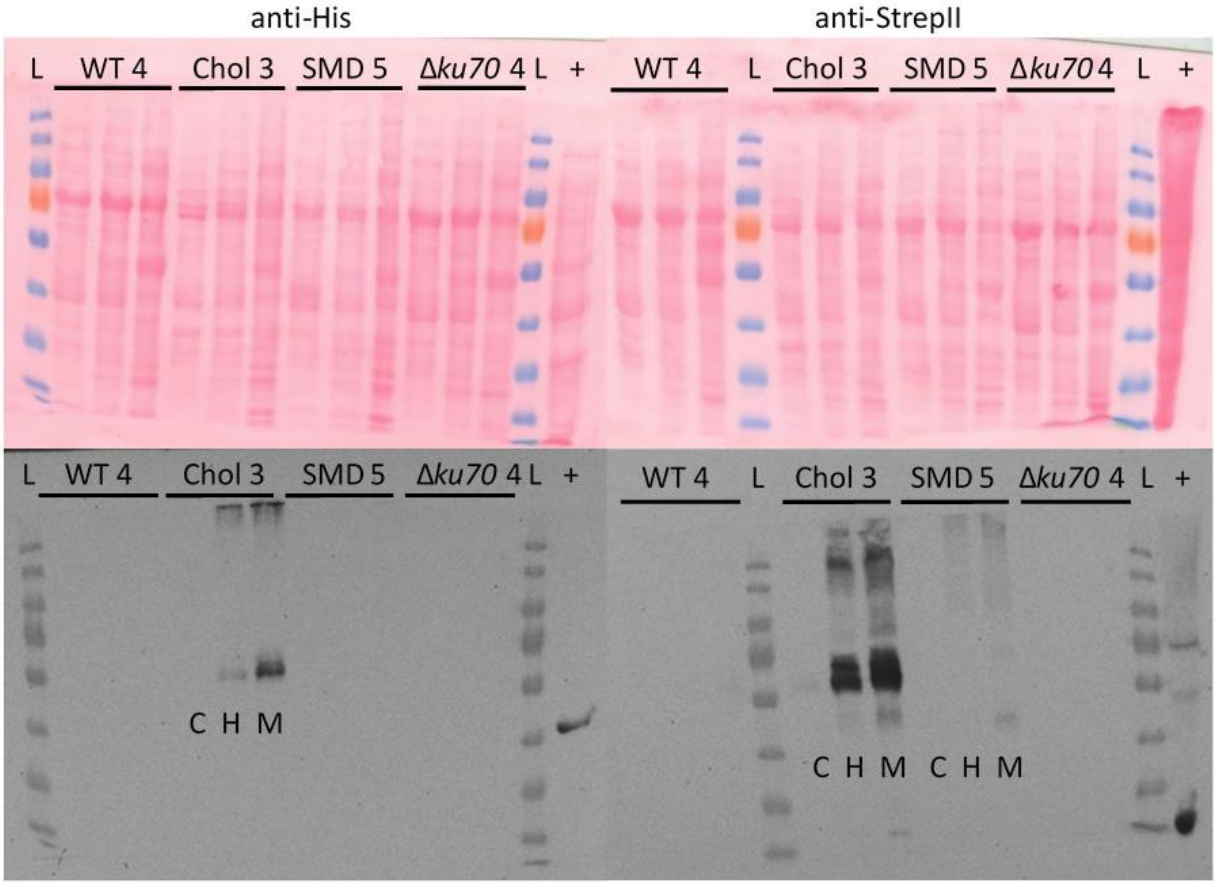

Figure 27: SDS-PAGE (10%) and WB of 20 µg protein of the cytosol (C), homogenate (H) = total cell lysate and total microsomes (M) after 48 h of MeOH induction with *P. pastoris* clones expressing β_2AR-StrepII, top: PonceauS staining of nitrocellulose membranes, bottom left: immunodetection with anti-His antibody, bottom right: immunodetection with anti-StrepII antibody; L: PageRuler™ Prestained Protein Ladder, +: positive control: protein with His-tag overexpressed in *E. coli* or protein with StrepII-tag overexpressed in *P. pastoris*, respectively.

3.1.2.1.3 Comparison to reference strains

As the cholesterol strains 2, 3 and 5 showed good signals, these strains were chosen for a comparison to reference strains from Christoph Reinhart that express a defined amount of active β_2AR. The reference strains are protease-deficient *P. pastoris* SMD1163 (Δ*prb1* Δ*pep4*) strains that have two different constructs of the β_2AR integrated. These five strains were cultivated, protein expression was induced and the total microsomes were isolated to do a comparative WB analysis. Figure 28 showed that the two reference strains expressed much more of the β_2AR than the cholesterol strains. The reference strains showed bands at about 55 kDa for the StrepII-tagged construct in the SMD1163 20 pmol/mg strain, at 70 kDa for the biotinylated construct in the SMD1163 50 pmol/mg strain and also at a high molecular weight, whereas the cholesterol strains only showed a smear at a high undefined molecular weight.

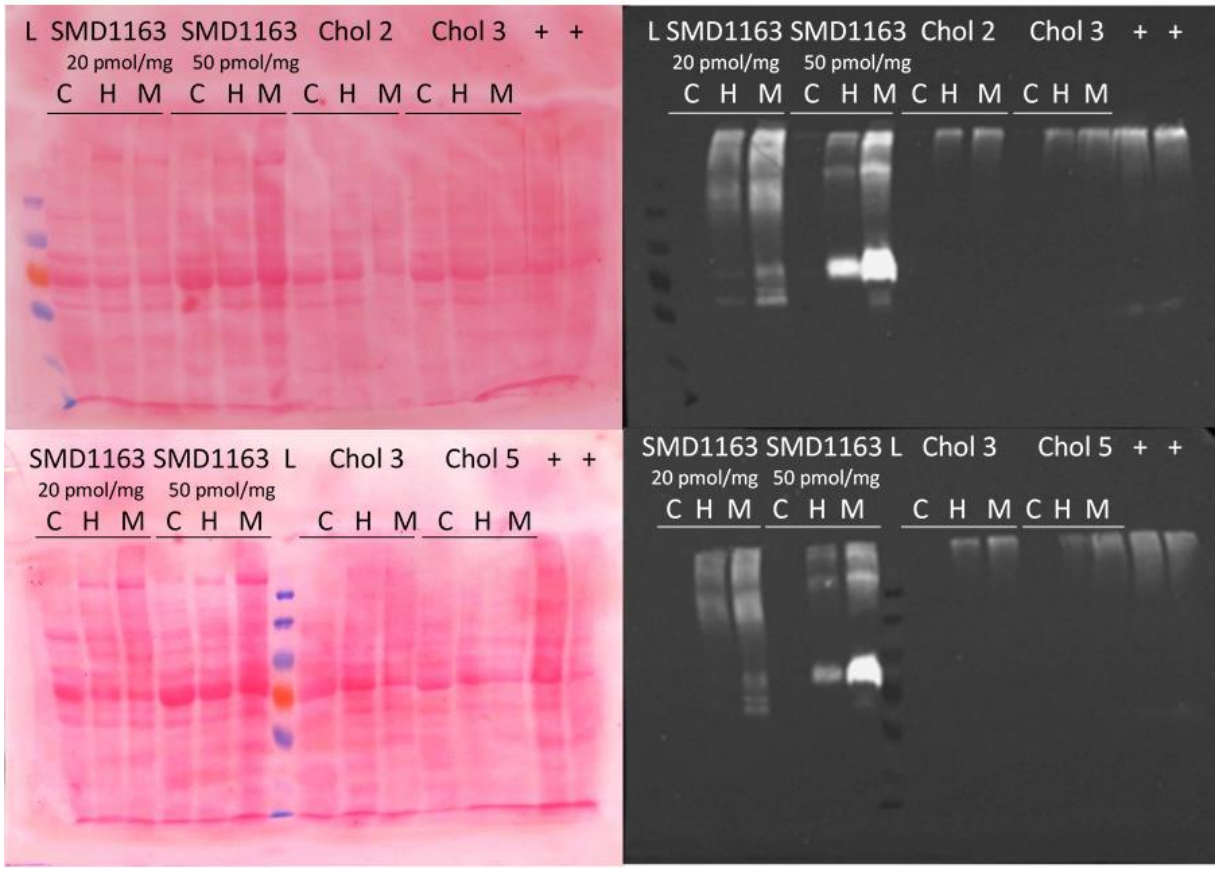

Figure 28: SDS-PAGE (10%) and WB of 20 µg protein of the cytosol (C), homogenate (H) = total cell lysate and total microsomes (M), after 48 h of MeOH induction with *P. pastoris* clones expressing β_2AR, left: PonceauS staining of nitrocellulose membranes, right: immunodetection with anti-His antibody, L: PageRuler™ Prestained Protein Ladder, *P. pas*toris SMD1163 pPIC9KFlagHis10TevΔGβ_2ARStrepII (20 pmol/mg), *P. pastoris* SMD1163 pPIC9KFlagHis10ΔGβ_2AR-Bio (50 pmol/mg), *P. pastoris* cholesterol strain pPpHygαHisβ_2ARStrepII 2, 3, 5; +: positive controls: total microsomes of *P. pastoris* cholesterol strain #3 expressing β_2AR-StrepII of last cultivation

For the positive controls, isolated microsomes of the cholesterol strain 3 from the last cultivation were used in two lanes. It appeared to have a slightly stronger signal than the newly cultivated cholesterol strains.

3.1.2.2 C3aR-StrepII

For analysis of C3aR expression, also five clones per strain background were cultivated and protein expression was induced. Total microsomes were isolated with the small-scale isolation method. The WB analysis of the microsomal fractions of five clones per strain using anti-StrepII antibody yielded no signal at all. Figure 29 shows the clones 2 and 3 of each strain as an example. The expected size of the C3aR monomer would be 60 kDa. The positive controls with the microsomes of the cholesterol strain 3 expressing β_2AR showed a strong signal upon anti-StrepII detection.

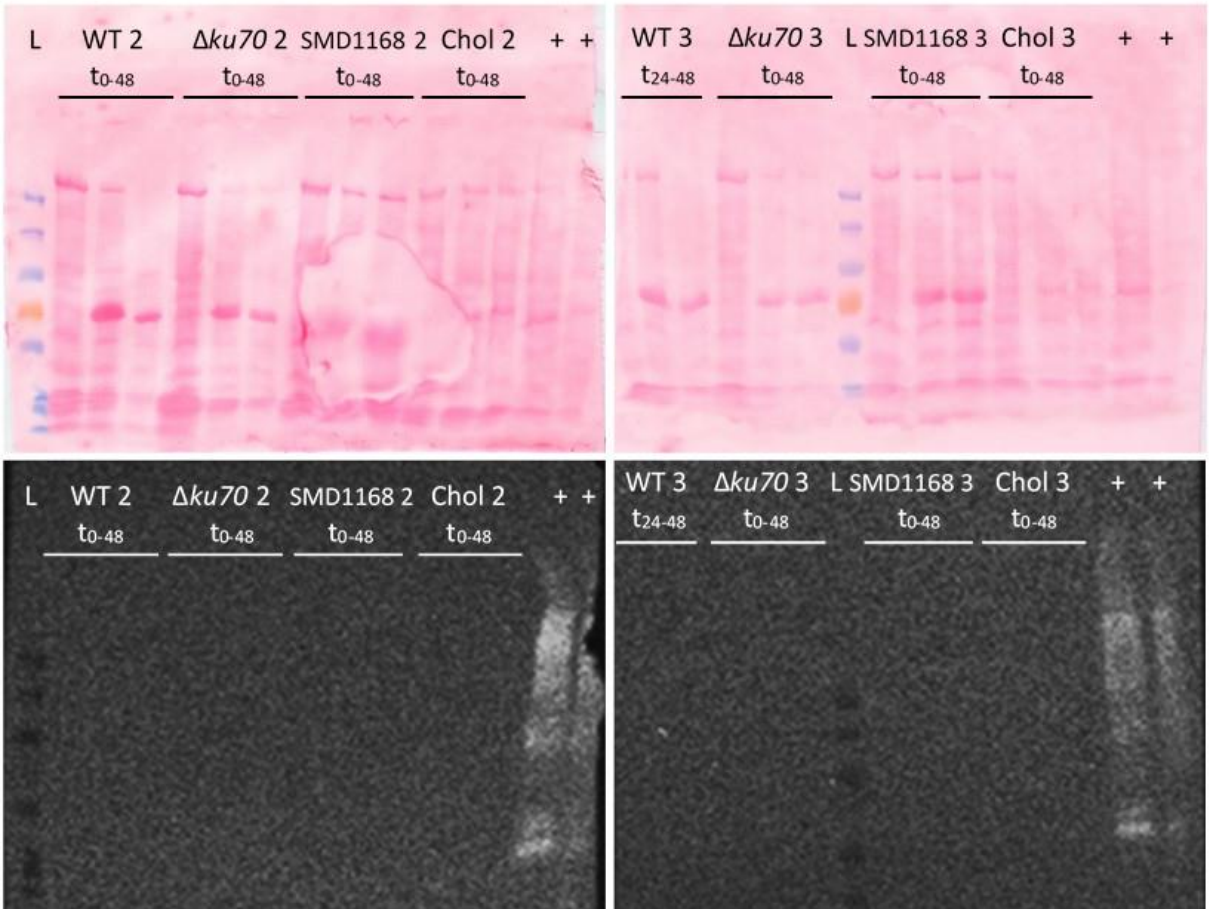

Figure 29: SDS-PAGE (10%) and WB against StrepII-tag of C3aR expressing *P. pastoris* clones. Total microsomes of t_0, t_{24} and t_{48} of MeOH induced cells. top: PonceauS staining of nitrocellulose membranes, bottom: immunodetection with anti-StrepII antibody, Samples: *P. pastoris* WT 2-3, *P. pastoris* Δ*ku70* 2-3, *P. pastoris* SMD1168 2-3, *P. pastoris* cholesterol strain 2-3, L: PageRuler™ Prestained Protein Ladder, +: positive control: microsomes of *P. pastoris* cholesterol strain #3 expressing β_2AR-StrepII

3.1.2.3 hB1R-StrepII

The expression of C-terminally StrepII-tagged hB1R was not further analyzed as the eGFP-tagged construct was easier to screen for.

3.1.3 Determination of possible multiple integration events

In order to find possible multiple integration events, transformants of *P. pastoris* WT and cholesterol strain were pinned onto YPD with increasing hygromycin concentrations from 300 µg/ml to 4000 µg/ml. Whereas all clones of WT background could grow on the highest hygromycin concentrations (Figure 30), the strains with the cholesterol background behaved differently. There were clones that grew on high hygromycin concentrations and some that showed no growth anymore (Figure 31). All clones of the WT seemed to be resistant against hygromycin irrespective of the copy number, but in the cholesterol strain background a correlation between hygromycin resistance and copy number is possible.

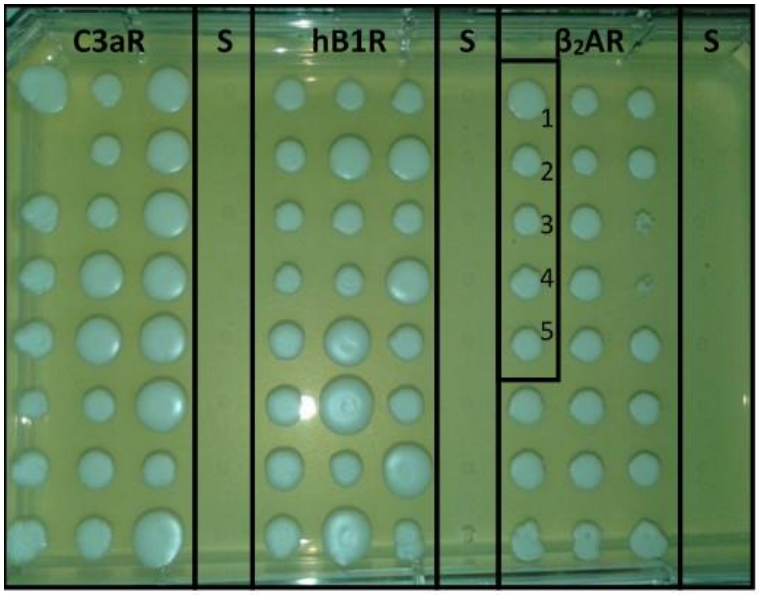

Figure 30: Determination of possible multiple integration events. *P. pastoris* WT transformants on YPD agar + 4000 µg/ml hygromycin; S: sterile control; lane 1: transformants 1-5 analyzed via cPCR, rest: randomly chosen transformants

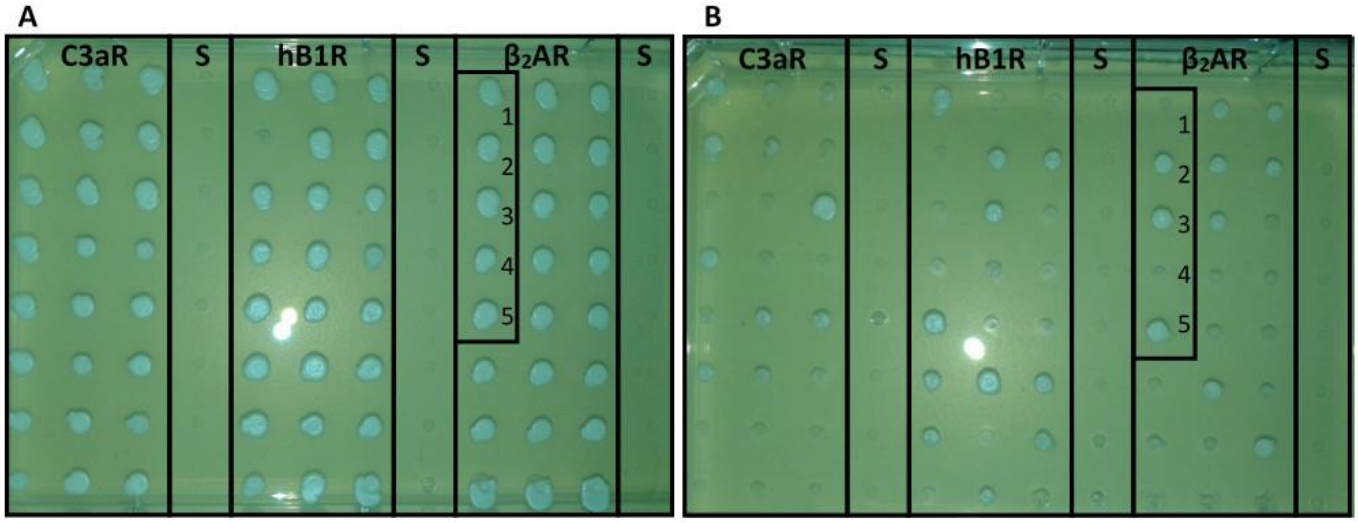

Figure 31: Determination of possible multiple integration events. (A) *P. pastoris* cholesterol strain transformants on YPD agar + 1000 µg/ml hygromycin, (B) *P. pastoris* cholesterol strain transformants on YPD agar + 4000 µg/ml hygromycin S: sterile control, lane 1: transformants 1-5 analyzed via cPCR, rest: randomly chosen transformants

Due to the fact that in DWP cultivation the cell density was quite high, all 20 cultivated strains with the β_2AR-StrepII construct were streaked onto YPD agar containing 300 µg/ml and 4000 µg/ml hygromycin (Figure 32), too. The WT, SMD1168 and Δ*ku70* strain (Fig. 32, B1, C1, D1) showed no difference in growth whereas the cholesterol strain showed the same result as in the first experiment (Figure 32, A2). Cholesterol strains 2, 3 and 5 could grow better on high hygromycin concentrations than strain 1 and 4 indicating an increased copy number of the expression cassette.

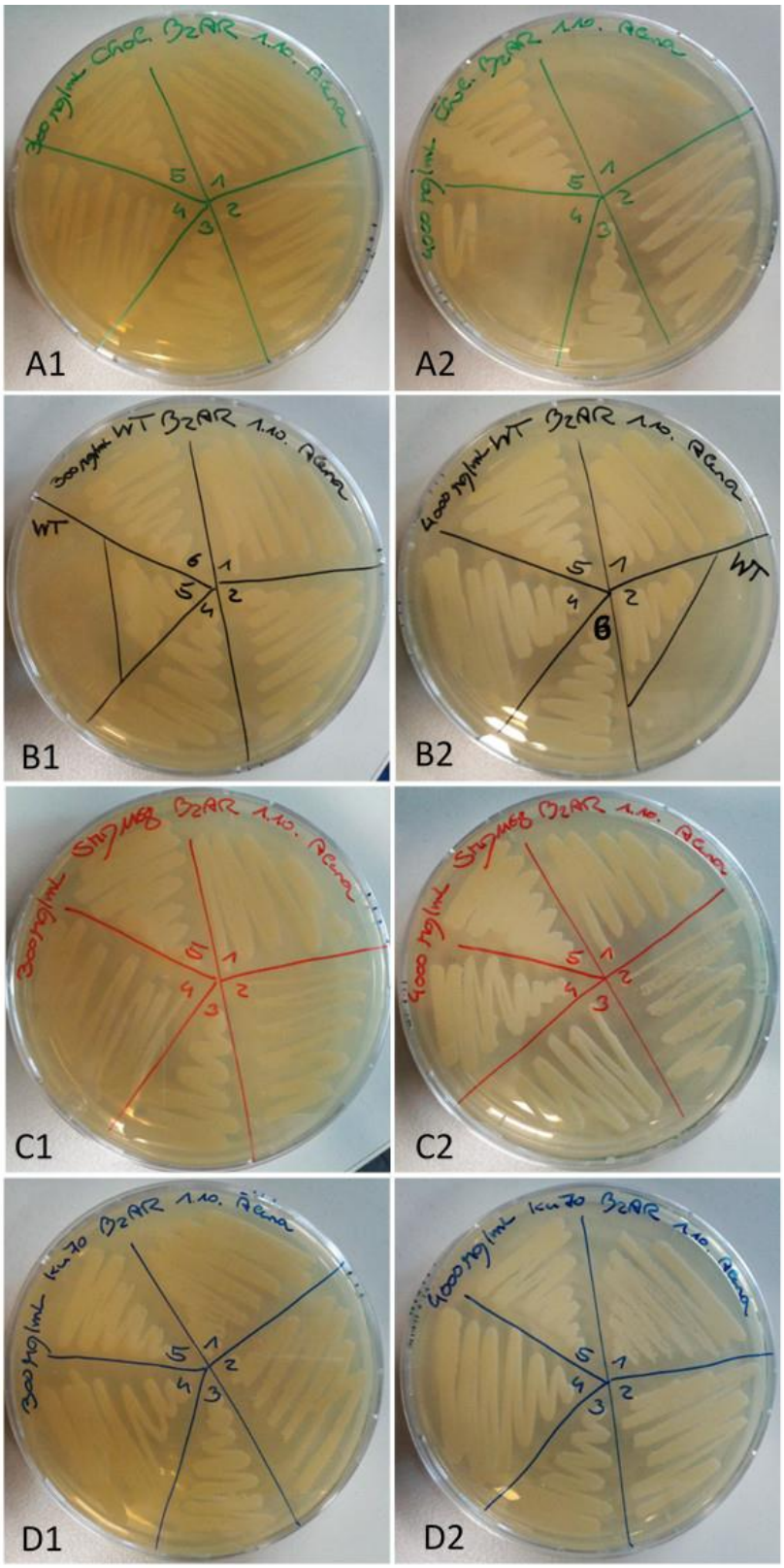

Figure 32: Different *P. pastoris* strains and transformants of β_2AR-StrepII on YPD agar plates with 300 µg/ml and 4000 µg/ml hygromycin. (A1) *P. pastoris* cholesterol strains 1-5 on 300 µg/ml hygromycin, (A2) *P. pastoris* cholesterol strains 1-5 on 4000 µg/ml hygromycin, (B1) *P. pastoris* WT strain 1, 2, 4-6 on 300 µg/ml hygromycin, WT: *P. pastoris* WT (negative control), (B2) *P. pastoris* WT strain 1, 2, 4-6 on 4000 µg/ml hygromycin, (C1) *P. pastoris* SMD1168 strain 1-5 on 300 µg/ml hygromycin, (C2) *P. pastoris* SMD1168 strain 1-5 on 4000 µg/ml hygromycin, (D1) *P. pastoris* Δ*ku70* strain 1-5 on 300 µg/ml hygromycin, (D2) *P. pastoris* Δ*ku70* strain 1-5 on 4000 µg/ml hygromycin

3.1.4 Quantitative PCR

To investigate a possible correlation between hygromycin resistance, signal in the WB and copy numbers, different strains expressing β_2AR-StrepII were analyzed by qPCR. Figure 33 shows isolated gDNA samples of different strains and Figure 34 the control PCR with the two different primer pairs and the isolated gDNA as template. Both PCR products could be formed, the *ARG4* gene was present in every strain as well as the hygromycin gene on the integrated expression cassette. The no template control was negative.

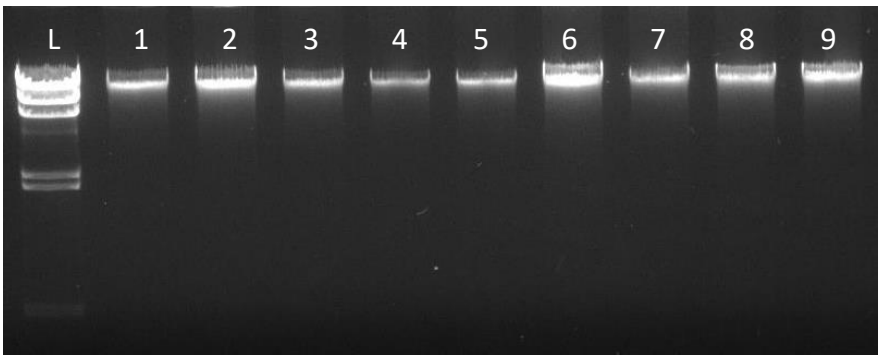

Figure 33: gDNA samples (2 µl) of different strains expressing β_2AR-StrepII. L: Lambda DNA/HindIII Marker, 1-5: *P. pastoris* cholesterol strain 1-5; 6,7: *P. pastoris* WT 4, 6; 8,9: *P. pastoris* SMD1168 4, 5

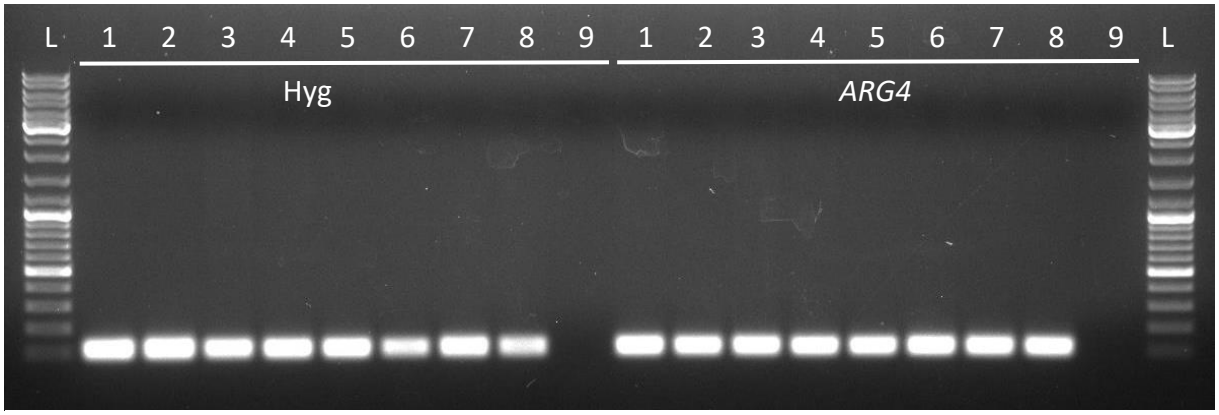

Figure 34: Control PCR of gDNA samples for qPCR. L: GeneRuler™ DNA Ladder Mix, Hyg: Hygromycin primer, *ARG4*: primer for *ARG4* gene, 1-5: *P. pastoris* cholesterol strain 1-5; 6,7: *P. pastoris* SMD1168 4,5; 8: *P. pastoris* WT 6; 9: no template control

Table 15 shows the calculated copy numbers of the five cultivated cholesterol strains as well as two SMD1168 and WT strains expressing β_2AR-StrepII. In general, the observed phenotypes of the strains as well as the signals in the WB matched the calculated copy numbers. The cholesterol strains that showed a signal in the WB and could grow at high hygromycin concentrations also seemed to have more than one copy of the expression cassette in the genome. The WT strains 4 and 6 seemed to have only one copy and gave no signal in the WB. The SMD1168 strain 5 also showed a signal in the WB and had more copies than the #4 strain that showed no signal. All calculations were triple checked and yielded these incredibly high values that were very hard to interpret.

Table 15: Quantitative PCR. Absolute and relative copy number (CN) of different strains expressing β_2AR-StrepII.

P. pastoris strain expressing β_2AR-StrepII	CN absolute	CN relative
Cholesterol strain 1	115.1*	104.6*
Cholesterol strain 2	719.5*	653.4*
Cholesterol strain 3	1090.7*	962.1*
Cholesterol strain 4	23.7*	21.8*
Cholesterol strain 5	370.7*	336.2*
WT 4	0.7	0.7
WT 6	1.0	1.0
SMD1168 4	1.1	1.1
SMD1168 5	25.3*	24.0*

*: should not be taken as absolute value

3.2 eGFP-tagged GPCR expression

3.2.1 Construction of C-terminal eGFP-tagged expression vectors

Table 16 lists the expected fragment sizes of the new pPpHygαHisGPCRTeveGFP vectors and the negative control vectors pPpHygαHisGPCRStrepII. Figure 35 shows the restriction analysis of the assembled vectors after the double digest with the restriction enzymes *SacI* and *PstI*.

Table 16: Expected fragment sizes of the pPpHygαHisGPCRTeveGFP vectors and the negative control vectors pPpHygαHisGPCRStrepII after double digest with *SacI* and *PstI*.

Vector	Expected fragment sizes (bp)				
pPpHygαHis-**β_2AR-StrepII**	1055	1188	1394	2163	
pPpHygαHis-**β_2AR-TeveGFP**	1055	1188	1394	2871	
pPpHygαHis-**hB1R-StrepII**	1055	1394	3246		
pPpHygαHis-**hB1R-TeveGFP**	1055	1394	3954		
pPpHygαHis-**C3aR-StrepII**	668	1055	1188	1394	1777
pPpHygαHis-**C3aR-TeveGFP**	668	1055	1394	1777	1896

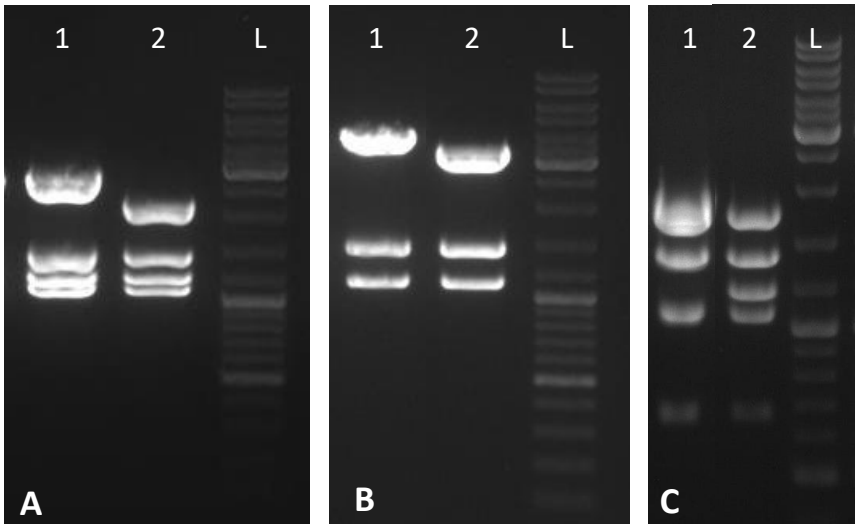

Figure 35: Restriction analysis of Gibson-assembled pPpHygαHisGPCRTeveGFP vectors with *PstI* and *SacI*. (A) 1: pPpHygαHisβ_2ARTeveGFP, 2: negative control pPpHygαHisβ_2ARStrepII, L: GeneRuler™ DNA Ladder Mix, (B) 1: pPpHygαHishB1RTeveGFP, 2: negative control pPpHygαHishB1RStrepII, (C) 1: pPpHygαHisC3aRTeveGFP, 2: negative control pPpHygαHisC3aRStrepII

After positive sequencing, the vectors pPpHygαHisGPCRTeveGFP were linearized with *SmiI*, purified and checked for integrity via agarose gel electrophoresis (Figure 36). The calculated sizes of the linearized vectors were 6790 bp for the C3aR, 6403 bp for the hB1R and 6508 bp for the β_2AR.

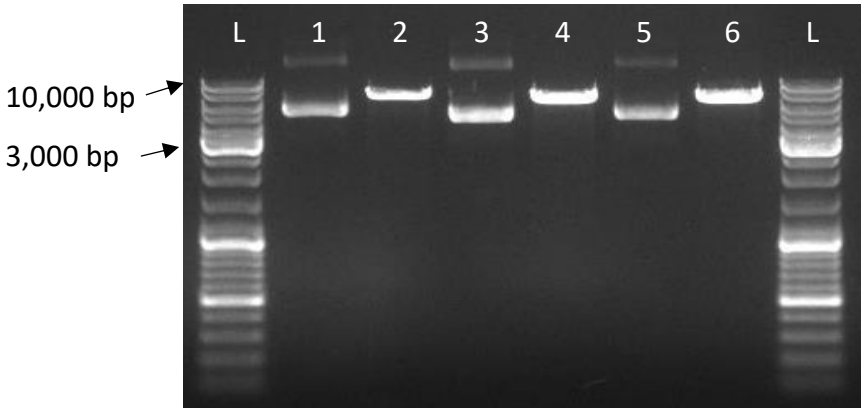

Figure 36: Linearized pPpHygαHisGPCRTeveGFP vectors with *SmiI*. L: GeneRuler™ DNA Ladder Mix, 1,2: pPpHygαHisC3aRTeveGFP uncut/cut, 3,4: pPpHygαHishB1RTeveGFP uncut/cut, 5,6: pPpHygαHisβ_2ARTeveGFP uncut/cut

3.2.2 Screening for fluorescence signal in DWPs

Directly after transformation, clones of each strain were cultivated in DWPs, induced and screened for fluorescence signals of the expressed eGFP-tag. Figures 37-39 show examples of the results of the screenings for fluorescence signals in DWPs with all three GPCRs. For the calculation of the fluorescence per OD_{600} unit, the values for the main fluorescence were divided by the main OD_{600} values. The main background value of the negative controls was subtracted.

3.2.2.1 β_2AR-GFP

Figure 37 shows the fluorescence signals of 40 clones of each strain containing the β_2AR-GFP construct. No strain had a tendency for higher signals, only single clones showed high values. The cholesterol strain showed generally lower values than the other strains.

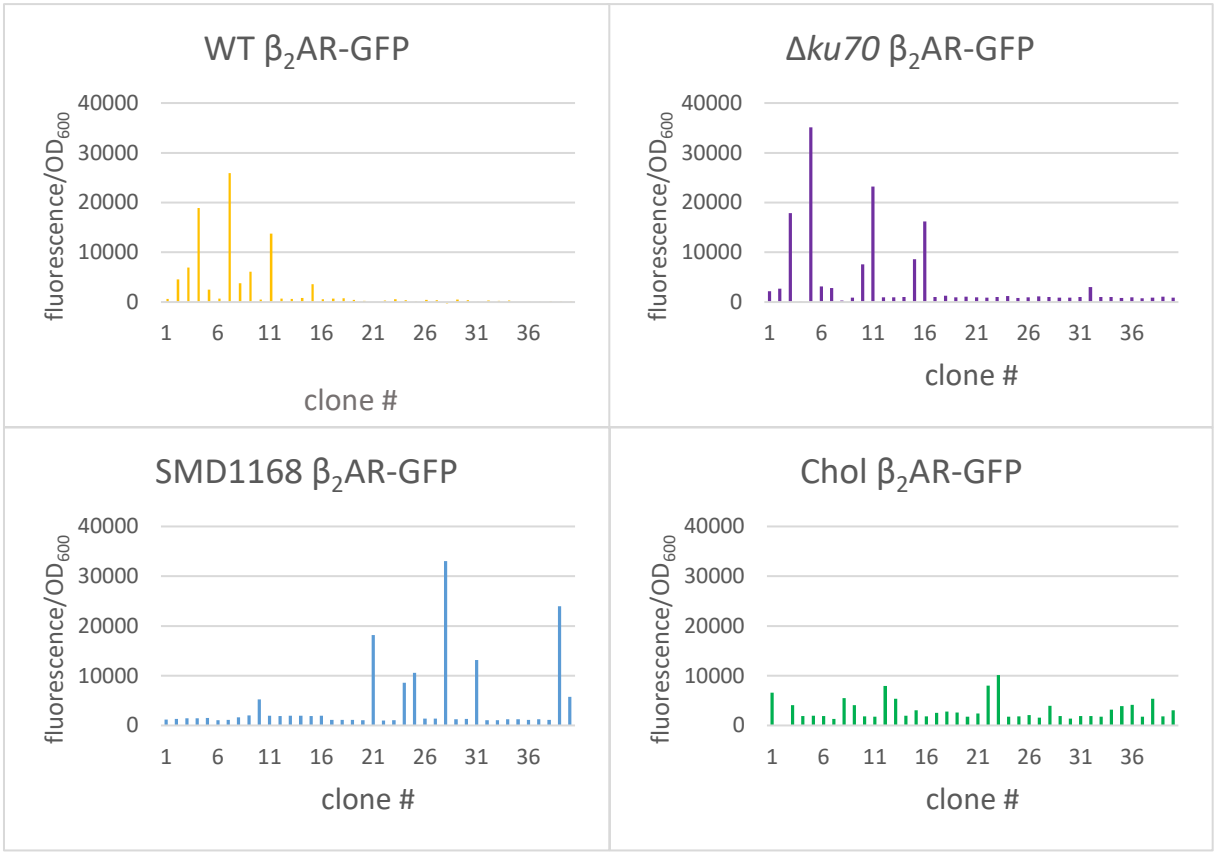

Figure 37: Screening for fluorescence signals in DWPs. The fluorescence values of the eGFP per OD_{600} for 40 clones of the different *P. pastoris* strains WT, Δ*ku70*, SMD1168 and cholesterol strain expressing β_2AR-GFP are shown.

3.2.2.2 hB1R-GFP

Figure 38 shows the fluorescence signals of 40 clones of each strain expressing hB1R-GFP. The picture was similar to the signal of the β_2AR-GFP, but the fluorescence signals were in general slightly weaker. The cholesterol strain showed again the lowest values.

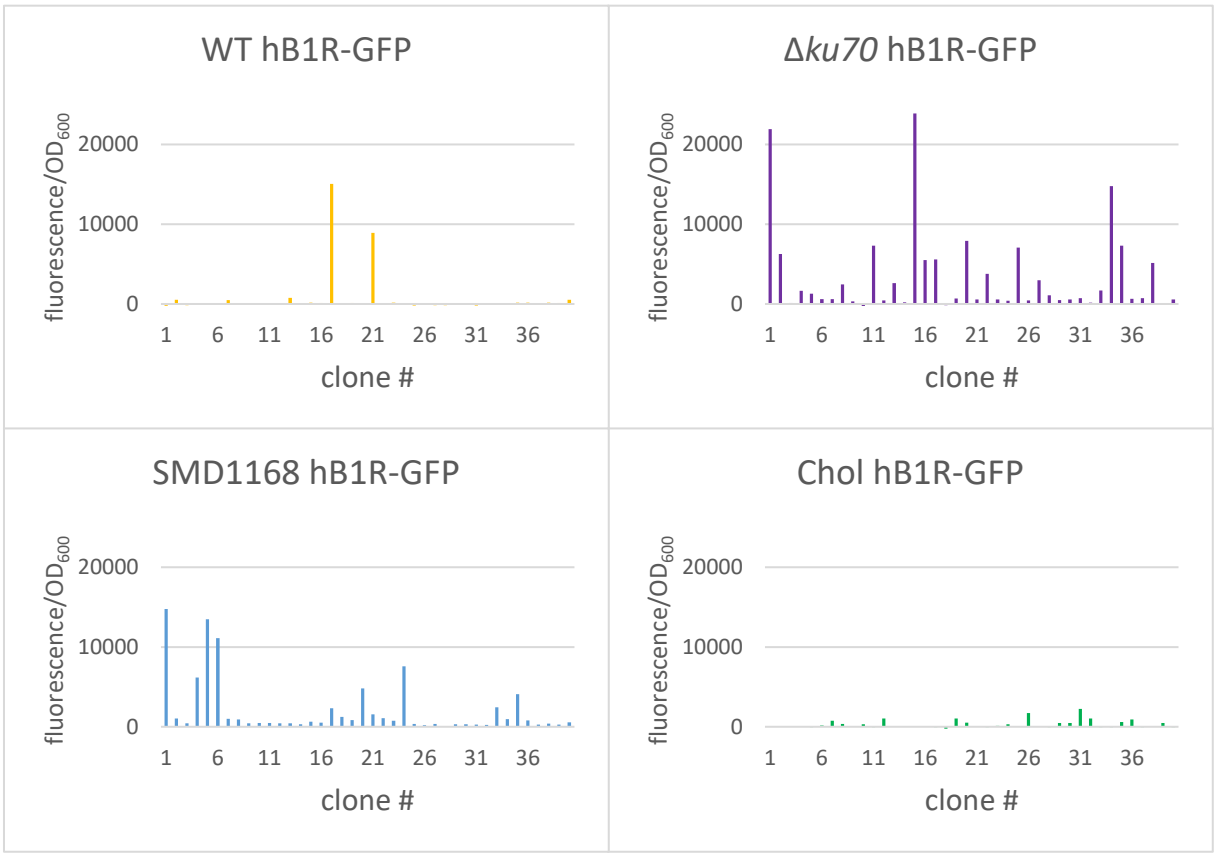

Figure 38: Screening for fluorescence signals in DWPs. The fluorescence values of the eGFP per OD_{600} for 40 clones of the different *P. pastoris* strains WT, Δ*ku*70, SMD1168 and cholesterol strain expressing hB1R-GFP are shown.

3.2.2.3 C3aR-GFP

Figure 39 shows the fluorescence signals of 40 clones of each strain expressing C3aR-GFP. There was no strong fluorescence signal that could be distinguished from the background and was comparable to signals of the β_2AR-GFP or the hB1R-GFP clones.

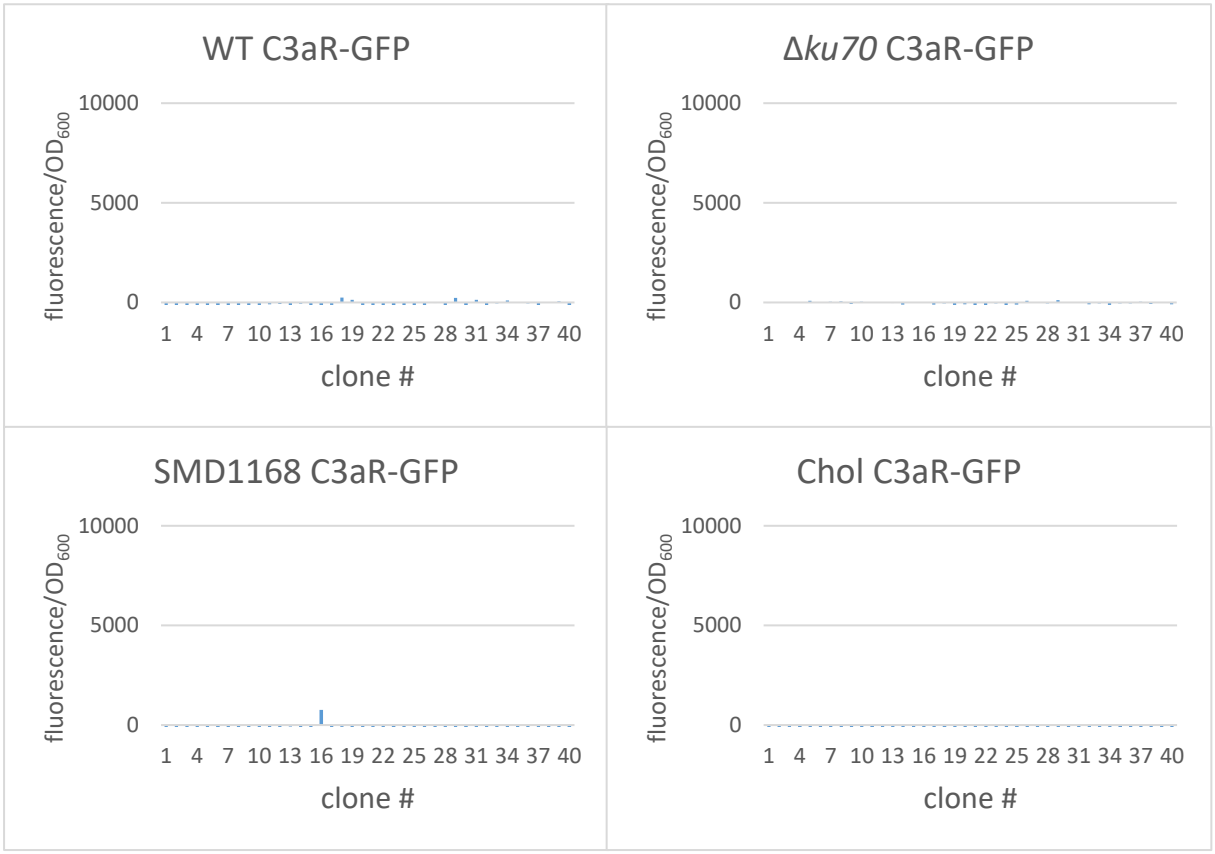

Figure 39: Screening for fluorescence signals in DWPs. The fluorescence values of the eGFP per OD_{600} for 40 clones of the different *P. pastoris* strains WT, Δ*ku70*, SMD1168 and cholesterol strain expressing C3aR-GFP are shown.

3.2.2.4 β_2AR-GFP in protease deficient cholesterol strains

The construction of protease-deficient cholesterol strains was partially successful. It was possible to create the cholesterol strain Δ*pep4* but not the double knock-out cholesterol strain Δ*prb1* Δ*pep4*.

Figure 40 shows the control cut of the ligated vector pPpKC3_pep4 and the linearized vector that was used for transformation into the *P. pastoris* cholesterol strains.

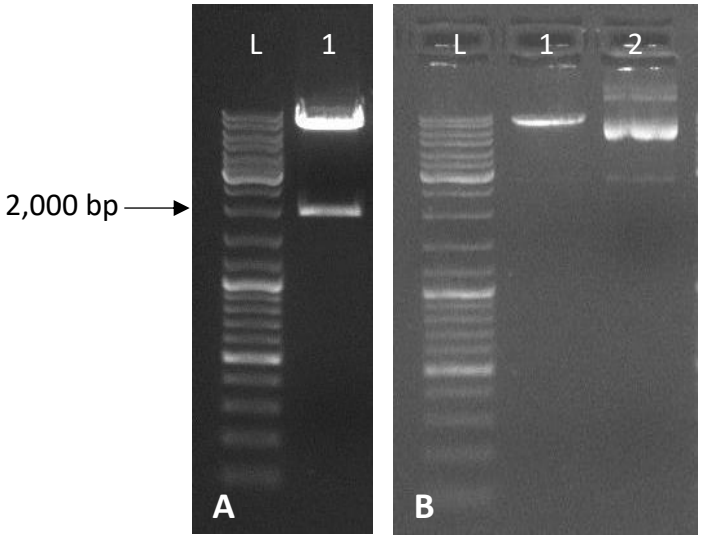

Figure 40: pPpKC3_pep4 vector. (A) L: GeneRuler™ DNA Ladder Mix, 1: control cut with *SfiI*: 7596 and 1936 bp fragments, (B) 1: linearized vector with 9532 bp; 2: uncut vector

After transformation into the *P. pastoris* cholesterol strain and cholesterol strain Δ*prb1*, twenty-four clones per strain were checked for vector integration into the *PEP4* locus via cPCR 1 and cPCR 2. In total, twenty-three of the twenty-four clones had the expression cassette successfully integrated into the *PEP4* locus. Figure 41 shows four and three representative clones, respectively. There was the expected product of 1568 bp but also an unspecific band of about 600 bp in cPCR 1 and 700 bp in cPCR 2 due to low annealing temperatures of 50°C. Negative controls were missing and cannot be shown here.

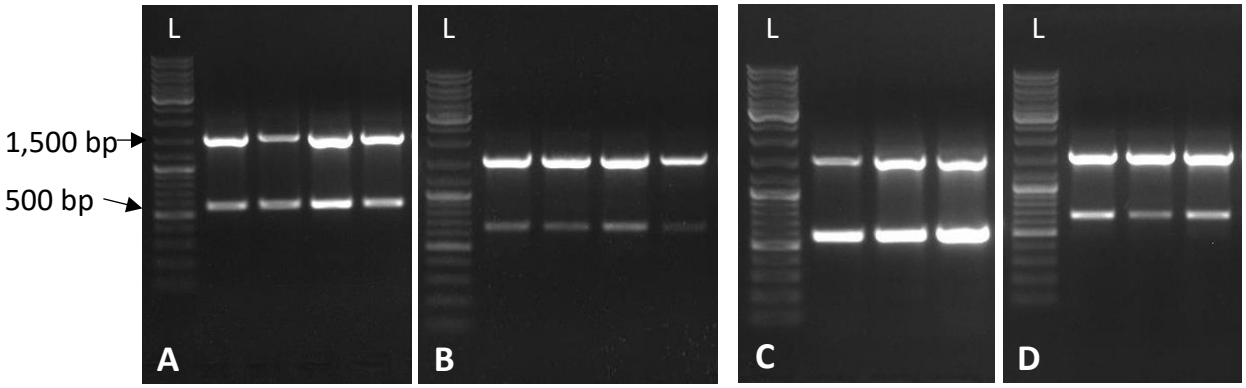

Figure 41: Control cPCRs of expression cassette integration into the *PEP4* locus. L: GeneRuler™ DNA Ladder Mix (A) cPCR 1 cholesterol strain 1-4, (B) cPCR 2 cholesterol strain 1-4, (C) cPCR 1 cholesterol strain Δ*prb1* 1-3 (D) cPCR 2 cholesterol strain Δ*prb1* 1-3

After marker recycling in BMMY medium, the clones were checked with primers specific for the *PEP4* gene via cPCR 3 (Figure 42). The cholesterol strain Δ*pep4* showed only the expected band of 180 bp which meant that the knockout had been successful and the marker had been recycled. The cholesterol strain Δ*prb1* Δ*pep4* showed a band at 180 bp but also an additional one at 1233 bp which represented the original *PEP4* gene. This strain may be a diploid strain or a mixed strain, as it seemed to have two different genome situations.

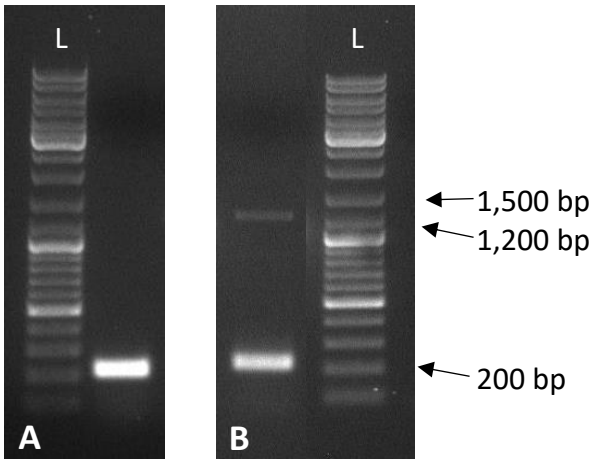

Figure 42: Control cPCRs after marker recycling of protease deficient cholesterol strains. L: GeneRuler™ DNA Ladder Mix. (A) cPCR 3 of cholesterol strain Δ*pep4*: 180 bp product (B) cPCR 3 of cholesterol strain Δ*prb1* Δ*pep4*: 180 bp and 1233 bp fragment

Nonetheless, the newly created, protease-deficient cholesterol strains, as well as the pre-existing cholesterol strain Δ*prb1*, were transformed with the β_2AR-GFP construct to check for better signals. Unfortunately, there was no general increase in fluorescence (Figure 43). Especially the cholesterol strain Δ*prb1* Δ*pep4* showed very low signals.

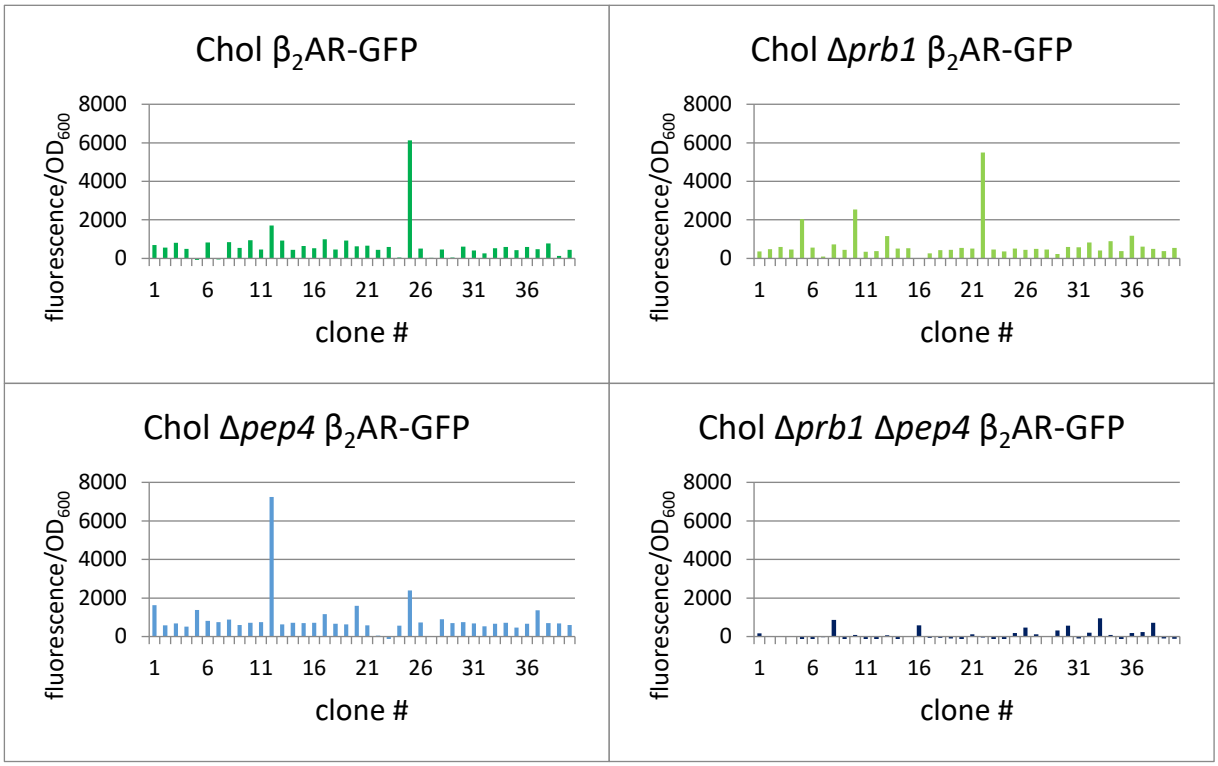

Figure 43: Screening for fluorescence signal in DWPs. The fluorescence values of the eGFP per OD_{600} for 40 clones of the *P. pastoris* cholesterol strain, cholesterol strain Δ*prb1*, cholesterol strain Δ*pep4*, cholesterol strain Δ*prb1* Δ*pep4* expressing β_2AR-GFP are shown.

3.2.2.5 C3aR-GFP in protease deficient cholesterol strains

The two protease-deficient cholesterol strains Δ*prb1* and Δ*pep4* were also transformed with the C3aR-GFP construct in order to get at least any signal for this GPCR, but no fluorescence was observed.

3.2.3 Fluorescence microscopy

3.2.3.1 β_2AR-GFP

3.2.3.1.1 Induction with methanol/sorbitol co-feed

The four best clones per strain of the DWP screening were cultivated, induced and taken for fluorescence microscopy to localize the receptor. Figures 44-47 show one clone per strain that had the best signal. These strains were further sent for functional analysis. The WT and Δ*ku70* strains showed several spots after 5 h of induction and from 24 h on only one patch of signal near the cell periphery could be detected (Figures 44, 45).

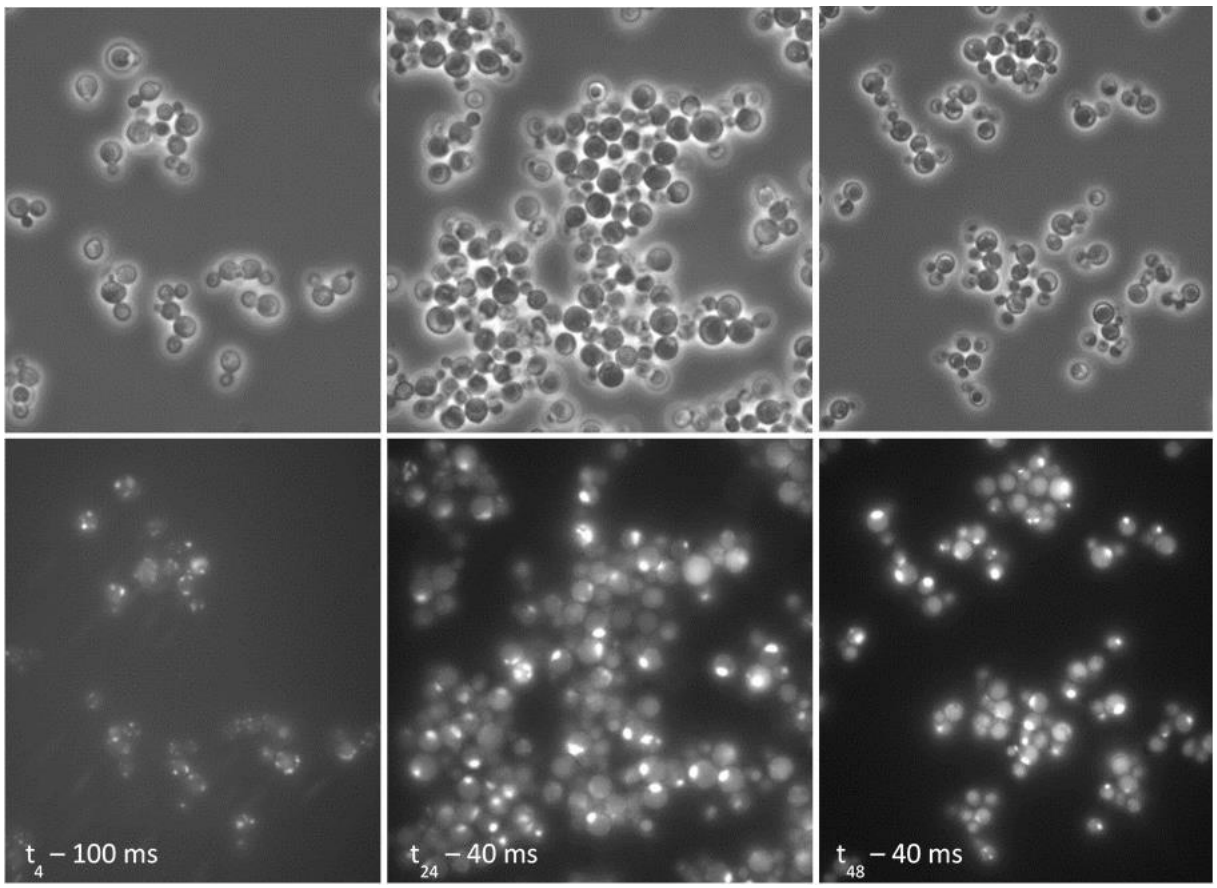

Figure 44: Fluorescence microscopy of *P. pastoris* WT expressing β_2AR-GFP after 4 h, 24 h and 48 h of induction in BMMSY. Upper pictures: phase contrast, lower pictures: fluorescence of eGFP

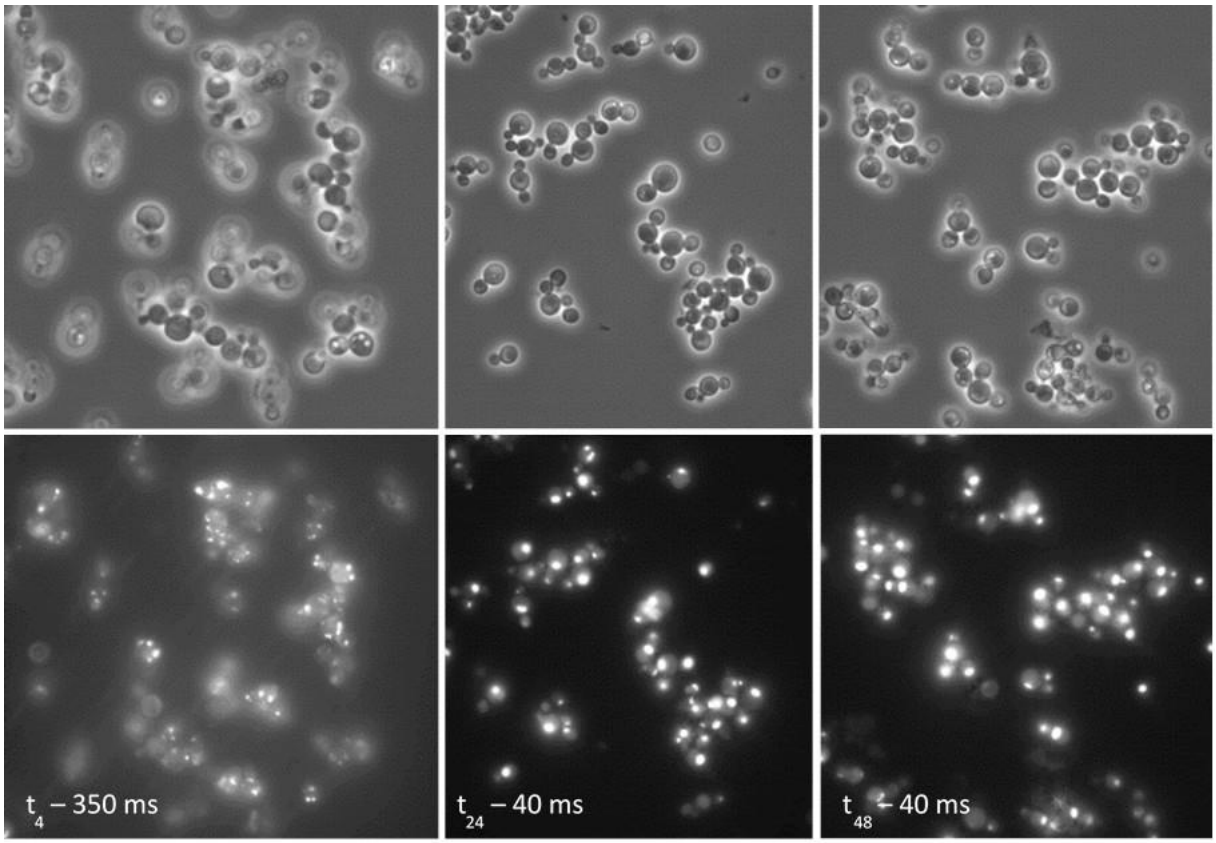

Figure 45: Fluorescence microscopy of *P. pastoris* Δ*ku70* expressing β_2AR-GFP after 4 h, 24 h and 48 h of induction in BMMSY. Upper pictures: phase contrast, lower pictures: fluorescence of eGFP

The SMD1168 strain showed a worse and different signal as there were always several small spots of signal beside undefined diffuse signal (Figure 46).

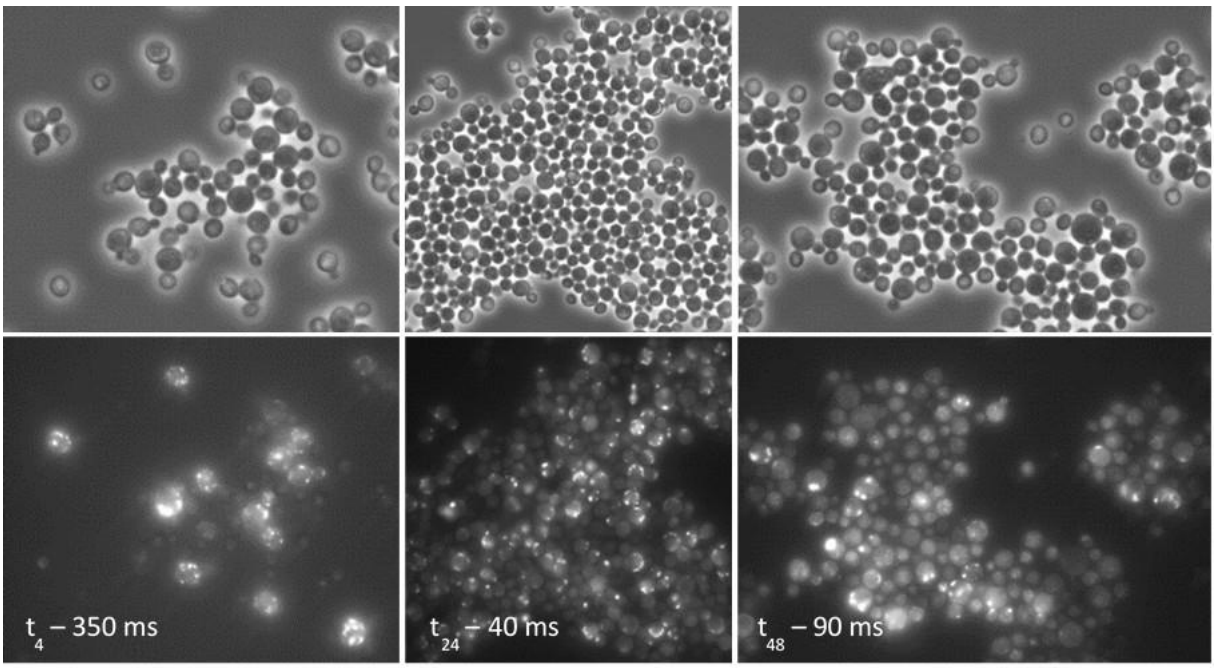

Figure 46: Fluorescence microscopy of *P. pastoris* SMD1168 expressing β_2AR-GFP after 4 h, 24 h and 48 h of induction in BMMSY. Upper pictures: phase contrast, lower pictures: fluorescence of eGFP

The cholesterol strain showed a weaker signal too which was partly in the vacuole and partly in some spots near the cell periphery (Figure 47).

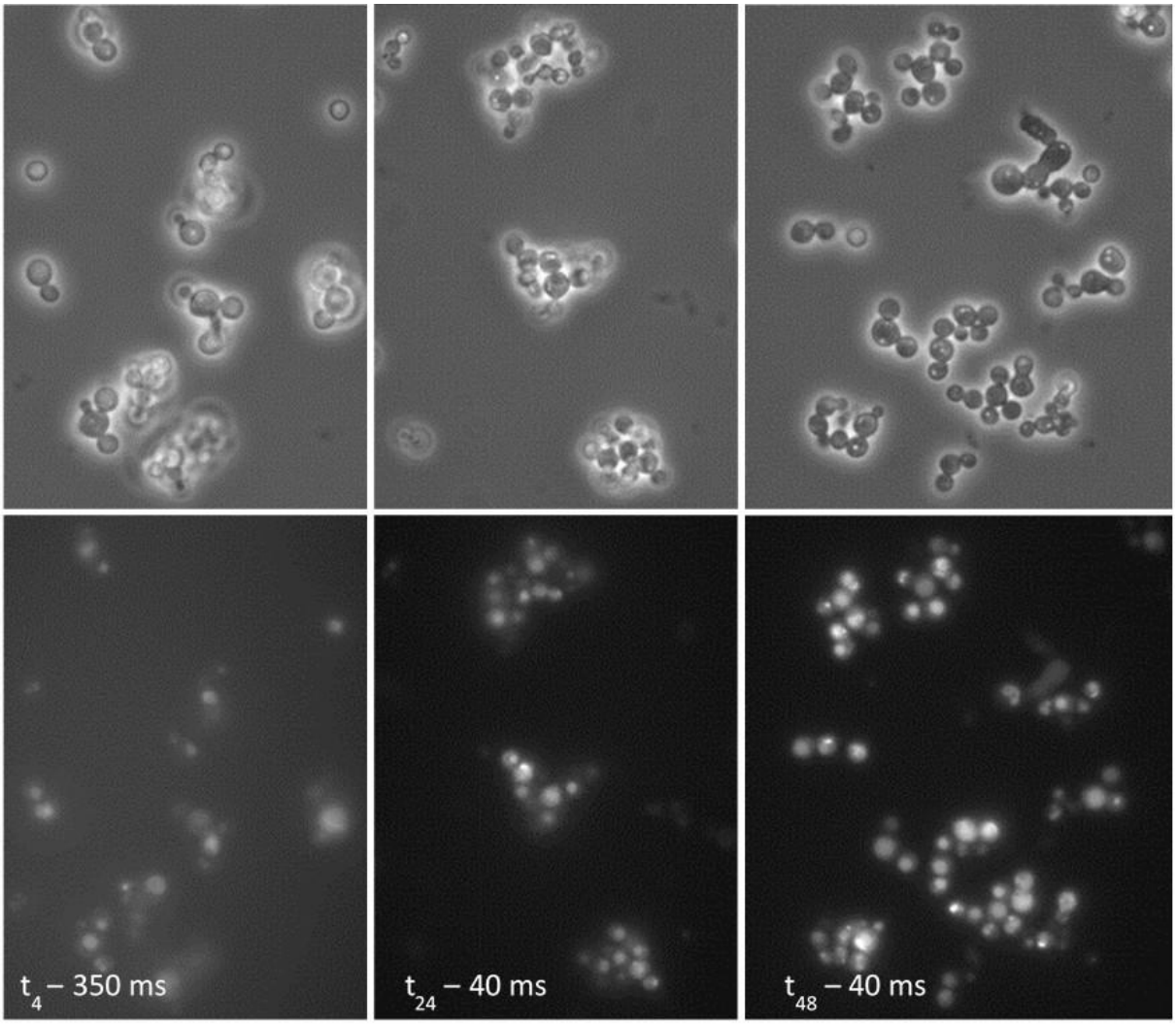

Figure 47: Fluorescence microscopy of *P. pastoris* cholesterol strain expressing β_2AR-GFP after 4 h, 24 h and 48 h of induction in BMMSY. Upper pictures: phase contrast, lower pictures: fluorescence of eGFP

3.2.3.1.2 Comparison of methanol/sorbitol co-feed with standard methanol induction

The clones were first induced with the methanol/sorbitol co-feed strategy for fluorescence microscopy in order to decrease receptor transport to the vacuole. Two clones that were further analyzed in more detail, the Δ*ku70* and the cholesterol strain expressing β_2AR-GFP, were also induced in parallel with the standard methanol induction protocol and the images of the fluorescence signals were compared (Figures 48, 49). The cholesterol strain with standard BMMY induction showed a strong signal of several spots near the cell periphery that differed from the BMMSY induction. Here, the signal was weaker, only one patch was visible and also the vacuole was stained (Figure 48). These images were comparable to the first microscopy pictures with BMMSY induction (Figure 47).

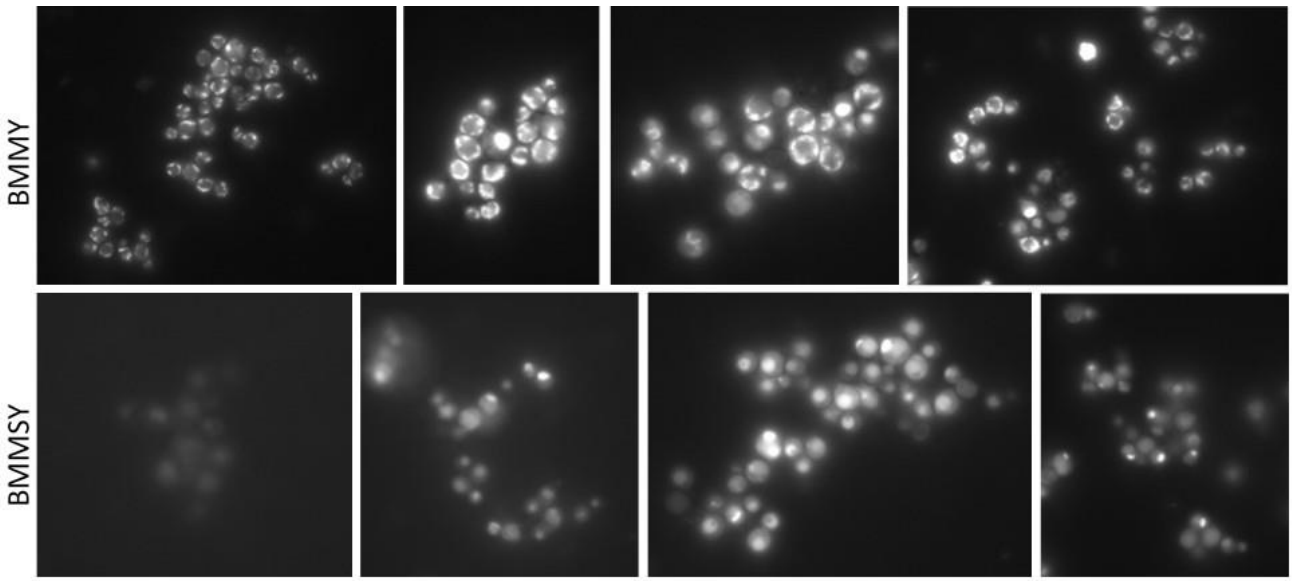

Figure 48: Fluorescence microscopy of *P. pastoris* cholesterol strain expressing β_2AR-GFP Upper pictures: Induction with standard BMMY: t_5 (40 ms), t_{24} (30 ms), t_{48} (30 ms), t_{72} (30 ms). Lower pictures: Induction with methanol/sorbitol co-feed (BMMSY): t_5 (350 ms) t_{24} (110 ms), t_{48} (90 ms), t_{72} (35 ms).

The Δ*ku70* strain showed the same image. With BMMY induction the signal was strong and several spots near the cell periphery were visible, whereas the BMMSY induction showed less structures and only this one patch of signal (Figure 49).

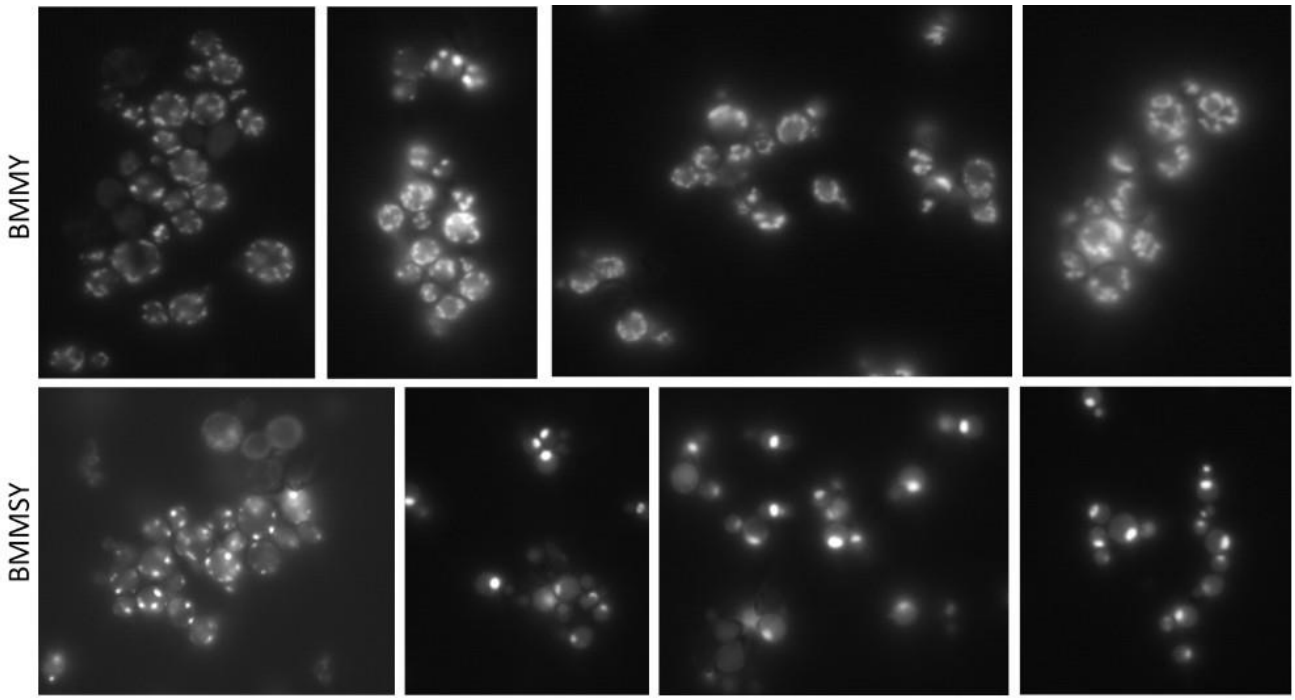

Figure 49: Fluorescence microscopy of *P. pastoris* Δ*ku70* expressing β_2AR-GFP. Upper pictures: Induction with standard BMMY. t_5 (40 ms), t_{24} (20 ms), t_{48} (10 ms), t_{72} (15 ms); Lower pictures: Induction with methanol/sorbitol co-feed (BMMSY): t_5 (300 ms), t_{24} (30 ms, t_{48} (25 ms), t_{72} (15 ms).

3.2.3.2 hB1R-GFP

Again, the four best clones of hB1R-GFP expressing strains identified in the DWP screening were cultivated, induced with BMMSY and analyzed by fluorescence microscopy to localize the receptor. Figures 50-53 show one clone per strain that had the best signal. In principle, the signals correspond to the β_2AR-GFP expressing strains. The WT strain showed one strong patch of signal (Figure 51). The Δ*ku70* and the cholesterol strain had a weaker signal of one spot and also a stained vacuole (Figure 50, 52). The SMD1168 strain showed again several spots of signal (Figure 53).

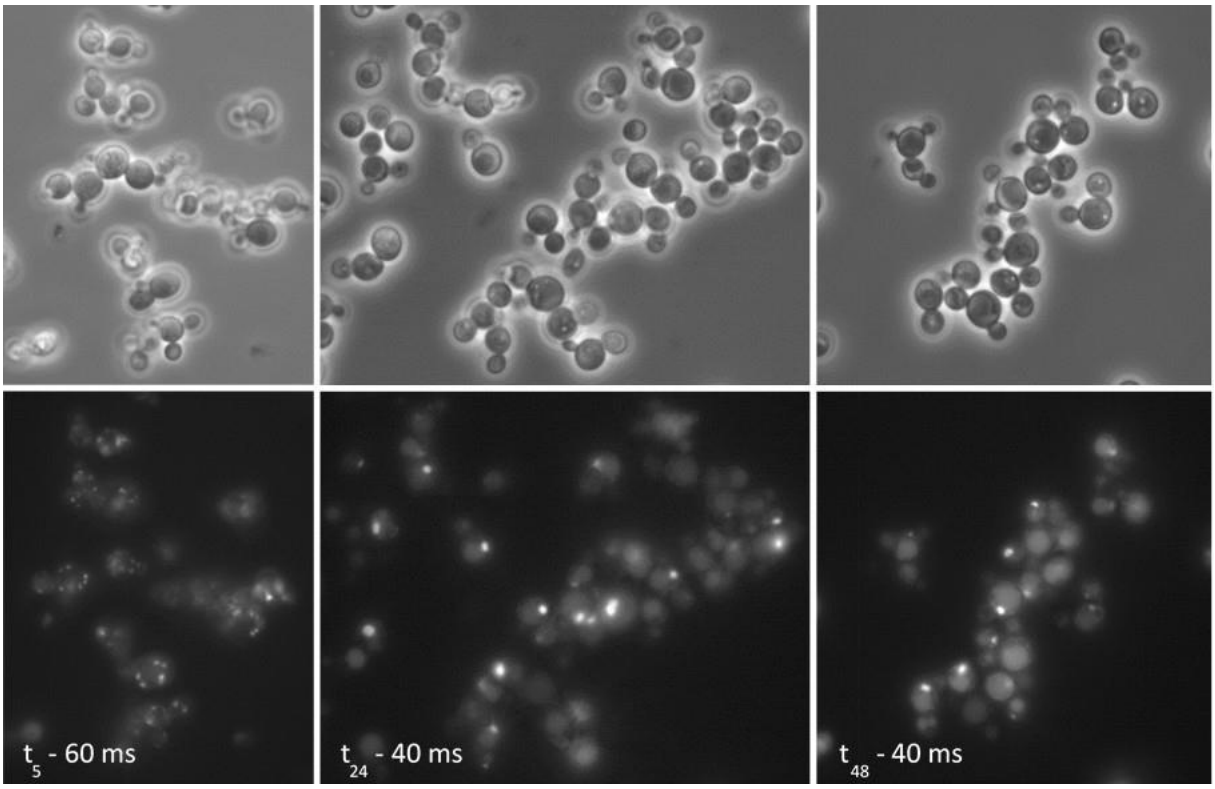

Figure 50: Fluorescence microscopy of *P. pastoris Δku70* expressing hB1R-GFP after 5 h, 24 h and 48 h of induction in BMMSY. Upper pictures: phase contrast, lower pictures: fluorescence of eGFP.

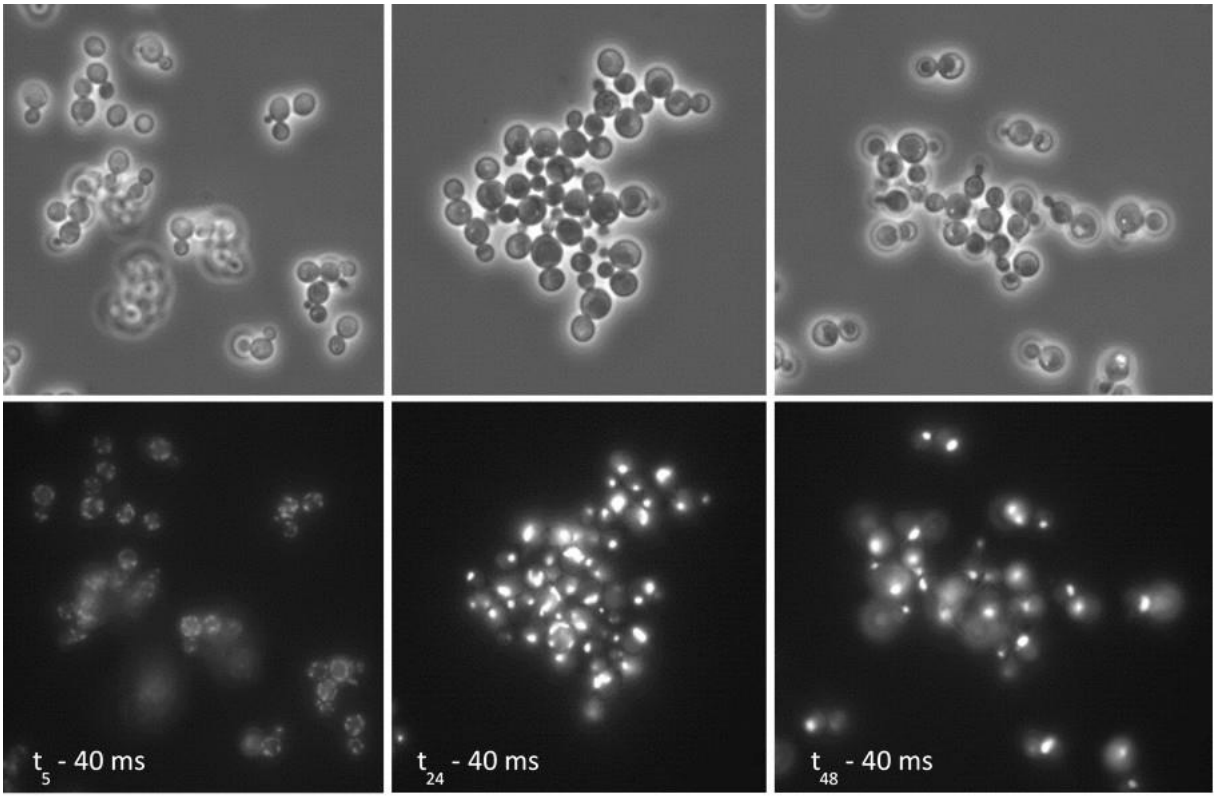

Figure 51: Fluorescence microscopy of *P. pastoris* WT expressing hB1R-GFP after 5 h, 24 h and 48 h of induction in BMMSY. Upper pictures: phase contrast, lower pictures: fluorescence of eGFP.

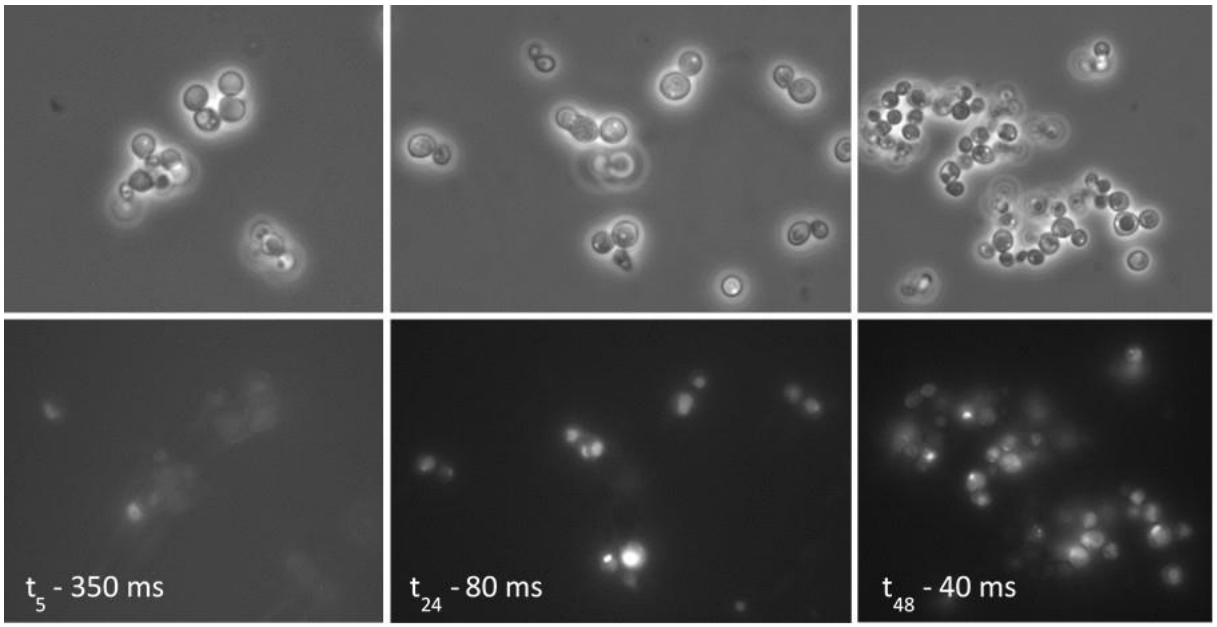

Figure 52: Fluorescence microscopy of *P. pastoris* cholesterol strain expressing hB1R-GFP after 5 h, 24 h and 48 h of induction in BMMSY. Upper pictures: phase contrast, lower pictures: fluorescence of eGFP.

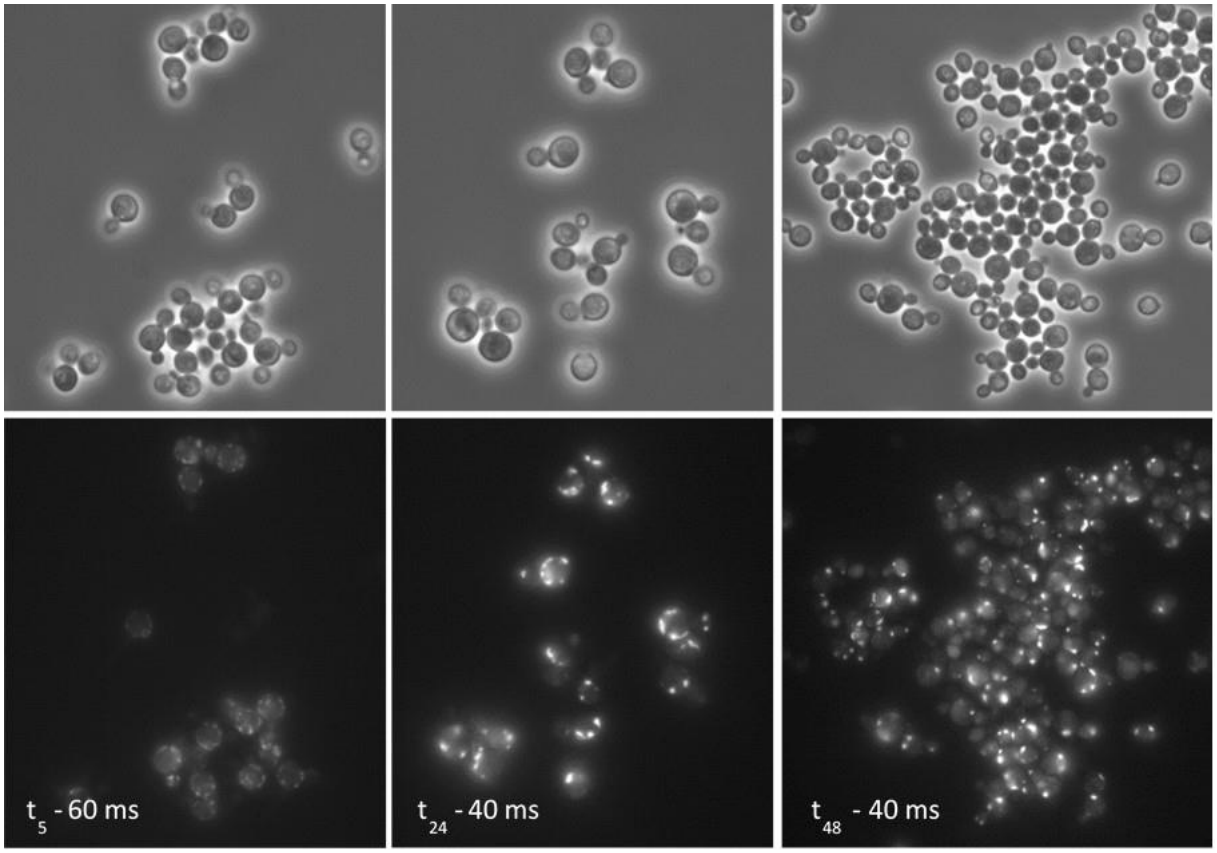

Figure 53: Fluorescence microscopy of *P. pastoris* SMD1168 expressing hB1R-GFP after 5 h, 24 h and 48 h of induction in BMMSY. Upper pictures: phase contrast, lower pictures: fluorescence of eGFP.

3.2.4 Functional analysis

3.2.4.1 β_2AR

One clone per strain of the eGFP-tagged construct that had been characterized by fluorescence microscopy was sent for functional analysis to Christoph Reinhart (Max-Planck-Institute, Frankfurt, Germany). Also, two clones of the StrepII-tagged construct were sent, which had shown a signal in the WB analysis especially when total microsomes were isolated. Table 17 lists the results of the functional analysis. The cholesterol strain seemed to have the highest fluorescence signal for the eGFP and expressed the most active eGFP-tagged receptor although the fluorescence microscopy and the DWP screening had shown a weaker signal compared to the other strains. The other strains with the eGFP-tagged constructs expressed much less active receptor. The two strains with the StrepII-tagged constructs showed only little active receptor which corresponded to the WB analysis with the reference strains of Christoph Reinhart. Additionally, the obtained values confirmed that the cholesterol strain expressed more receptor than the SMD1168 strain.

The two SMD1163 reference strains that should express 20 and 50 pmol/mg of β_2AR, showed much less signal in the measurement with our strains. The exact values, however, were not announced by C. Reinhart.

Table 17: Functional analysis of β_2AR with the antagonist [3H](-)CGP-12177. Listed are (A) the pmol of bound ligand per mg of total membrane protein, (B) the RFU (=relative fluorescence units) per 100 µg of membrane protein and (C) the pmol of bound ligand per 100 RFU. The shown values are the mean of measurements in triplicate.

		A	B	C
***P. pastoris* strain**	construct	pmol/ mg	RFU/ 100 µg	pmol/ 100 RFU
Cholesterol	pPpHygαHisβ$_2$ARTeveGFP	12.17	652.66	4.66
SMD1168	pPpHygαHisβ$_2$ARTeveGFP	2.75	280.89	2.44
Δ*ku70*	pPpHygαHisβ$_2$ARTeveGFP	1.47	356.01	1.03
WT	pPpHygαHisβ$_2$ARTeveGFP	0.88	556.36	0.40
Cholesterol (#3)	pPpHygαHisβ$_2$ARStrepII	0.73	-	-
SMD1168 (#5)	pPpHygαHisβ$_2$ARStrepII	0.20	-	-

3.2.4.2 hB1R

One clone per hB1R-GFP expressing strain was also sent for functional analysis. However, no ligand binding could be detected.

Figure 54 shows a WB against the hB1R N-terminal His-tag of isolated membranes of the sent strains. The expressed hB1R-GFP should have a predicted size of 73 kDa. Here, several bands from 50 up to 80 kDa were visible which made it difficult to interpret which band represented the monomeric form of the hB1R-GFP. According to Christoph Reinhart, the Δ*ku70* and cholesterol strains showed less signal of the receptor than the WT and SMD1168 strain. These observations would correspond to the results of the fluorescence microscopy.

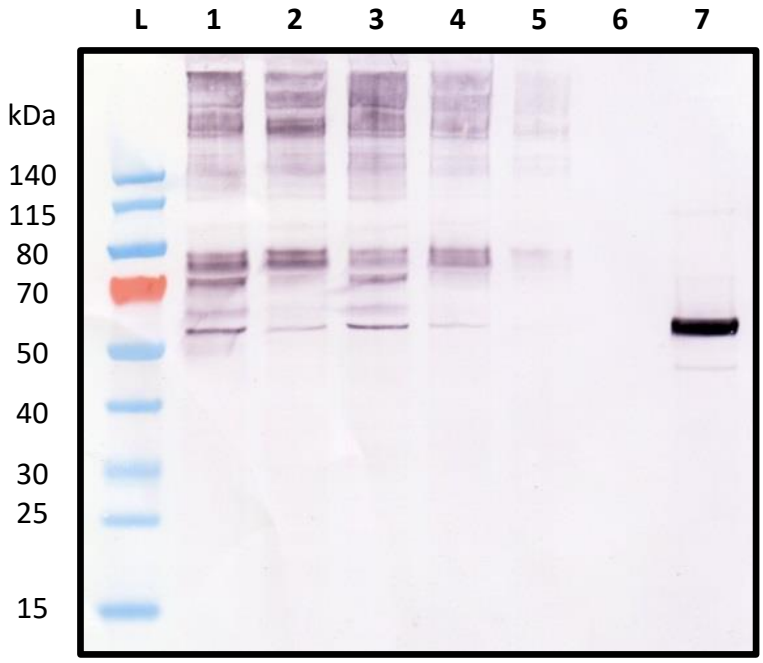

Figure 54: His-blot of prepared membranes of *P. pastoris* strains expressing hB1R-GFP. 30 µg membranes per lane. 1: WT, 2: Δ*ku70*, 3: SMD1168, 4: cholesterol strain, 5: cholesterol strain DMSO, 6: empty, 7: positive control H10M11-VKORC1L1 (GAP1)

3.2.5 Cell fractionation

Two clones that were sent for functional analysis and showed good signals of active receptor, were taken to analyze the localization of the receptor in more detail. Here, the cholesterol strain expressing β_2AR-GFP as well as the Δ*ku70* strain expressing β_2AR-GFP were chosen for cell fractionation. Figure 55 shows that the protein pattern of the two strains was quite similar.

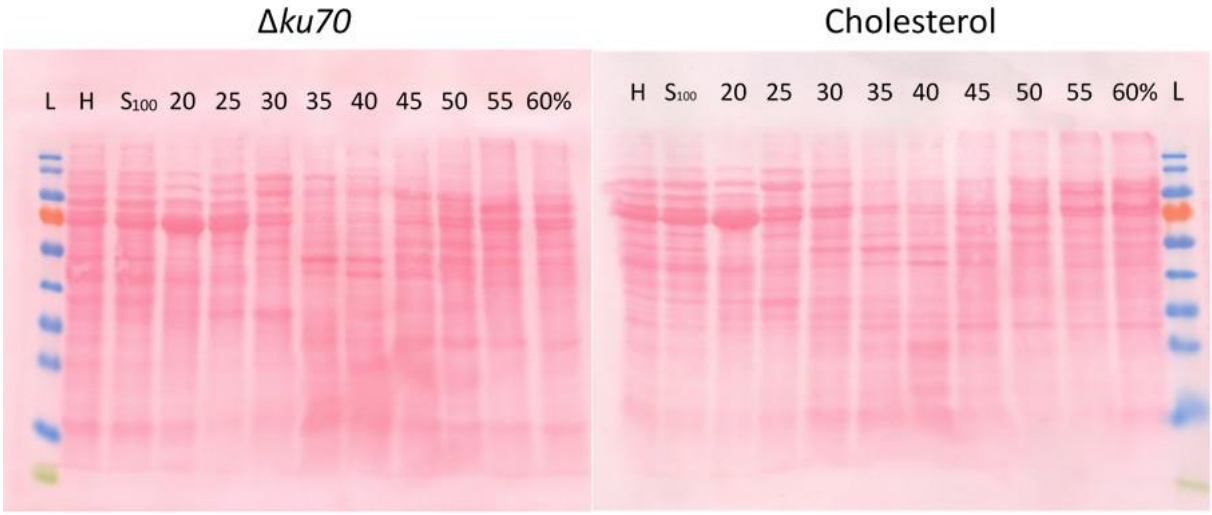

Figure 55: Protein pattern after cell fractionation of the *P. pastoris* Δ*ku70* and cholesterol strain expressing β_2AR-GFP. H… homogenate, S_{100}… supernatant after 100 000 x g (= cytosol), 20-60%... microsomal fraction in 20-60% sucrose, L: PageRuler™ Prestained Protein Ladder

In Figure 56 different immunoblots of the protein fractions are shown. The β_2AR was detected with the anti-His antibody. Different other antibodies were applied to visualize the localization of several marker proteins that are representing the plasma membrane (Pma1p, Gas1p), the ER (HDEL, ER 40 kDa), the mitochondria (Por1p) and the peroxisomes (AOX1p).

The β_2AR localized in both strains in the dense fractions of 55-60% and showed a size of about 100 kDa. The two plasma membrane markers had the predicted sizes of 100 kDa for the Pma1p and 130 kDa for the Gas1p[54], and showed the same localization pattern in each case, however, it differed between the two strains. In the Δ*ku70* strain they were visible in the 45-50% fractions whereas in the cholesterol strain they were in the 50-55% fractions. By comparison, the localization pattern of the two plasma membrane markers was more overlapping with the localization of the β_2AR in the cholesterol strain. This fact might indicate that in the cholesterol strain, there was more β_2AR transported and maybe also stabilized in the plasma membrane.

The HDEL marker did not give any indication of the receptor localization as the pattern looked the same in the two strains. The ER 40 kDa marker overlapped with the plasma membrane markers which could indicate that the ER 40 kDa marker protein might be a plasma membrane associated protein in *P. pastoris*. The mitochondrial porin with 30 kDa localized differently in the two strains. The Aox1p in the Δ*ku70* strain was only seen as faint bands in the dense fractions whereas in the cholesterol strain there were strong bands in the 25-30% and also in the 50-60% fractions. This little amount of Aox1p in the Δ*ku70* strain indicated a possible MutS phenotype which was later confirmed by streaking the strain out onto MDH and MMH agar plates.

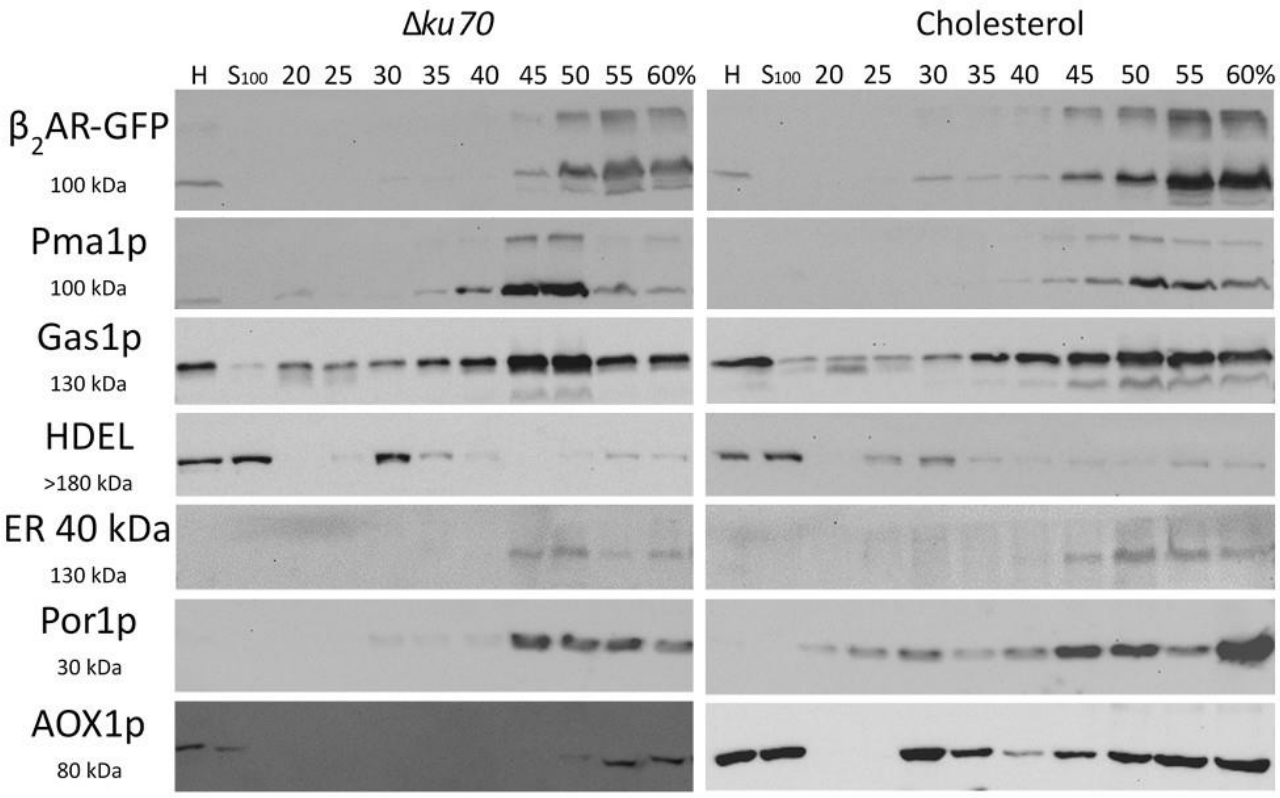

Figure 56: Immunoblot of different marker proteins after cell fractionation of the *P. pastoris* Δ*ku70* and cholesterol strains expressing β_2AR-GFP. H… homogenate, S_{100}… supernatant after 100,000 x g (= cytosol), 20-60%... microsomal fraction in 20-60% sucrose, Pma1p: plasma membrane H^+-ATPase, Gas1p: plasma membrane GPI anchored β-(1,3)-glucanosyl transferase, HDEL: ER retention signal, ER 40 kDa: 40 kDa protein of ER, Por1p: 30 kDa porin in outer mitochondrial membrane, Aox1p: alcohol oxidase 1 in peroxisomes

To monitor time-dependent receptor expression, 1 ml samples were taken during cultivation of these two strains and total microsomes were isolated as described in sections 2.2.6.1.1 and 2.2.7.1.1. The microsomal fractions were then analyzed via SDS-PAGE and WB against the N-terminal His-tag (Figure 57). The PonceauS stain confirmed the low abundance of the Aox1p in the Δ*ku70* strain. The Δ*ku70* strain had the most intense band of the β_2AR after 8 h of induction and then the signal decreased. By contrast, the cholesterol stain showed a slightly increasing signal over induction time. This trend was comparable with the first WBs of the StrepII-tagged receptors and indicated a stabilized receptor in the cholesterol strain.

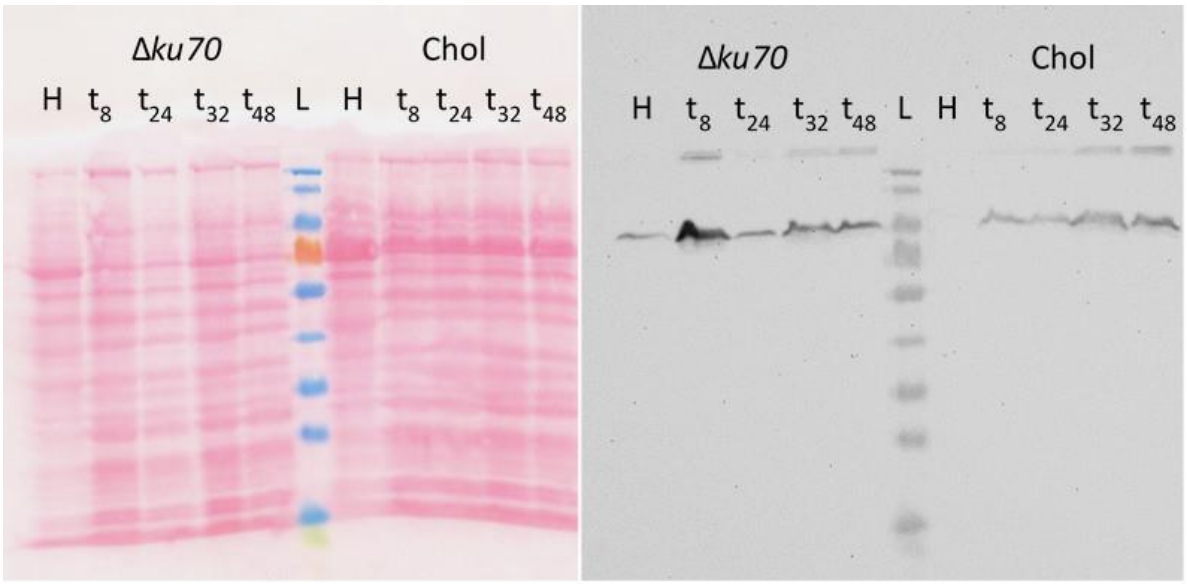

Figure 57: SDS-PAGE (12.5%) and WB of microsomal samples of *P. pastoris* Δ*ku70* and cholesterol strain expressing β_2AR-GFP. H = homogenate, $t_{8\text{-}48}$: total microsome fractions after 8-48 h induction with MeOH, left: PonceauS staining of nitrocellulose membrane, right: immunodetection with anti-His antibody; L: PageRuler™ Prestained Protein Ladder

3.3 Expression of GPCRs under the control of P_{GAP}

3.3.1 Construction of GPCR expression vectors under P_{GAP}

Figure 58 shows the restriction analysis of the assembled vectors after the double digest with the restriction enzymes *SacI* and *PstI*. Table 18 lists the expected fragment sizes of the new pPpHyg**pGAP**αHisGPCRStrepII/TeveGFP vectors and the corresponding negative control vectors pPpHygαHisGPCRStrepII/TeveGFP.

Table 18: Expected fragment sizes of the new pPpHygpGAPαHisGPCRStrepII/TeveGFP vectors and the negative control vectors pPpHygαHisGPCRStrepII/TeveGFP after double digest with *SacI* and *PstI*.

Vector pPpHyg-	Expected fragment sizes (bp)				
αHisβ$_2$ARStrepII	1055	1188	1394	2163	
pGAPαHisβ$_2$ARStrepII	1394	1798	2163		
αHishB1RStrepII	1055	1394	3246		
pGAPαHishB1RStrepII	1394	3856			
αHisC3aRStrepII	668	1055	1188	1394	1777
pGAPαHisC3aRStrepII	668	1188	1394	2387	
αHisβ$_2$ARTeveGFP	1055	1188	1394	2871	
pGAPαHisβ$_2$ARTeveGFP	1394	1798	2871		
αHishB1RTeveGFP	1055	1394	3954		
pGAPαHishB1RTeveGFP	1394	4564			
αHisC3aRTeveGFP	668	1055	1394	1777	1896
pGAPαHisC3aRTeveGFP	668	1394	1896	2387	

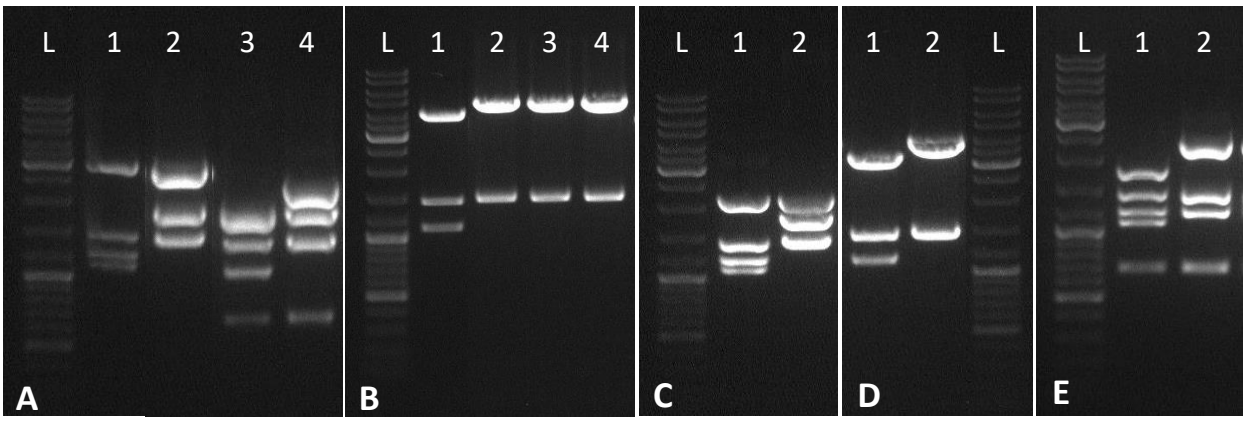

Figure 58: Restriction analysis of assembled pPpHygpGAPαHisGPCRStrepII/TeveGFP vectors with *SacI* and *PstI*. L: GeneRuler™ DNA Ladder Mix.
(A) 1: negative control pPpHygαHisβ$_2$ARTeveGFP 2: pPpHygpGAPαHisβ$_2$ARTeveGFP
3: negative control pPpHygαHisC3aRTeveGFP, 4: pPpHygpGAPαHisC3aRTeveGFP
(B) 1: negative control pPpHygαHishB1RTeveGFP, 2-4: pPpHygpGAPαHishB1RTeveGFP
(C) 1: negative control pPpHygαHisβ$_2$ARStrepII, 2: pPpHygpGAPαHisβ$_2$ARStrepII
(D) 1: negative control pPpHygαHishB1RStrepII, 2: pPpHygpGAPαHishB1RStrepII
(E) 1: negative control pPpHygαHisC3aRStrepII, 2: pPpHygpGAPαHishB1RStrepII

A summary of the vector constructs under the control of P_{GAP} is shown in Table 19. After sequencing of several vectors, the construct pPpHygpGAPαHishB1RTeveGFP had to be dropped because of critical mutations around the start codon. The pPpHygpGAPαHisC3aRStrepII construct had no mutations but was not transformed into *P. pastoris* as it was not promising to give signals.

Table 19: Vector constructs with P_{GAP}, sequencing result and transformation into *P. pastoris*

vector	sequencing	transformed
pPpHygpGAPαHisβ$_2$ARStrepII	No mutation	yes
pPpHygpGAPαHishB1RStrepII	No mutation	yes
pPpHygpGAPαHisC3aRStrepII	No mutation	no
pPpHygpGAPαHisβ$_2$ARTeveGFP	No mutation	yes
pPpHygpGAPαHishB1RTeveGFP	mutations	no
pPpHygpGAPαHisC3aRTeveGFP	No mutation	yes

Nevertheless, four of the six vectors pPpHygpGAPαHisGPCR-StrepII/TeveGFP were linearized with *SmiI*, purified and analyzed via agarose gel electrophoresis (Figure 59).

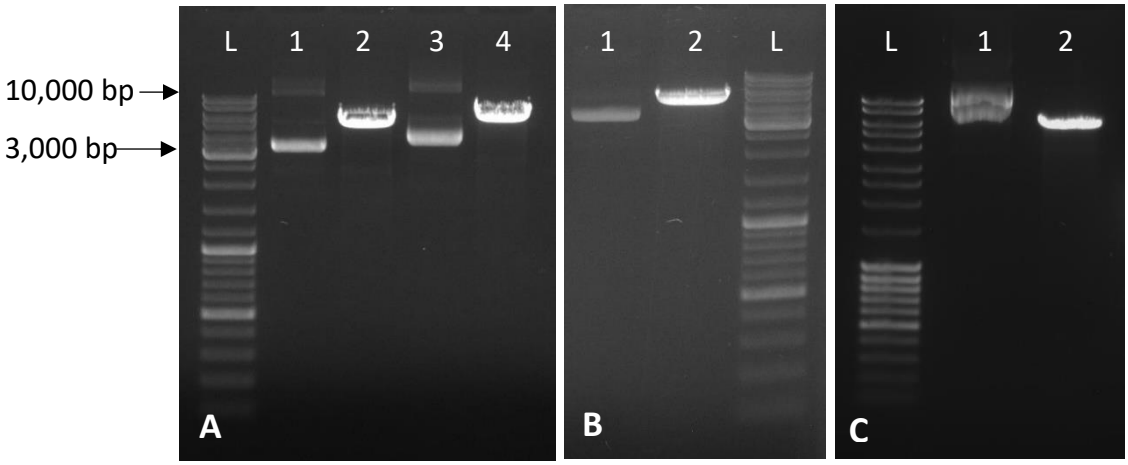

Figure 59: Linearized pPpHygpGAPαHisGPCR-StrepII/TeveGFP vectors with *SmiI*. L: GeneRuler™ DNA Ladder Mix, (A) 1,2: pPpHygpGAPαHisβ$_2$ARStrepII uncut/cut (5355 bp), 3,4: pPpHygαHisβ$_2$ARTeveGFP uncut/cut (6063 bp), (B) 1,2: pPpHygpGAPαHishB1RStrepII uncut/cut (5250 bp), (C) 1,2: pPpHygpGAPαHisC3aRTeveGFP uncut/cut (6345 bp)

3.3.2 Transformation of GPCR expression vectors under P_{GAP}

Unfortunately, the transformation efficiency of the expression constructs under the control of P_{GAP} was not as high as with the first constructs under P_{AOX1}. Especially the Δ*ku70* and the cholesterol strain showed only very few transformants.

3.3.3 Analysis of C-terminally StrepII-tagged constructs

The C-terminally StrepII-tagged constructs of all three GPCRs were correctly assembled, but only the β_2AR and hB1R constructs were linearized and transformed into *P. pastoris*. Transformants were cultivated in several 96-DWPs and analyzed via DotBlot, but no signal was obtained with one of the two GPCRs.

3.3.4 Analysis of C-terminally eGFP-tagged constructs

The C-terminally eGFP-tagged constructs were assembled for the β_2AR and C3aR cassettes. They were linearized, transformed into *P. pastoris* and screened for fluorescence signal in DWP cultivation.

3.3.4.1 Screening in DWP for fluorescence signal

3.3.4.1.1 β_2AR-GFP

Several transformations were performed with the pPpHygαHispGAPβ$_2$ARTeveGFP construct. Several DWPs were filled with YPD or BMGY and were inoculated with clones of each strain but only two clones showed a fluorescence signal that was clearly above the background (Figure 60). They were further named WT #21 and SMD1168 #13. The values for the fluorescence/OD_{600} were about 10x lower compared to the expression under the control of P_{AOX1}.

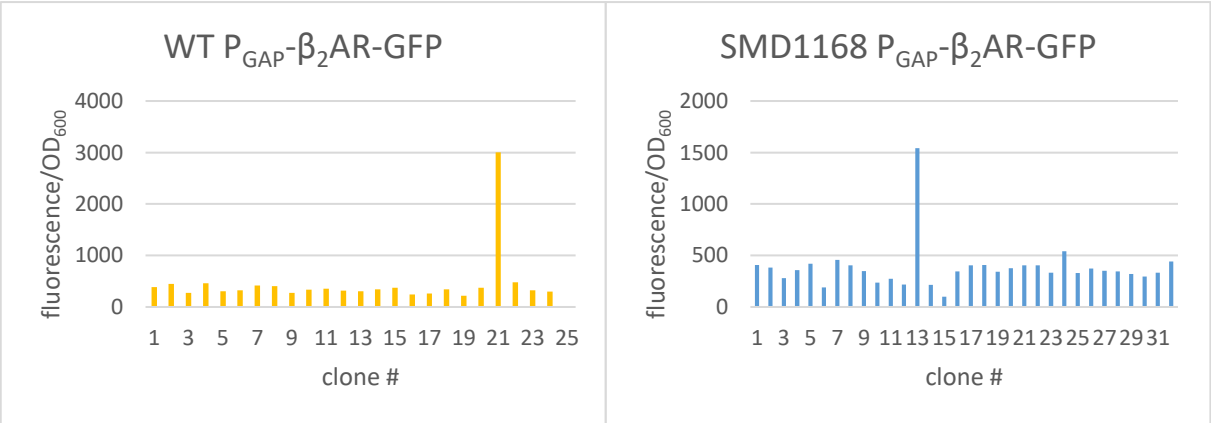

Figure 60: Screening for fluorescence signal in DWPs. The eGFP fluorescence values per OD_{600} for the different *P. pastoris* clones in WT and SMD1168 background that were expressing β_2AR-GFP under the control of P_{GAP} are shown. The WT clones were cultivated in YPD, the SMD1168 clones in BMGY.

3.3.4.1.2 C3aR-GFP

As the pPpHygαHispGAPC3aRTeveGFP vector could be constructed without mutations, one attempt was made to measure possible fluorescence for the C3aR under the control of P_{GAP}. Figure 61 shows the results of the fluorescence screening but there was no clear signal above the background. All values were below the positive control of the *P. pastoris* WT #21 expressing β_2AR-GFP under P_{GAP} that showed values of about 120 fluorescence units/OD_{600} in this series of experiments.

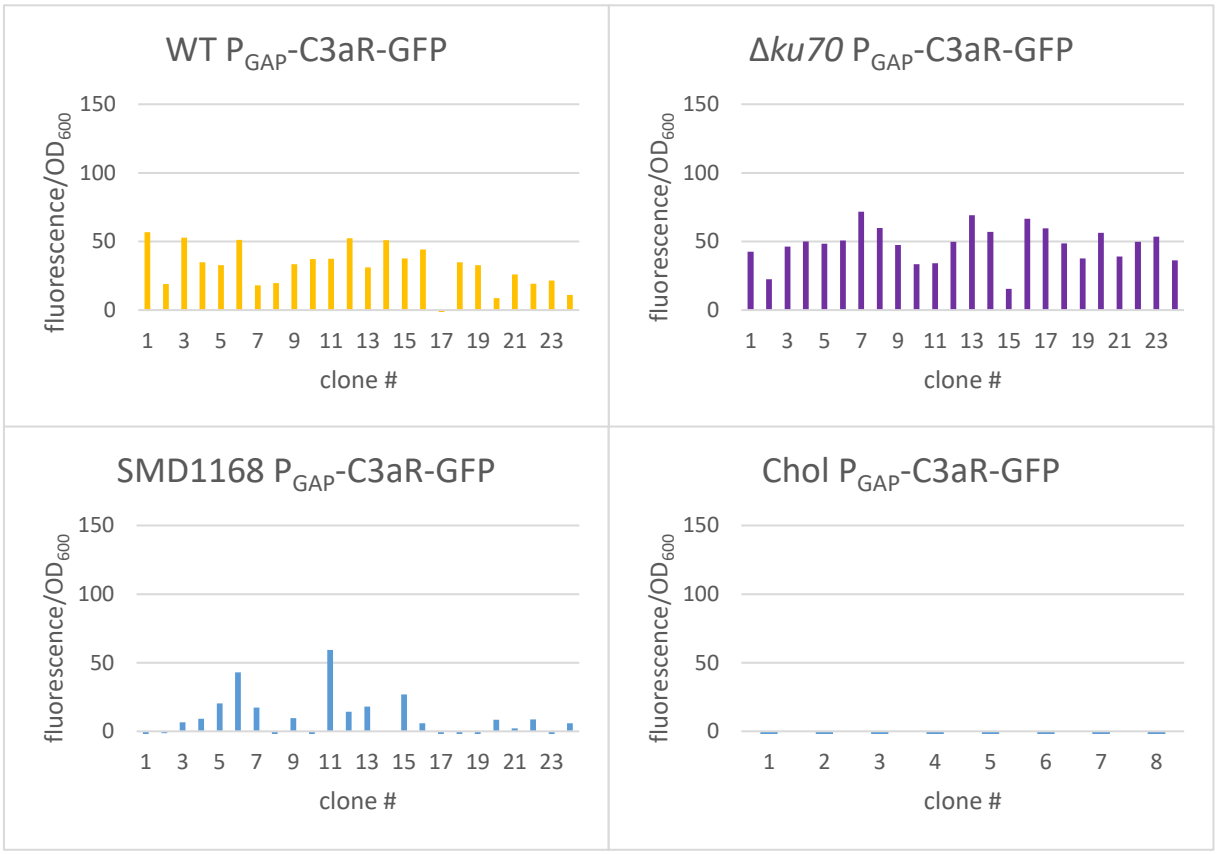

Figure 61: Screening for fluorescence signal in DWPs. The eGFP fluorescence values per OD_{600} for the different *P. pastoris* strains WT, Δ*ku70*, SMD1168 and cholesterol strain that were expressing C3aR-GFP under the control of P_{GAP} are shown.

3.3.4.2 Fluorescence microscopy

As two clones expressing β_2AR-GFP showed a signal in the DWP screening, they were further analyzed by fluorescence microscopy (Figures 62, 63). After cultivation in YPD there was fluorescence but the intensity was much weaker with the P_{GAP} compared to the P_{AOX1}. In the SMD1168 strain the localization looked interesting as it showed an elongated signal next to the plasma membrane. In the WT strain, there were some spots near the cell periphery.

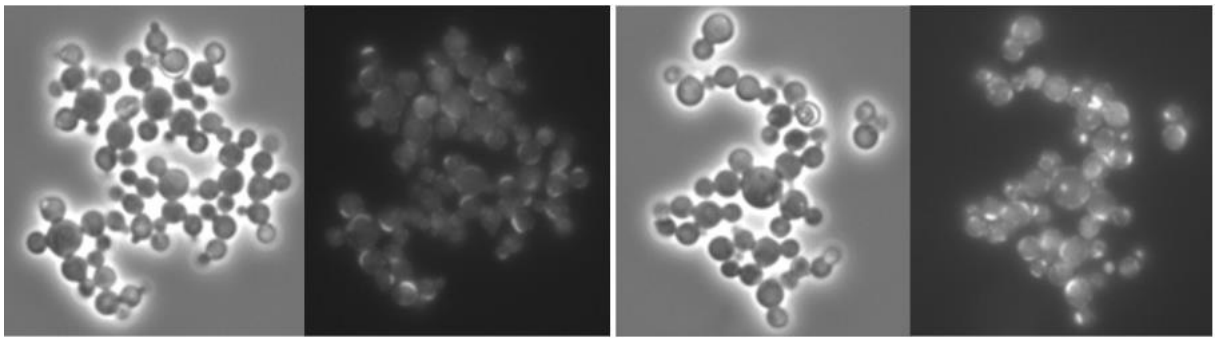

Figure 62: Fluorescence microscopy of *P. pastoris* SMD1168 #13 expressing β_2AR-GFP under P_{GAP} after 24 h growth in YPD. Left pictures: phase contrast and fluorescence of eGFP (110 ms), right pictures: phase contrast and fluorescence of eGFP (350 ms)

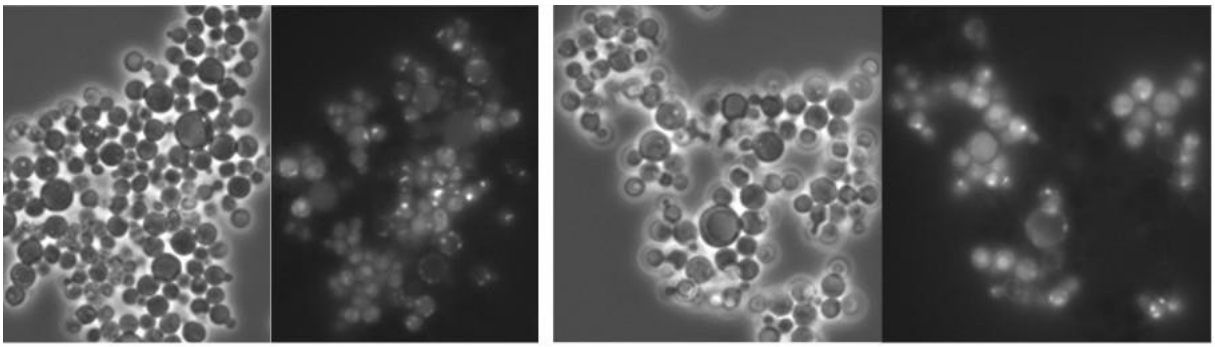

Figure 63: Fluorescence microscopy of *P. pastoris* WT #21 expressing β_2AR-GFP under P_{GAP} after 24 h growth in YPD. Left pictures: phase contrast, right pictures: fluorescence of eGFP (110 ms)

These two strains were also cultivated in BMGY for 24 h and the fluorescence microscopy images showed faint signals of ER and plasma membrane structures as well as a round structure that could represent either the nucleus, or more likely, the vacuole (Figures 64, 65)

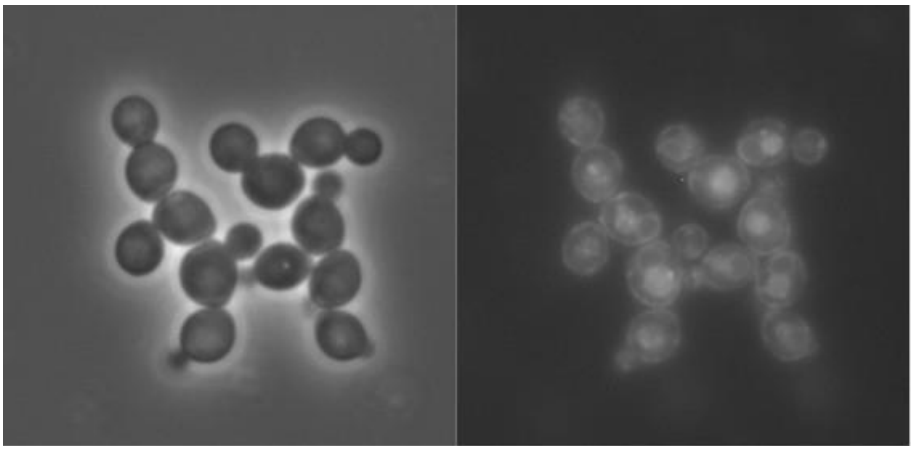

Figure 64: Fluorescence microscopy of *P. pastoris* SMD1168 #13 expressing β_2AR-GFP under the control of P_{GAP} after 24 h growth in BMGY. Left picture: phase contrast, right picture: fluorescence of eGFP (430 ms)

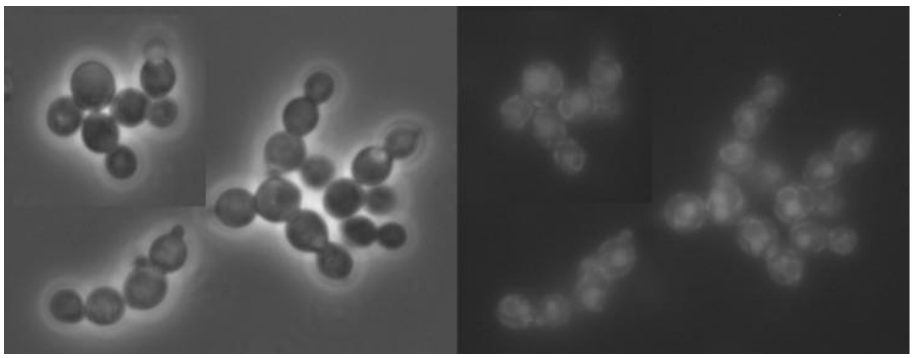

Figure 65: Fluorescence microscopy of *P. pastoris* WT #21 expressing β_2AR-GFP under the control of P_{GAP} after 24 h growth in BMGY. Left picture: phase contrast, right picture: fluorescence of eGFP (350 ms)

4 Discussion

4.1 Expression of β_2AR

4.1.1 StrepII-tagged β_2AR

The C-terminal StrepII-tagged β_2AR could be detected in different strains in the total cell lysates and, even better, in the microsomal fractions. The first WB experiments showed that the cholesterol strain tended to express a stable receptor as the signal got stronger over induction time whereas in the other strains the signal always decreased and had the strongest signal after 8 hours of induction. This indicated that the receptor was less stable without cholesterol in the plasma membrane and was degraded. The expected size of the β_2AR monomer would have been 49.8 kDa which was calculated with the Compute pI/MW online tool of Expasy. In the WB, we saw a band of about 55 kDa which was only slightly bigger and could be due to either a not correctly processed N-terminus or due to some post-translational modifications which may occur naturally in yeast. In addition, the folding state of the membrane protein might influence the apparent migration behavior. There were also undefined bands at a high molecular weight which are representing different forms of oligomeric or aggregated receptor due to its hydrophobicity.

In the determination of possible multiple integration events by qPCR, the cholesterol strain showed a correlation between a possible higher copy number and increasing hygromycin resistance, whereas the WT as well as the Δ*ku70* and the SMD1168 strain did not behave similarly. At the moment, the reason for this phenomenon is not fully understood as the antibiotic hygromycin inhibits protein biosynthesis[68] and should therefore not differentiate between the WT and the cholesterol strain as it does not target the cell wall or the plasma membrane. One possible explanation would be the different growth rate. The *P. pastoris* WT has a specific growth rate of 0.25 h^{-1} whereas the cholesterol strain grows slower with a rate of only 0.11 h^{-1} [52]. This may have caused the difference in growth on high hygromycin concentrations.

The correlation between copy number and hygromycin resistance was confirmed by several quantitative PCR experiments. Those strains that could grow on high hygromycin concentrations and/or showed a signal in the WB, always seemed to have higher copy

numbers than the other strains. The high copy number values of up to 1,000 copies cannot be trusted, as this high number of expression cassettes integrated in the genome is not credible and would mean that every 10,000 bp there was one expression cassette integrated. After the application of different calculation methods, we could be quite sure that the reason for these high values had to do with the strains themselves. On the one hand, the qPCR strategy based on the hygromycin marker was not fully developed, but it was rather a first attempt to find out about possible multiple integration events. There could be, for instance, formation of unspecific products although no substantial evidence was found neither in agarose gel electrophoresis of the PCR products nor in the analysis of the melt curve. Moreover, the values for the copy quantities of the cholesterol strain samples were always outside of the calibration curve. Several attempts to bring these results into the calibration range failed. On the other hand, a possible reason for these high numbers is the reference strain that was only thought to have one copy of the expression cassette integrated. It has never been checked in detail if this assumption is true. Unfortunately, there was no other reference strain available which corresponded to our demands and could be compared to our transformants. The important part of this experiment was to find out whether there was a connection between increased copy numbers and hygromycin resistance in the cholesterol strain. In addition, a connection between signals in the WB and an increased copy number in the SMD1168 strain could be found. In our experiments, the higher copy number seemed to be favorable for heterologous receptor expression, but experience shows that the best copy number for optimal expression levels must always be determined experimentally[13].

One obvious explanation for the higher copy numbers in the cholesterol strains might be the fact that the hygromycin is almost certainly transported out of the cell via a transport protein. The different sterol composition in the cholesterol strain might have affected the activity of these transporters and they might not work as efficiently as in the WT strain background. Souza et al. (2011) described something similar for a transporter of weak organic acids that belongs to the multidrug resistance family[69]. On this assumption, the local concentration of hygromycin was supposedly higher in the cholesterol strain and lead to higher copy numbers of the expression cassette that contained the hygromycin resistance gene.

In the comparative WB of the β_2AR-expressing cholesterol strains and the reference strains of Christoph Reinhart, the cholesterol strains did not show that strong signal anymore as before. Surprisingly, the positive control showed a stronger signal for the β_2AR than the newly

cultivated cholesterol strains although it was the same strain and the same amount of protein was loaded. This observation implied that the expression behavior of one strains can differ from cultivation to cultivation despite the apparently same conditions. Despite this low signal of expressed β_2AR in the cholesterol strains compared to the reference strains, functional analysis revealed that the StrepII-tagged β_2AR was active and that the cholesterol strain expressed more of active β_2AR than the SMD1168 strain.

4.1.2 eGFP-tagged β_2AR

The reason for tagging the GPCR constructs with an C-terminal eGFP was that the eGFP is much easier to screen for, especially for the screening of a great number of clones and it also provides the possibility of receptor localization via fluorescence microscopy.

The fluorescence screening in DWPs did not correlate to our expectations that the β_2AR expression was favored in the cholesterol strain. The eGFP-tagged constructs of the β_2AR did not follow the trend of the StrepII-tagged constructs and did not show a higher level of fluorescence signal. Only single clones showed higher signals irrespective of the strain background. This might be due to different copy numbers or integration loci. The fluorescence microscopy showed that all strains express the β_2AR-GFP to a certain extent. However, the observed structures under the fluorescence microscope were neither conclusive nor the localization of the receptor could be figured out in detail.

The eGFP has already been used to localize a GPCR via fluorescence microscopy[70]. In this study, the authors also got several punctual structures near the cell periphery with standard BMMY induction which were assumed to correspond to local concentrations of intracellular membrane networks, deriving either from the ER or the Golgi. It has to be kept in mind that a hydrophobic membrane protein was highly overexpressed under the control of P_{AOX1}. Therefore, it is possible that the receptor forms aggregates. Moreover, it has been shown that high expression of eGFP in *P. pastoris* can lead to aggregate formation of 5-10 particles per cell[71]. These particles were also seen in 10-fold lower expression of GFP with sorbitol as carbon source.

Concerning the formation of the one strong spot of signal with the BMMSY induction strategy, this may imply the formation of so-called aggresomes. This has been already reported for yeasts[72]. This aggresome formation should be connected to a survival mechanism of the cell

when the proteasomal machinery is overloaded with the overexpression of abnormal proteins. They are either degraded via autophagy, but can also be quite stable[73] as seen in our pictures. Lately, it has been described that it is possible to produce functional inclusion bodies in *P. pastoris*[74]. They resembled inclusion bodies in *E. coli* and were expressed under the control of P_{GAP}.

The functional analysis of the β_2AR-constructs in different strains revealed active receptor even with the eGFP-tagged constructs. Moreover, it confirmed the advantage of the cholesterol strain for receptor functionality. The cholesterol strain could express more active β_2AR per fluorescence unit. The value of about 12 pmol/mg for the β_2AR in the cholesterol strain represented at least a mid-range level expression[75]. The second best strain was the SMD1168 which might express more active receptor than the WT strains due to its protease deficiency. Surprisingly, the standardized fluorescence intensities did not match our values, neither those of the fluorescence screening nor of the fluorescence microscopy images with the BMMSY induction. However, the screening method as well as this special induction in combination with the quality of the fluorescence microscopy images may be misleading concerning the strength of signal. By comparison with the standard BMMY induction, the images of the Δ*ku70* and the cholesterol strain expressing β_2AR-GFP looked quite similar.

The closer look on the localization of the receptor via cell fractionation revealed certain differences of the cholesterol strain compared to its background strain Δ*ku70*. Especially the plasma membrane protein Pma1p and the plasma membrane associated Gas1p showed a slightly different localization pattern. In the cholesterol strain, this pattern was more overlapping to the β_2AR localization which could be a hint that more of the receptor is transported to the plasma membrane and is stably integrated there. The size of the detected β_2AR-GFP was 100 kDa which was again bigger than the calculated size of 77 kDa. This difference is explainable due to aggregation phenomena, post-translational modifications and the fact that a fusion protein was expressed. The localization of the β_2AR-GFP into the dense sucrose fractions might also indicate aggregation processes. The ER 40 kDa marker of *S. cerevisiae* showed bands at 130 kDa in *P. pastoris*. This size shift might be caused by a cross-reaction. As this ER marker co-localized with the plasma membrane markers in *P. pastoris*, the antibody raised against a protein of *S. cerevisiae* might target a plasma membrane associated protein in *P. pastoris.* The WB of the time-dependent expression confirmed a stabilized receptor in the cholesterol strain once more.

The side project of creating protease deficient cholesterol strains did not yield any improvement of receptor expression. Examples were shown with the β_2AR-GFP in Figure 43. In principle, it showed that only single clones had a good signal and there was no trend for generally higher signals in a protease deficient strain. The Δ*prb1* Δ*pep4* double knock-out strain seemed to be completely unable to express the β_2AR-GFP as it showed very low fluorescence signals in the screening. The reason might have been due to its diploid background as the control cPCRs after marker recycling showed corresponding bands for a successful *pep4* knockout but also for a remaining intact *PEP4* locus (Figure 42B). The reason why the double knockout cholesterol strain could not be constructed is not clear. Maybe the cholesterol strain is not able to cope with the knock-out of both, the *pep4* and *prb1* genes.

4.2 Expression of hB1R

In the analysis of hB1R expression, only the eGFP-tagged constructs were analyzed as it was easier to screen more clones. The signals in fluorescence screening in DWPs and in fluorescence microscopy looked quite good and were comparable to the β_2AR-GFP expression. Unfortunately, the functional analysis revealed that the receptor was not active. The first explanation would be that the C-terminal eGFP somehow hindered the functionality of the receptor as the eGFP itself is a quite big tag with a size of about 240 amino acids. The hB1R itself only has about 380 amino acids. The His-Blot with the isolated membranes done by Christoph Reinhart did not give any useful information about hB1R expression either. We could not figure out which of these bands corresponded to our receptor. Anyway, as the expressed hB1Rs were inactive, they were not further analyzed.

4.3 Expression of C3aR

The C3aR could not be detected in any way. Under the control of P_{AOX1}, neither the microsomal samples of the StrepII-tagged constructs in the WB, nor the eGFP-tagged constructs in the fluorescence screening gave a signal. The attempt of expressing the C3aR-GFP in the protease deficient cholesterol strains failed too. The eGFP-tagged construct under the control of P_{GAP} was not successfully expressed either. For this screening, another fluorescence reader was used which was the reason for the generally low fluorescence values compared to previous screenings. Due to the fact that absolutely no signal could be obtained from the C3aR, the question arose whether *P. pastoris* is able to express this receptor at all.

4.4 Expression of GPCRs under the control of P_{GAP}

Unfortunately, the expression of different constructs under the control of P_{GAP} was not successful. On the one hand, the transformation of the constructs was difficult, as the integration efficiency was not as high as compared to the P_{AOX1} constructs. On the other hand, although there was a signal with the β_2AR eGFP-tagged constructs, the signal intensity was much lower than with the P_{AOX1}-driven constructs.

The transformants were cultivated in YPD and BMGY media with glucose or glycerol as the major carbon source. Both of them were reported to be preferable carbon sources for expression under P_{GAP}[76,77]. One WT strain was found to express the β_2AR-GFP in YPD cultivation and one SMD1168 strain with BMGY cultivation. Unfortunately, the transformation with the Δ*ku70* and the cholesterol strain did not work out. Only a few clones were obtained and these did not show a fluorescence signal. Maybe these two strains, which both had the Δ*ku70* background, showed less integration efficiency of the P_{GAP} construct than the other two strains which had a WT background. Nevertheless, the pictures of fluorescence microscopy of the two confirmed clones showed interesting new localization patterns. Especially with the SMD1168 strain cultivated in YPD an elongated structure next to the plasma membrane could be detected which was not found upon expression under the control of P_{AOX1} before. After 24 h of cultivation in BMGY, very faint signals of ER and plasma membrane structures could be seen. These may represent the initial localizations of the expressed β_2AR-GFP under the control of P_{GAP}. The round structure may represent the vacuole or the nucleus, which has also been reported to be a localization target for the eGFP.

The attempt of finding good expression clones under the control of P_{GAP} with the DotBlot screening method failed. This could be due to an imperfectly adapted protocol, or the expression level of the GPCRs under the control of P_{GAP} was below the detection limit of this screening method.

5 Conclusion & outlook

All in all, several conclusions can be drawn from our results. The β_2AR could be well expressed in moderate to high amounts in *P. pastoris*. Moreover, functional receptors could be detected with the StrepII- as well as the eGFP-tagged constructs especially in the cholesterol strains. The cholesterol in the cell membrane seemed to stabilize the β_2AR, which confirmed previous results and could now be shown also in a cholesterol-producing *P. pastoris* strain. The exact localization remained undetermined but there was a hint that parts of the receptor were located at the plasma membrane. The copy number determination of the cholesterol strains expressing β_2AR-StrepII indicated that more copies lead to signals in WB as well as an increasing hygromycin resistance.

For the eGFP-tagged hB1R, a good fluorescence signal was obtained, but in the functional analysis only inactive receptor was found. It would be necessary to analyze the constructs without the eGFP-tag in more detail and to find a proper screening method for well expressing clones.

Unfortunately, we could not detect any signal for the C3aR expression. In this case, further experiments would be necessary to analyze if the construct is transcribed and translated at all, and what happens to the protein afterwards concerning, for example, possible proteasomal degradation.

The P_{GAP}-driven expression constructs also did not yield any improvement of receptor expression at all. It would be necessary to try different expression vectors and constructs to enhance transformation efficiency, screen more clones that express under the control of P_{GAP} and analyze them further.

Despite the difficulties encountered with GPCR expression in *P. pastoris*, we showed that the strategy to alter the membrane sterols is also applicable for at least expression of the human β_2AR. In the future, it will be interesting to investigate additional receptors and set up new, improved expression protocols.

6 References

1. Fredriksson, R., Lagerström, M. C., Lundin, L.-G. & Schiöth, H. B. The G-protein-coupled receptors in the human genome form five main families. Phylogenetic analysis, paralogon groups, and fingerprints. *Mol Pharmacol* **63,** 1256–1272 (2003).
2. Venter, J. C., Adams, M. D., Myers, E. W., Li, P. W. & Mural, R. J., et al. The sequence of the human genome. *Science* **291,** 1304–1351 (2001).
3. Bjarnadottir, T. K., Gloriam, D. E., Hellstrand, S. H., Kristiansson, H., Fredriksson, R. & Schiöth, H. B. Comprehensive repertoire and phylogenetic analysis of the G protein-coupled receptors in human and mouse. *Genomics* **88,** 263–273 (2006).
4. Alexander, S. P., Davenport, A. P., Kelly, E., Marrion, N., Peters, J. A., Benson, H. E., Faccenda, E., Pawson, A. J., Sharman, J. L., Southan, C. & Davies, J. A. The Concise Guide to PHARMACOLOGY 2015/16: G protein-coupled receptors. *Br J Pharmacol* **172,** 5744–5869 (2015).
5. Zhang, D., Zhao, Q. & Wu, B. Structural Studies of G Protein-Coupled Receptors. *Mol Cells* **38,** 836–842 (2015).
6. Schiöth, H. B. & Fredriksson, R. The GRAFS classification system of G-protein coupled receptors in comparative perspective. *Gen Comp Endocrinol* **142,** 94–101 (2005).
7. Rosenbaum, D. M., Rasmussen, S. G. F. & Kobilka, B. K. The structure and function of G-protein-coupled receptors. *Nature* **459,** 356–363 (2009).
8. Sun, Y., Huang, J., Xiang, Y., Bastepe, M., Juppner, H., Kobilka, B. K., Zhang, J. J. & Huang, X.-Y. Dosage-dependent switch from G protein-coupled to G protein-independent signaling by a GPCR. *EMBO J* **26,** 53–64 (2007).
9. Heng, B. C., Aubel, D. & Fussenegger, M. An overview of the diverse roles of G-protein coupled receptors (GPCRs) in the pathophysiology of various human diseases. *Biotechnol Adv* **31,** 1676–1694 (2013).
10. Cherezov, V., Rosenbaum, D. M., Hanson, M. A., Rasmussen, S. G. F., Thian, F. S., Kobilka, T. S., Choi, H.-J., Kuhn, P., Weis, W. I., Kobilka, B. K. & Stevens, R. C. High-resolution crystal structure of an engineered human beta2-adrenergic G protein-coupled receptor. *Science* **318,** 1258–1265 (2007).
11. Overington, J. P., Al-Lazikani, B. & Hopkins, A. L. How many drug targets are there? *Nat Rev Drug Discov* **5,** 993–996 (2006).
12. Lagerström, M. C. & Schiöth, H. B. Structural diversity of G protein-coupled receptors and significance for drug discovery. *Nat Rev Drug Discov* **7,** 339–357 (2008).
13. Byrne, B. *Pichia pastoris* as an expression host for membrane protein structural biology. *Curr Opin Struct Biol* **32,** 9–17 (2015).
14. Schütz, M., Schöppe, J., Sedlák, E., Hillenbrand, M., Nagy-Davidescu, G., Ehrenmann, J., Klenk, C., Egloff, P., Kummer, L. & Plückthun, A. Directed evolution of G protein-coupled receptors in yeast for higher functional production in eukaryotic expression hosts. *Sci Rep* **6,** 21508 (2016).
15. Chakraborty, R., Xu, B., Bhullar, R. P. & Chelikani, P. Expression of G protein-coupled receptors in Mammalian cells. *Methods Enzymol* **556,** 267–281 (2015).

16. Claes, K., Vandewalle, K., Laukens, B., Laeremans, T., Vosters, O., Langer, I., Parmentier, M., Steyaert, J. & Callewaert, N. Modular Integrated Secretory System Engineering in *Pichia pastoris* To Enhance G-Protein Coupled Receptor Expression. *ACS Synth Biol* **5,** 1070–1075 (2016).

17. Johnson, M. Molecular mechanisms of beta(2)-adrenergic receptor function, response, and regulation. *J Allergy Clin Immunol* **117,** 18-24; quiz 25 (2006).

18. Taylor, M. R. G. Pharmacogenetics of the human beta-adrenergic receptors. *Pharmacogenomics J* **7,** 29–37 (2007).

19. Turki, J., Pak, J., Green, S. A., Martin, R. J. & Liggett, S. B. Genetic polymorphisms of the beta 2-adrenergic receptor in nocturnal and nonnocturnal asthma. Evidence that Gly16 correlates with the nocturnal phenotype. *J Clin Invest* **95,** 1635–1641 (1995).

20. Woo, A. Y. H. & Xiao, R.-p. beta-Adrenergic receptor subtype signaling in heart: from bench to bedside. *Acta Pharmacol Sin* **33,** 335–341 (2012).

21. Tilley, D. G. & Rockman, H. A. Role of beta-adrenergic receptor signaling and desensitization in heart failure: new concepts and prospects for treatment. *Expert Rev Cardiovasc Ther* **4,** 417–432 (2006).

22. Azar, A. F., Jazani, N. H., Bazmani, A., Vahhabi, A. & Shahabi, S. Polymorphisms in Beta-2 Adrenergic Receptor Gene and Association with Tuberculosis. *Lung* **195,** 147–153 (2017).

23. Richard A. Bond, David B. Bylund, Douglas C. Eikenburg, J. Paul Hieble, Rebecca Hills, Kenneth P. Minneman, Sergio Parra. IUPHAR/BPS Guide to PHARMACOLOGY Adrenoceptors: β2-adrenoceptor. *Br J Pharmacol* **2016**.

24. Dixon, R. A., Kobilka, B. K., Strader, D. J., Benovic, J. L., Dohlman, H. G., Frielle, T., Bolanowski, M. A., Bennett, C. D., Rands, E., Diehl, R. E., Mumford, R. A., Slater, E. E., Sigal, I. S., Caron, M. G., Lefkowitz, R. J. & Strader, C. D. Cloning of the gene and cDNA for mammalian beta-adrenergic receptor and homology with rhodopsin. *Nature* **321,** 75–79 (1986).

25. Kobilka, B. K., Dixon, R. A., Frielle, T., Dohlman, H. G., Bolanowski, M. A., Sigal, I. S., Yang-Feng, T. L., Francke, U., Caron, M. G. & Lefkowitz, R. J. cDNA for the human beta 2-adrenergic receptor: a protein with multiple membrane-spanning domains and encoded by a gene whose chromosomal location is shared with that of the receptor for platelet-derived growth factor. *Proc Natl Acad Sci U.S.A* **84,** 46–50 (1987).

26. Rosenbaum, D. M., Cherezov, V., Hanson, M. A., Rasmussen, S. G. F., Thian, F. S., Kobilka, T. S., Choi, H.-J., Yao, X.-J., Weis, W. I., Stevens, R. C. & Kobilka, B. K. GPCR engineering yields high-resolution structural insights into beta2-adrenergic receptor function. *Science* **318,** 1266–1273 (2007).

27. Rasmussen, S. G. F., Choi, H.-J., Rosenbaum, D. M., Kobilka, T. S., Thian, F. S., Edwards, P. C., Burghammer, M., Ratnala, V. R. P., Sanishvili, R., Fischetti, R. F., Schertler, G. F. X., Weis, W. I. & Kobilka, B. K. Crystal structure of the human beta2 adrenergic G-protein-coupled receptor. *Nature* **450,** 383–387 (2007).

28. Palczewski, K. Crystal Structure of Rhodopsin. A G Protein-Coupled Receptor. *Science* **289,** 739–745 (2000).

29. Zeder-Lutz, G., Cherouati, N., Reinhart, C., Pattus, F. & Wagner, R. Dot-blot immunodetection as a versatile and high-throughput assay to evaluate recombinant GPCRs produced in the yeast *Pichia pastoris*. *Protein Expr Purif* **50,** 118–127 (2006).

30. Weiss, H. M., Haase, W., Michel, H. & Reilander, H. Comparative biochemical and pharmacological characterization of the mouse 5HT5A 5-hydroxytryptamine receptor and the human beta2-adrenergic receptor produced in the methylotrophic yeast *Pichia pastoris. Biochem J* **330 (Pt 3),** 1137–1147 (1998).

31. Adamian, L., Naveed, H. & Liang, J. Lipid-binding surfaces of membrane proteins: evidence from evolutionary and structural analysis. *Biochim Biophys Acta* **1808,** 1092–1102 (2011).

32. Yao, Z. & Kobilka, B. Using synthetic lipids to stabilize purified beta2 adrenoceptor in detergent micelles. *Anal Biochem* **343,** 344–346 (2005).

33. Hanson, M. A., Cherezov, V., Griffith, M. T., Roth, C. B., Jaakola, V.-P., Chien, E. Y. T., Velasquez, J., Kuhn, P. & Stevens, R. C. A specific cholesterol binding site is established by the 2.8 A structure of the human beta2-adrenergic receptor. *Structure* **16,** 897–905 (2008).

34. Rasmussen, S. G. F., DeVree, B. T., Zou, Y., Kruse, A. C., Chung, K. Y., Kobilka, T. S., Thian, F. S., Chae, P. S., Pardon, E., Calinski, D., Mathiesen, J. M., Shah, S. T. A., Lyons, J. A., Caffrey, M., Gellman, S. H., Steyaert, J., Skiniotis, G., Weis, W. I., Sunahara, R. K. & Kobilka, B. K. Crystal structure of the beta2 adrenergic receptor-Gs protein complex. *Nature* **477,** 549–555 (2011).

35. Zhou, W. The new face of anaphylatoxins in immune regulation. *Immunobiology* **217,** 225–234 (2012).

36. Ali, H. & Panettieri, R. A., JR. Anaphylatoxin C3a receptors in asthma. *Respir Res* **6,** 19 (2005).

37. Guo, Q., Subramanian, H., Gupta, K. & Ali, H. Regulation of C3a receptor signaling in human mast cells by G protein coupled receptor kinases. *PLoS One* **6,** e22559 (2011).

38. Fischer, W. H. & Hügli, T. E. Regulation of B cell functions by C3a and C3a(desArg): suppression of TNF-alpha, IL-6, and the polyclonal immune response. *J Immunol* **159,** 4279–4286 (1997).

39. Ames, R. S., Li, Y., Sarau, H. M., Nuthulaganti, P., Foley, J. J., Ellis, C., Zeng, Z., Su, K., Jurewicz, A. J., Hertzberg, R. P., Bergsma, D. J. & Kumar, C. Molecular Cloning and Characterization of the Human Anaphylatoxin C3a Receptor. *J Biol Chem* **271,** 20231–20234 (1996).

40. Voronina, L. & Rizzo, T. R. Spectroscopic studies of kinetically trapped conformations in the gas phase: the case of triply protonated bradykinin. *Phys Chem Chem Phys* **17,** 25828–25836 (2015).

41. Maurer, M., Bader, M., Bas, M., Bossi, F., Cicardi, M., Cugno, M., Howarth, P., Kaplan, A., Kojda, G., Leeb-Lundberg, F., Lotvall, J. & Magerl, M. New topics in bradykinin research. *Allergy* **66,** 1397–1406 (2011).

42. Leeb-Lundberg, L. M. F., Marceau, F., Muller-Esterl, W., Pettibone, D. J. & Zuraw, B. L. International union of pharmacology. XLV. Classification of the kinin receptor family: from molecular mechanisms to pathophysiological consequences. *Pharmacol Rev* **57,** 27–77 (2005).

43. Enquist, J., Skroder, C., Whistler, J. L. & Leeb-Lundberg, L. M. F. Kinins promote B2 receptor endocytosis and delay constitutive B1 receptor endocytosis. *Mol Pharmacol* **71,** 494–507 (2007).

44. Marceau, F., Hess, J. F. & Bachvarov, D. R. The B1 receptors for kinins. *Pharmacol Rev* **50,** 357–386 (1998).

45. Hess, J. F., Borkowski, J. A., Young, G. S., Strader, C. D. & Ransom, R. W. Cloning and pharmacological characterization of a human bradykinin (BK-2) receptor. *Biochem Biophys Res Com* **184,** 260–268 (1992).

46. Menke, J. G., Borkowski, J. A., Bierilo, K. K., MacNeil, T., Derrick, A. W., Schneck, K. A., Ransom, R. W., Strader, C. D., Linemeyer, D. L. & Hess, J. F. Expression cloning of a human B1 bradykinin receptor. *J Biol Chem* **269,** 21583–21586 (1994).

47. Ahmad, M., Hirz, M., Pichler, H. & Schwab, H. Protein expression in *Pichia pastoris*: recent achievements and perspectives for heterologous protein production. *Appl Microbiol Biotechnol* **98,** 5301–5317 (2014).

48. Küberl, A., Schneider, J., Thallinger, G. G., Anderl, I., Wibberg, D., Hajek, T., Jaenicke, S., Brinkrolf, K., Goesmann, A., Szczepanowski, R., Puhler, A., Schwab, H., Glieder, A. & Pichler, H. High-quality genome sequence of *Pichia pastoris* CBS7435. *J Biotechnol* **154,** 312–320 (2011).

49. Singh, S., Hedley, D., Kara, E., Gras, A., Iwata, S., Ruprecht, J., Strange, P. G. & Byrne, B. A purified C-terminally truncated human adenosine A(2A) receptor construct is functionally stable and degradation resistant. *Protein Expr Purif* **74,** 80–87 (2010).

50. Shiroishi, M., Kobayashi, T., Ogasawara, S., Tsujimoto, H., Ikeda-Suno, C., Iwata, S. & Shimamura, T. Production of the stable human histamine H(1) receptor in *Pichia pastoris* for structural determination. *Methods* **55,** 281–286 (2011).

51. Shimamura, T., Shiroishi, M., Weyand, S., Tsujimoto, H., Winter, G., Katritch, V., Abagyan, R., Cherezov, V., Liu, W., Han, G. W., Kobayashi, T., Stevens, R. C. & Iwata, S. Structure of the human histamine H1 receptor complex with doxepin. *Nature* **475,** 65–70 (2011).

52. Hirz, M., Richter, G., Leitner, E., Wriessnegger, T. & Pichler, H. A novel cholesterol-producing *Pichia pastoris* strain is an ideal host for functional expression of human Na,K-ATPase alpha3beta1 isoform. *Appl Microbiol Biotechnol* **97,** 9465–9478 (2013).

53. Hirz, M. Masterarbeit: Membrane Protein Expression in *Pichia pastoris* (2012).

54. Carotti, C., Ragni, E., Palomares, O., Fontaine, T., Tedeschi, G., Rodriguez, R., Latge, J. P., Vai, M. & Popolo, L. Characterization of recombinant forms of the yeast Gas1 protein and identification of residues essential for glucanosyltransferase activity and folding. *Eur J Biochem* **271,** 3635–3645 (2004).

55. Pelham, H. R., Hardwick, K. G. & Lewis, M. J. Sorting of soluble ER proteins in yeast. *EMBO J* **7,** 1757–1762 (1988).

56. Grillitsch, K., Tarazona, P., Klug, L., Wriessnegger, T., Zellnig, G., Leitner, E., Feussner, I. & Daum, G. Isolation and characterization of the plasma membrane from the yeast *Pichia pastoris*. *Biochim Biophys Acta* **1838,** 1889–1897 (2014).

57. Näätsaari, L., Mistlberger, B., Ruth, C., Hajek, T., Hartner, F. S. & Glieder, A. Deletion of the *Pichia pastoris* KU70 homologue facilitates platform strain generation for gene expression and synthetic biology. *PLoS One* **7,** e39720 (2012).

58. Schmidt, T. G. M. & Skerra, A. The Strep-tag system for one-step purification and high-affinity detection or capturing of proteins. *Nat Protoc* **2,** 1528–1535 (2007).

59. Lin-Cereghino, J., Wong, W. W., Xiong, S., Giang, W., Luong, L. T., Vu, J., Johnson, S. D. & Lin-Cereghino, G. P. Condensed protocol for competent cell preparation and transformation of the methylotrophic yeast *Pichia pastoris*. *Biotechniques* **38,** 44, 46, 48 (2005).

60. Hoffman, C. S. & Winston, F. A ten-minute DNA preparation from yeast efficiently releases autonomous plasmids for transformation of *Escherichia coli*. *Gene* **57,** 267–272 (1987).

61. Abad, S., Kitz, K., Hormann, A., Schreiner, U., Hartner, F. S. & Glieder, A. Real-time PCR-based determination of gene copy numbers in *Pichia pastoris*. *Biotechnol J* **5,** 413–420 (2010).

62. Schiefer, A. Master's thesis: Molecular characterization of yeast strains made by synthetic biology (2014).

63. Lee, C., Kim, J., Shin, S. G. & Hwang, S. Absolute and relative QPCR quantification of plasmid copy number in *Escherichia coli*. *J Biotechnol* **123,** 273–280 (2006).

64. Livak, K. J. & Schmittgen, T. D. Analysis of relative gene expression data using real-time quantitative PCR and the 2(-Delta Delta C(T)) Method. *Methods* **25,** 402–408 (2001).

65. Pfaffl, M. W. A new mathematical model for relative quantification in real-time RT-PCR. *Nucleic Acids Res* **29,** e45 (2001).

66. Gibson, D. G. Synthesis of DNA fragments in yeast by one-step assembly of overlapping oligonucleotides. *Nucleic Acids Res* **37,** 6984–6990 (2009).

67. Gibson, D. G., Young, L., Chuang, R.-Y., Venter, J. C., Hutchison, C. A. 3. & Smith, H. O. Enzymatic assembly of DNA molecules up to several hundred kilobases. *Nat Methods* **6,** 343–345 (2009).

68. Gritz, L. & Davies, J. Plasmid-encoded hygromycin B resistance. The sequence of hygromycin B phosphotransferase gene and its expression in *Escherichia coli* and *Saccharomyces cerevisiae*. *Gene* **25,** 179–188 (1983).

69. Souza, C. M., Schwabe, T. M. E., Pichler, H., Ploier, B., Leitner, E., Guan, X. L., Wenk, M. R., Riezman, I. & Riezman, H. A stable yeast strain efficiently producing cholesterol instead of ergosterol is functional for tryptophan uptake, but not weak organic acid resistance. *Metab Eng* **13,** 555–569 (2011).

70. Sarramegna, V., Talmont, F., Seree de Roch, M., Milon, A. & Demange, P. Green fluorescent protein as a reporter of human μ-opioid receptor overexpression and localization in the methylotrophic yeast *Pichia pastoris*. *J Biotechnol* **99,** 23–39 (2002).

71. Lenassi Zupan, A., Trobec, S., Gaberc-Porekar, V. & Menart, V. High expression of green fluorescent protein in *Pichia pastoris* leads to formation of fluorescent particles. *J Biotechnol* **109,** 115–122 (2004).

72. Wang, Y., Meriin, A. B., Zaarur, N., Romanova, N. V., Chernoff, Y. O., Costello, C. E. & Sherman, M. Y. Abnormal proteins can form aggresome in yeast: aggresome-targeting signals and components of the machinery. *FASEB J* **23,** 451–463 (2009).

73. Kopito, R. R. Aggresomes, inclusion bodies and protein aggregation. *Trends Cell Biol* **10,** 524–530 (2000).

74. Rueda, F., Gasser, B., Sanchez-Chardi, A., Roldan, M., Villegas, S., Puxbaum, V., Ferrer-Miralles, N., Unzueta, U., Vazquez, E., Garcia-Fruitos, E., Mattanovich, D. & Villaverde, A. Functional inclusion bodies produced in the yeast *Pichia pastoris*. *Microb Cell Fact* **15,** 166 (2016).

75. André, N., Cherouati, N., Prual, C., Steffan, T., Zeder-Lutz, G., Magnin, T., Pattus, F., Michel, H., Wagner, R. & Reinhart, C. Enhancing functional production of G protein-coupled receptors in *Pichia pastoris* to levels required for structural studies via a single expression screen. *Protein Sci* **15,** 1115–1126 (2006).

76. Zhang, A.-L., Luo, J.-X., Zhang, T.-Y., Pan, Y.-W., Tan, Y.-H., Fu, C.-Y. & Tu, F.-Z. Recent advances on the GAP promoter derived expression system of *Pichia pastoris*. *Mol Biol Rep* **36,** 1611–1619 (2009).

77. Waterham, H. R., Digan, M. E., Koutz, P. J., Lair, S. V. & Cregg, J. M. Isolation of the *Pichia pastoris* glyceraldehyde-3-phosphate dehydrogenase gene and regulation and use of its promoter. *Gene* **186,** 37–44 (1997).

7 Appendix

7.1 Sequences

10xHis-tag StrepII-tag

7.1.1 α-factor signal sequence

ATGAGATTCCCATCTATTTTCACCGCTGTCTTGTTCGCTGCCTCCTCTGCATTGGCTGCCCCTGTTAAC
ACTACCACTGAAGACGAGACTGCTCAAATTCCAGCTGAAGCAGTTATCGGTTACTCTGACCTTGAGG
GTGATTTCGACGTCGCTGTTTTGCCTTTCTCTAACTCCACTAACAACGGTTTGTTGTTCATTAACACCA
CTATCGCTTCCATTGCTGCTAAGGAAGAGGGTGTCTCTCTCGAGAAGAGA

7.1.2 His-β_2AR-StrepII

CATCACCATCACCATCACCATCACCATCACGGGGATCCCAATAGAAGCCATGCGCCGGACCACGACG
TCACGCAGCAAAGGGACGAGGTGTGGGTGGTGGGCATGGGCATCGTCATGTCTCTCATCGTCCTGG
CCATCGTGTTTGGCAATGTGCTGGTCATCACAGCCATTGCCAAGTTCGAGCGTCTGCAGACGGTCAC
CAACTACTTCATCACTTCACTGGCCTGTGCTGATCTGGTCATGGGCCTGGCAGTGGTGCCCTTTGGGG
CCGCCCATATTCTTATGAAAATGTGGACTTTTGGCAACTTCTGGTGCGAGTTTTGGACTTCCATTGAT
GTGCTGTGCGTCACGGCCAGCATTGAGACCCTGTGCGTGATCGCAGTGGATCGCTACTTTGCCATTA
CTTCACCTTTCAAGTACCAGAGCCTGCTGACCAAGAATAAGGCCCGGGTGATCATTCTGATGGTGTG
GATTGTGTCAGGCCTTACCTCCTTCTTGCCCATTCAGATGCACTGGTACCGGGCCACCCACCAGGAAG
CCATCAACTGCTATGCCAATGAGACCTGCTGTGACTTCTTCACGAACCAAGCCTATGCCATTGCCTCTT
CCATCGTGTCCTTCTACGTTCCCCTGGTGATCATGGTCTTCGTCTACTCCAGGGTCTTTCAGGAGGCCA
AAAGGCAGCTCCAGAAGATTGACAAATCTGAGGGCCGCTTCCATGTCCAGAACCTTAGCCAGGTGG
AGCAGGATGGGCGGACGGGGCATGGACTCCGCAGATCTTCCAAGTTCTGCTTGAAGGAGCACAAAG
CCCTCAAGACGTTAGGCATCATCATGGGCACTTTCACCCTCTGCTGGCTGCCCTTCTTCATCGTTAACA
TTGTGCATGTGATCCAGGATAACCTCATCCGTAAGGAAGTTTACATCCTCCTAAATTGGATAGGCTAT
GTCAATTCTGGTTTCAATCCCCTTATCTACTGCCGGAGCCCAGATTTCAGGATTGCCTTCCAGGAGCTT
CTGTGCCTGCGCAGGTCTTCTTTGAAGGCCTATGGGAATGGCTACTCCAGCAACGGCAACACAGGGG
AGCAGAGTGGATATCACGTGGAACAGGAGAAAGAAAATAAACTGCTGTGTGAAGACCTCCCAGGCA
CGGAAGACTTTGTGGGCCATCAAGGTACTGTGCCTAGCGATAACATTGATTCACAAGGGAGGAATT
GTAGTACAAATGACTCACTGCTGTGGAGTCATCCTCAATTTGAAAAATAATAA

7.1.3 His-C3aR-StrepII

CATCACCATCACCATCACCATCACCATCACGGGGATCGCGAAAACCTGTACTTTCAAGGTCATATGGC
GTCTTTCTCTGCTGAGACCAATTCAACTGACCTACTCTCACAGCCATGGAATGAGCCCCCAGTAATTCT
CTCCATGGTCATTCTCAGCCTTACTTTTTTACTGGGATTGCCAGGCAATGGGCTGGTGCTGTGGGTGG
CTGGCCTGAAGATGCAGCGGACAGTGAACACAATTTGGTTCCTCCACCTCACCTTGGCGGACCTCCTC
TGCTGCCTCTCCTTGCCCTTCTCGCTGGCTCACTTGGCTCTCCAGGGACAGTGGCCCTACGGCAGGTT
CCTATGCAAGCTCATCCCCTCCATCATTGTCCTCAACATGTTTGCCAGTGTCTTCCTGCTTACTGCCATT
AGCCTGGATCGCTGTCTTGTGGTATTCAAGCCAATCTGGTGTCAGAATCATCGCAATGTAGGGATGG
CCTGCTCTATCTGTGGATGTATCTGGGTGGTGGCTTTTGTGATGTGCATTCCTGTGTTCGTGTACCGG
GAAATCTTCACTACAGACAACCATAATAGATGTGGCTACAAATTTGGTCTCTCCAGCTCATTAGATTA

TCCAGACTTTTATGGAGATCCACTAGAAAACAGGTCTCTTGAAAACATTGTTCAGCCGCCTGGAGAA
ATGAATGATAGGTTAGATCCTTCCTCTTTCCAAACAAATGATCATCCTTGGACAGTCCCCACTGTCTTC
CAACCTCAAACATTTCAAAGACCTTCTGCAGATTCACTCCCTAGGGGTTCTGCTAGGTTAACAAGTCA
AAATCTGTATTCTAATGTATTTAAACCTGCTGATGTGGTCTCACCTAAAATCCCCAGTGGGTTTCCTAT
TGAAGATCACGAAACCAGCCCACTGGATAACTCTGATGCTTTTCTCTCTACTCATTTAAAGCTGTTCCC
TAGCGCTTCTAGCAATTCCTTCTACGAGTCTGAGCTACCACAAGGTTTCCAGGATTATTACAATTTAG
GCCAATTCACAGATGACGATCAAGTGCCAACACCCCTCGTGGCAATAACGATCACTAGGCTAGTGGT
GGGTTTCCTGCTGCCCTCTGTTATCATGATAGCCTGTTACAGCTTCATTGTCTTCCGAATGCAAAGGG
GCCGCTTCGCCAAGTCTCAGAGCAAAACCTTTCGAGTGGCCGTGGTGGTGGTGGCTGTCTTTCTTGTC
TGCTGGACTCCATACCACATTTTTGGAGTCCTGTCATTGCTTACTGACCCAGAAACTCCCTTGGGGAA
AACTCTGATGTCCTGGGATCATGTATGCATTGCTCTAGCATCTGCCAATAGTTGCTTTAATCCCTTCCT
TTATGCCCTCTTGGGGAAAGATTTTAGGAAGAAAGCAAGGCAGTCCATTCAGGGAATTCTGGAGGC
AGCCTTCAGTGAGGAGCTCACACGTTCCACCCACTGTCCCTCAAACAATGTCATTTCAGAAAGAAATA
GTACAACTGTGGGCGGCCGCTGGAGTCATCCTCAATTTGAAAAATAATAA

7.1.4 His-hB1R-StrepII

CATCACCATCACCATCACCATCACCATCACGGGGATCGCGAAAACCTGTACTTTCAAGGTCATATGGC
TTCTTCCTGGCCTCCACTCGAGTTGCAATCAAGTAATCAAAGTCAGCTGTTCCCACAGAATGCTACTG
CCTGCGACAACGCTCCCGAAGCCTGGGATTTGCTGCACAGGGTCTTGCCCACCTTCATCATTTCCATC
TGTTTCTTTGGCCTTCTCGGTAACCTTTTCGTTTTGCTGGTGTTTCTTCTCCCAAGACGTCAATTGAATG
TGGCTGAAATCTACCTGGCCAACCTTGCTGCCTCAGACTTGGTCTTCGTACTGGGACTTCCCTTTTGG
GCCGAAAACATTTGGAATCAGTTCAACTGGCCTTTTGGAGCTTTGCTGTGCCGTGTCATCAATGGCGT
AATTAAGGCCAACCTGTTCATCAGCATTTTTCTTGTTGTGGCTATCTCTCAAGACCGTTATAGGGTTCT
GGTGCATCCTATGGCCTCTGGCAGGCAACAGAGGCGCAGACAGGCTCGCGTCACTTGCGTATTGATT
TGGGTCGTAGGTGGACTTCTCTCCATCCCTACCTTCTTGCTGAGGTCAATTCAAGCCGTTCCTGACTTG
AACATCACAGCTTGTATTCTTCTCTTGCCACACGAGGCTTGGCATTTCGCCCGCATCGTTGAACTCAAT
ATTTTGGGCTTTCTGCTTCCCTTGGCTGCCATCGTGTTCTTTAACTACCACATTCTGGCCAGTCTTCGCA
CAAGAGAGGAAGTCAGCCGTACTAGGGTTCGCGGTCCTAAGGATTCCAAAACTACCGCTCTCATTTT
GACACTGGTTGTGGCTTTCCTGGTGTGCTGGGCTCCTTATCATTTCTTTGCTTTTCTCGAGTTCTTGTTT
CAAGTTCAGGCTGTGAGAGGTTGTTTCTGGGAAGACTTTATCGATCTTGGACTCCAGTTGGCTAATTT
CTTTGCCTTCACTAATAGCTCTTTGAACCCAGTGATTTACGTCTTCGTAGGTAGACTCTTTCGTACCAA
GGTCTGGGAGCTGTATAAGCAATGTACACCCAAATCACTGGCTCCTATCTCCTCAAGTCACAGAAAA
GAAATTTTCCAGTTGTTTTGGCGTAACGGCGGCCGCTGGAGTCATCCTCAATTTGAAAAATAATAA

7.1.5 eGFP

GCTAGCAAAGGAGAAGAACTTTTCACTGGAGTTGTCCCAATTCTTGTTGAATTAGATGGTGATGTTA
ATGGGCACAAATTTTCTGTCAGTGGAGAGGGTGAAGGTGATGCTACATACGGAAAGCTTACCCTTAA
ATTTATTTGCACTACTGGAAAACTACCTGTTCCATGGCCAACACTTGTCACTACTTTGACTTATGGTGT
TCAATGCTTTTCCCGTTATCCTGATCATATGAAACGGCATGACTTTTTCAAGAGTGCCATGCCCGAAG
GTTATGTACAGGAACGCACTATATCTTTCAAAGATGACGGGAACTACAAGACGCGTGCTGAAGTCAA
GTTTGAAGGTGATACCCTTGTTAATCGTATCGAGTTAAAAGGTATTGATTTTAAAGAAGATGGAAAC
ATTCTCGGACACAAACTTGAGTACAACTATAACTCACACAATGTATACATCACGGCAGACAAACAAA
AGAATGGAATCAAAGCTAACTTCAAAATTCGCCACAACATTGAAGATGGTTCCGTTCAACTAGCAGA
CCATTATCAACAAAATACTCCAATTGGCGATGGCCCTGTCCTTTTACCAGACAACCATTACCTGTCGAC
ACAATCTGCCCTTTCGAAAGATCCCAACGAAAAGCGTGACCACATGGTCCTTCTTGAGTTTGTAACTG
CTGCTGGGATTACACATGGCATGGATGAATTGTACAAGTAA

7.2 Glycerol stock list

Table 20: List of strains preserved as glycerol stocks

#	Strain description	Details		
#1	*P. pastoris* cholesterol strain pPpHygαHisβ$_2$ARStrepII #1-5	cPCR + F	WB -	qPCR
#2			WB +	
#3			WB +	FA +
#4			WB -	
#5			WB +	
#6	*P. pastoris* WT pPpHygαHisβ$_2$ARStrepII #1, 2, 4-6	cPCR + F	WB -	
#7				
#8				qPCR
#9				
#10				qPCR
#11	*P. pastoris Δku70* pPpHygαHisβ$_2$ARStrepII #1-5	cPCR + F	WB -	
#12			WB -	
#13			WB -	
#14			WB +	
#15			WB -	
#16	*P. pastoris* SMD1168 pPpHygαHisβ$_2$ARStrepII #1-5	cPCR + F	WB -	
#17			WB -	
#18			WB +	
#19			WB -	qPCR
#20			WB +	FA + qPCR
#21	*E. coli* Top10 pPpHygαHishB1RTEVeGFP	Sequenced *P. pastoris* transformation		
#22	*E. coli* Top10 pPpHygαHisβ$_2$ARTEVeGFP			
#23	*E. coli* Top10 pPpHygαHisC3aRTEVeGFP			
#24	*E. coli* Top10 pPpKC3_pep4	No sequencing		
#25	*P. pastoris* WT pPpHygαHisβ$_2$ARTeveGFP #3	cPCR +; FM: -		
#26	*P. pastoris* WT pPpHygαHisβ$_2$ARTeveGFP #8	cPCR +; FM: +		
#27	*P. pastoris* cholesterol strain pPpHygαHisβ$_2$ARTeveGFP #1-4	cPCR + FM + Positive controls for DWP		
#28				
#29				
#30				
#31	*P. pastoris* WT pPpHygαHisβ$_2$ARTeveGFP #1-4	DWP FM +		
#32				
#33				
#34			FA +	
#35	*P. pastoris Δku70* pPpHygαHisβ$_2$ARTeveGFP #1-4	DWP FM +		
#36			FA +	CF
#37				
#38				
#39	*P. pastoris* SMD1168 pPpHygαHisβ$_2$ARTeveGFP #1-4	DWP FM +		
#40			FA +	

#41			
#42			
#43			
#44	*P. pastoris* cholesterol strain pPpHygαHisβ$_2$ARTeveGFP #1-4	DWP FM +	
#45			
#46			FA + CF
#47	*P. pastoris* WT pPpHygαHishB1RTeveGFP #1-3	DWP FM +	
#48			FA -
#49			
#50	*P. pastoris Δku70* pPpHygαHishB1RTeveGFP #1, 2, 4	DWP FM +	
#51			FA -
#52			
#53	*P. pastoris* SMD1168 pPpHygαHishB1RTeveGFP #1-3	DWP FM +	
#54			FA -
#55			
#56	*P. pastoris* cholesterol strain pPpHygαHishB1RTeveGFP #1-3	DWP FM +	
#57			
#58			FA -
#59	*P. pastoris* cholesterol strain *Δpep4*	marker recycelt, knockout verified by cPCR	
#60	*P. pastoris* cholesterol strain *Δprb1 Δpep4*	marker recycelt, knockout NOT verified by cPCR	
#61	*P. pastoris* WT CBS7435	empty strains	
#62	*P. pastoris* WT *Δku70*		
#63	*P. pastoris* SMD1168		
#64	*P. pastoris* cholesterol strain		
#65	*P. pastoris* cholesterol strain *Δprb1*		
#66	*E. coli Top10* pPpHygpGAPαHisβ$_2$ARStrepII	Sequenced *P. pastoris* transformation	
#67	*E. coli Top10* pPpHygpGAPαHisβ$_2$ARTEVeGFP		
#68	*E. coli Top10* pPpHygpGAPαHishB1RStrepII		
#69	*E. coli Top10* pPpHygpGAPαHosC3aRTEVeGFP		
#70	*P. pastoris* WT pPpHyg**pGAP**αHisβ$_2$ARTeveGFP #21	DWP FM: +	
#71	*P. pastoris* SMD1168 pPpHyg**pGAP**αHosβ$_2$ARTeveGFP #13		
#72	*P. pastoris* cholesterol strain pPpHygαHisβ$_2$ARTeveGFP #1-8	Positive controls for DWP	
#73			
#74			
#75			
#76			
#77			
#78			
#79			

cPCR +: cPCR positive, F: fermentation, WB +/-: signal/no signal in WB analysis, FA +/-: functional analysis positive(functional)/negative (not functional), qPCR: quantitative PCR, CF: cell fractionation, FM +/-: fluorescence microscopy positive signal/negative signal, DWP: best clones in DWP screening